Risk and Resilience Assessment of Complex Infrastructure Networks

– A system-of-systems approach to rail networks

Ohiowaobo Ilalokhoin **CEng FICE**

Keble College

University of Oxford

A Thesis submitted for the degree of

Doctor of Philosophy

Trinity Term 2021

Abstract

The railway is an important critical national infrastructure network in many western countries and by its nature is exposed to diverse threats ranging from extreme weather and climate change risks, man-made and malevolent activities. The complex nature of the interdependencies across the respective systems that make up a typical rail network can result in the propagation of network failures with serious consequences for the movement of trains, passengers, goods and services. Recent disruption events have shown how rapid and widescale the impact of failures can be on complex interdependent rail networks, and with the projection of increased risk from extreme weather and climate change events, there is a need for robust methodologies that can address this growing complexity with applicability to real-world networks.

The aim of this thesis is therefore to develop models and methodologies for analysing the risk and resilience of large scale interdependent rail infrastructure networks. It introduces multi-scale, system-of-systems based methodologies and applied analysis that provides important new insights into interdependent infrastructure network risk and resilience at national scale using real-world case studies. The thesis comprises three parts. First, a theoretical network-based model of the multi-track layout is built to replicate the actual operational functionality of the rail network which is tested using a real-world national timetable dataset for Great Britain. This model is calibrated using an empirical dataset of journey disruptions to arrive at a robust journey disruption network model. Next, by adopting a complex network-based modelling approach, real-world asset data is integrated from the respective systems of the national rail network in Great Britain to represent the physical interconnectivity that exists within and between its interdependent infrastructure systems. The coupling of both models give rise to an integrated infrastructure network model which is used to simulate scenarios of risk to the traction power network and resilience modelling. Lastly, the impact of extreme weather risks is studied with the development of a flood risk methodology which is tested by carrying out a comprehensive risk assessment of the national rail network in Great Britain. The criticality of individual assets is calculated by summing the direct impacts, with the indirect impacts measured in terms of train and passenger disruptions.

The development of robust methodologies and research models that represent the actual physical, geographic and functional interdependencies across rail networks using real-world asset datasets allows for the testing of multiple scenarios of risk and resilience which can be used to support robust decision making in complex networks. This research therefore presents new theoretical insights and practical methodologies with direct applicability to academia, infrastructure managers, policy and decision makers across Great Britain and beyond.

Acknowledgements

First, I am extremely grateful to God for the blessing of life and His continued mercy and grace over the years. To my mum and dad, Mary and Joseph Ilalokhoin, who from a very young age during our early years growing up in Benin City, Nigeria, instilled on us the virtues of a sound education, making huge financial and personal sacrifices despite limited resources to ensure we got the best possible education available at that time.

I am grateful to my supervisors, Professor Jim Hall and Dr Raghav Pant for their tireless academic guidance throughout my doctoral research study at Oxford. I am very proud to have been awarded a highly competitive, fully funded academic scholarship at Oxford for the duration of my doctoral research study and I am grateful to the Engineering and Physical Sciences Research Council (EPSRC) for this.

My DPhil journey is a true reflection of the African proverb that *'it takes a village to train a child*'. In my case, there have been a number of close friends who have been instrumental to my DPhil journey and wellbeing at Oxford. I am grateful for this.

Lastly, and because the best needs to be saved for last, I cannot overstress the heartfelt gratitude to my loving wife, Faith, and my children who have endured the ups and downs of my entire academic journey over the years with me. I am indebted to the loving support my wife, Faith has shown to me over the years, the selfless and personal sacrifices made which is more than I could ever imagined and without asking for anything in return.

September 2021
Oxford, England

Table of Contents

List of figures

List of tables

1 Introduction

1.1 Background

The importance of infrastructure systems to everyday life is widely acknowledged across research and industry circles (PCCIP, 1997; EPCIP, 2008; Sahoo et al, 2012; World Bank, 2013; Dash & Sahoo, 2010; Menson, 2012). These infrastructure systems, comprising transport, energy, communication, water, digital technologies underpin the smooth functioning of society and their loss can result in great socio-economic impacts, disruptions to citizen's livelihoods, threat to national security and loss of lives (Cabinet Office, 2010). Due to their vital importance, they are often referred to as critical national infrastructures. Across many countries around the world, the railway network plays a significant role in the movement of passengers and freight. The complex interdependencies across the respective systems that make up a typical rail network is such that perturbation affecting one system can quickly percolate across the entire network resulting in consequences beyond the initiating system. It is imperative therefore for rail networks to be resilient enough to maintain an acceptable level of operational functionality under failure conditions.

But rail networks are peculiar when compared with other infrastructure networks by the nature of their topological, functional, operational characteristics and the complex interactions that exist across their interdependent asset systems. This therefore presents a practical challenge in the adoption of conventional methodologies for assessing their vulnerability and resilience to threats. In some cases, these challenges can be made worse by virtue of their historical challenges, with many of the existing rail networks built in the past when little was known of the current projection of risks that they would be subject to today. For example, in Great Britain, research shows that the circumstances surrounding the initial construction of the railway network in the 1800's where the lack of central planning or coordination of railway expansion meant that many sections of the

railway were built in cuttings and tunnel which were lower than their surrounding and on flat low-lying land with limited drainage which made it susceptible to heavy rain and flooding (Bogart et al, 2017). With much of the existing network today still based on original design specifications and following their original routes, recent hazard events have exposed their vulnerability. For example, in July 2021, several notable rail networks were subject to severe flooding across Great Britain, other parts of Western Europe, North America and China (Network Rail, 2021; Trains, 2021, Nytimes, 2021, BBC, 2021). Future projections (Collins, 2013) show that the risk from extreme weather events will increase due to the challenge of climate change with the potential for it to be subject to vulnerabilities from extreme weather hazards with increased flooding, strong winds, sea level rises and rising temperatures. Despite this challenge, research methodologies and models that focus extensively on risk and resilience assessment of rail networks remain very few. While some acknowledged progress has being made (Pagani et al, 2019; Pant et al, 2016; Johansson et al, 2011), more still needs to be done, especially in the area of methodological development which takes into account network vulnerability from a system-of-systems perspective (RSSB, 2016). Also, when these networks are subject to perturbation, an important factor in measuring the extent of vulnerability is the correct assessment of the disruptive impact of risk. In practical real-world scenarios, this is measured using the metrics of train and passenger delays (ORR, 2019; DAB, 2019). However, across research literature, there are currently no studies which specifically model network vulnerability impacts in terms of delay minutes. To do this requires complex modelling of the rail asset systems with passenger journeys simulated such that the impact from perturbation can be measured in terms of disruption to trains and passengers on the track model. While some research progress has been made previously in this area (Pant et al, 2016), it has focussed exclusively on simulating train journeys on single track models which, although makes a notable contribution to research knowledge

in this area, is limited in the estimation of impacts when this is compared with real-world train journeys made on multi-track networks. This presents gaps in methodology and model development of ways in which risk and resilience are assessed, the metrics for performance measurement to reflect real-world scenarios and the simulation of trains and passenger journeys to reflect their actual journey paths on multi-track models.

These are the gaps which this thesis seeks to address by making a significant contribution in methodological and model development with applicability to real-world scenarios. The models developed in this thesis are calibrated where available, using empirical datasets from Great Britain's rail network and are used to simulate and stress test a range of extreme weather hazard scenarios to assist with informed and robust decision making by railway Infrastructure Managers and policy makers.

1.2 Aims and objectives

This aim of this thesis is to develop novel methodological formulations for rail infrastructure and train journey modelling to enable a system-of-systems analysis of its risk and resilience at national scale, making significant steps in the modelling of train operations, disruptions, interdependencies and simulating extreme weather-related hazards.

To achieve this aim, the following objectives have been identified:

(i) To build a tractable integrated rail infrastructure network model that correctly replicates the complex system-of-systems interdependencies that exists across the respective rail systems and allows for the correct simulation of journeys on the rail network according to their actual multi-track pathways.

(ii) To correctly model the formulation of industry-relevant systemic performance metrics into an integrated rail network model for use in carrying out vulnerability and resilience assessment of rail networks.

(iii) To evaluate systemic risk to the rail network from extreme weather flood events and use the system-of-system model and methodology developed in (i) and (ii) to quantify flood risk and impacts based on real-world scenarios on the national rail network in Great Britain.

1.3 Research questions for the thesis

The overarching research question for this thesis is:

- How can the risk and resilience of complex interdependent rail networks be assessed?

Based on the overarching question, three research questions are outlined below which are structured to align with the three (3) research papers that form the core sections of this thesis.

Research question 1: What methods can be used to study and correctly replicate the operational functionality of large, complex interdependent rail networks?

Research question 2: What methods and models can be developed to assess risk and resilience of interdependent railway?

Research question 3: How can flood risk on complex interdependent rail networks be assessed at large scale?

1.4 Research publications

The following first author journal research papers make up the substantive content of this DPhil Thesis. The papers have been integrated into the thesis through their inclusion as Chapters 4-6. The research paper contribution statements are signed by all co-authors and detailed in Appendix A. A description of each paper, including its status in terms of publication, is given below:

1.4.1 Paper 1:

Ilalokhoin, O., Pant, R. and Hall, J., (2021), 'A multi-track rail model for estimating journey impacts from extreme weather events - case study of Great Britain's rail network', International Journal of Rail Transportation, DOI: 10.1080/23248378.2021.1891582.

1.4.2 Paper 2:

Ilalokhoin, O., Pant, R. and Hall, J., 'A model and methodology for risk and resilience assessment of interdependent rail networks – case study of Great Britain's rail network, JRESS-D-21-00945, submitted to the Journal of Reliability Engineering and System Safety, in Review.

1.4.3 Paper 3:

Ilalokhoin, O., Pant, R. and Hall, J., 'A flood risk assessment methodology for complex railway networks: application to the national rail network in Great Britain', submitted to Risk Analysis, in Review.

1.5 Thesis structure

This thesis is divided into 7 chapters. Following the introduction, Chapters 2 and 3 provide a literature review that underpins the theoretical and methodological development of the thesis. Chapter 2 introduces the railway, its complex system-of-systems interdependencies and an in-depth review of modelling approaches. Chapter 3 introduces the literature on risk and resilience assessment of rail networks including climate change and extreme weather risks and adaptation on rail networks.

Chapter 4 responds to research question 1 by presenting a multi-track model and methodology for estimating journey impacts from weather events. This model is applied to an empirical case study of actual weather events in Great Britain.

Chapter 5 responds to research question 2 by discussing the development of a model and methodology for risk and resilience assessment of interdependent rail networks. This model is applied to a case study of the traction power systems on the southern region rail network in Great Britain.

Chapter 6 responds to research question 3 by presenting a flood risk assessment methodology for complex railway networks which is applied to a comprehensive analysis of the national rail network in Great Britain.

Chapter 7 presents the conclusions of the thesis, the main contribution of the thesis and its implications for engineering, regulatory and policy making. This chapter concludes by outlining areas of future research development.

Supporting materials are presented in the Appendix including an overview of the software tools used and developed in this thesis.

2 The railway network as a complex system-of-systems

While the concept of *systems*, *systems thinking* and *systems engineering* is still generally regarded as a growing areas in transport systems, its roots can be traced back to very early works by von Bertalanffy (1928) on the foundation of the General System Theory who articulated that in biological systems, the *"…investigation of the single parts and processes cannot provide a complete explanation….and gives no information about the coordination of parts and process".* Over time, the concept of systems has gained increasing traction across research literature and particularly in the literature on infrastructure networks which are characterised by complex system-of-systems interdependencies (Rinaldi et al, 2001).

Two important descriptions of the term *systems* are ascribed to Ackoff (1981) and Checkland (1981). Ackoff (1981) described a system as a set of two or more elements which satisfy the following three conditions:

- The behaviour of each element has an effect on the behaviour of the whole
- The behaviour of the elements and their effects on the whole are interdependent
- However subgroup of the elements are formed, each has an effect on the behaviour of the whole and none has an independent effect on it.

Checkland (1981) went further to discuss the central concept of *systems* in the context of a set of connected elements with interactions between its different parts to form a whole. He described viewing systems from a broad view of the combination of all its constituent parts.

A typical rail network comprises several interconnected systems which work together to facilitate the movement of passengers and freight on trains from an origin to a destination. In Figure 2.1, a description of the core systems that make up a typical rail network is presented. The track system comprises twin longitudinal rails on which trains run

including switches and crossings that allows for change in train paths and directions on the network. The civil engineering system comprises the bridges, tunnels, buildings, stations, drainage systems, earthworks and structural support for the track and other assets. The signalling control system directs railway traffic and keep trains at a safe distance apart from each other and in many modern systems, relies on digital telecommunication to support a secure and reliable driver-signaller communication across the network. The energy system provides power for running trains which can be obtained from electricity, fossil fuels and other sustainable sources. Together, these systems form a complex network of interdependencies in facilitating the effective functionality of the rail network. This interdependent relationship is such that failure of a component in one of its systems can quickly result in a cascade of failure across other systems resulting in higher order effects and eventual disruption to train services. The large number of interconnected parts across the network gives rise to the possibility of multiple failure points across the respective network, with each subsystem influencing the overall behaviour of the whole network. Together these form a complex structure of system-of-systems relationship.

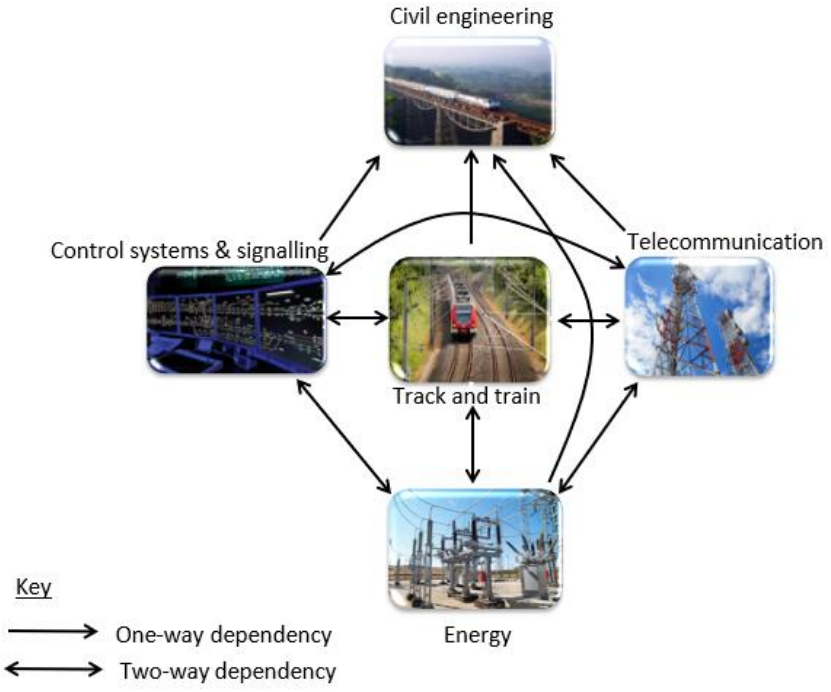

Figure 2.1 Key interdependent infrastructure systems that make up a typical railway network

While the discussions above have focussed on the internal complexities of interdependent relationships across the respective infrastructure systems that make up the rail network, there are equally huge complexities in the external dependencies and interdependencies of the railway network. For example, the reliance on the railway network for the movement of goods and services by freight trains and commuter journeys using trains across many countries as well as the reliance of the railway network on external infrastructure systems like the national grid for electricity to run electric trains. Also, with third party non-railway assets located within close geographical proximities to railway assets, direct and indirect impacts can often be aggravated. For example, a freight train derailment in Baltimore's Howard Street Tunnel in the United States resulted in fire leading to a breakdown of water mains above the tunnel, loss of electricity, disruption in phone services, emails, web services to thousands of Baltimore residences as well as disruption to rail transport across several States with huge socio-economic impact (Pederson et al, 2006). Similarly, the World Trade Centre terrorist attack in 2001 resulted in the breaking of water mains which led to flooding of rail tunnels and vaults containing some of the world's largest telecommunication nodes some of which were connected to the New York Stock Exchange resulting in international financial instability (Pederson et al, 2006). In Great Britain, extreme weather event led to the collapse of the Dawlish sea wall supporting the rail line into Devon and Cornwall, severing all rail services to this part of the country as well as loss of power and damage to properties (Armstrong et al, 2017) and an estimated overall economic loss of up to £1.2 billion excluding the cost of repair to the infrastructure (DMF, 2015). Despite the challenges in the complexities of rail networks, a notable gap in research literature is the absence of research methodologies which are specifically focussed on system-of-systems interdependencies on railways with very little published beyond a handful of peer reviewed papers (Ilalokhoin et al, 2021). While the scale of the problem is widely acknowledged and the theory is known (RSSB,

2016), there are still gaps in practical methodologies which brings to the fore the need for a shift in focus in research scholarship to tackling these challenges.

An even greater challenge is the increasing complexities occasioned by digitalisation of the railway network through the use of digital train control technology, automated traffic management systems, in-cab signalling - European Train Control system (ETCS), Automatic Train Operation (ATO), Connected Driver Advisory systems (CDAS) and the enabling telecommunications network. This increasing complexity of infrastructure systems and the advancement in digital technologies means that the interactions across these systems will transcend mere physical and geographical boundaries, with migration to fully computer-based telecommunication controls (CBTC) and remote signalling controls. Similarly, in many countries including the United Kingdom, electrification control systems are now digitally controlled with the implementation of the Supervisory Control and Data Acquisition (SCADA), while rail telecommunication systems are being migrated towards Internet Protocol (RailEngineer, 2015). Across Europe, there is a migration of signalling systems to the European Rail Traffic Management System (ERTMS) establishing an interoperable rail framework across the European Union territory using ETCS and a roll out of the global system for mobile communications on railway (GSM-R). The United Kingdom, despite leaving the European Union following the end of the Brexit transition in 2020, is still committed to the ERTMS and ETCS in line with the objectives of the launch of its Digital Railway programme in 2018.

2.1 Types of interdependencies

An important element of complex railway networks is the existence of mutually dependent relationships across the respective asset systems. Rinaldi et al (2001) defined these in terms of four principal types namely – physical, geographic, cyber, logical interdependencies.

Physical interdependencies applies when there is a physical linkage between two or more systems, with one system relying on the output of the other system. A good example is the reliance of the station assets on the electricity generated by the distribution network operators (DNO) for lighting, electronics and customer information systems (CIS). The implication of disruption of service provided by the DNO is the corresponding effect it has on the station assets and eventual delay to passenger journeys and possibly, delay to trains.

Geographical interdependencies exist by virtue of different systems being in close spatial proximities within the same footprint and do not require any physical connections between the respective assets that make up the systems. An example is an overline bridge running above a railway line which supports a cable trough connected to its abutment and an overhead line electrification (OLE) return conductor cable underslung from the bridge deck. In the event of a failure to the bridge, both assets are in turn affected, not because they have any connection between each other, but by the mere fact they are co-located within the same hazard footprint.

Cyber interdependencies exist between two systems if they rely on the transfer of information transmitted through an information network. With the proliferation of computerised and digital systems, the respective systems that make up these networks are relying more on information transfer through different medium, for example, the Global System for Mobile Communications-Railway (GSM-R) which delivers digital communications between drivers and signallers on the rail network via Fixed Telecommunication Network (FTN/FTNx), Supervisory Control and Data Acquisition (SCADA) connections between traction substations and electrical controllers. These connections through electronic and digital informational links create cyber interdependencies across the respective systems.

Logical interdependencies refer to the interrelationship that links two systems without the need for a physical, cyber or geographical connection. In infrastructure systems, external influence, e.g., human decision making can play a more significant role in creating logical interdependency between systems. For example, on a railway network, government policy on toll charges for vehicles during days of high pollution in a city like Paris, may result in commuters switching to rail and public transport on those days and a surge in congestion in trains and busses. In this example, a logical interdependency exists between the environmental and transport systems as a result of government policy decision making rather than a physical, cyber or geographical interaction between the systems.

2.2 Approaches to interdependency modelling

Across the rail network, systems can have one or more of the types of interdependencies discussed above, resulting in complex interactions across the network. Due to these complexities, modelling methodologies have become a favourable method adopted across several research literatures for studying interdependencies of critical infrastructure networks (Pederson et al, 2006). These cut across multiple dimensions with the different modelling techniques varying in their degree of abstraction, intricacy of systems and complexity of interactions which often determine their choice of use for specific research types (Eusgeld & Kroger, 2008).

While there are several approaches for modelling complex infrastructure systems, four types with direct applicability to railway networks are discussed here and are based on the literature discussed in Ouyang (2014) namely – (i) empirical approaches (ii) input-output based approach (iii) agent-based approach and (iv) network based approach.

Empirical approaches to interdependency modelling involve analysing interdependencies according to historical data of hazard impact and expert opinions, identifying failure patterns to inform and quantify the interdependency metrics for

empirical based analysis. For example, on a railway network, the existence of historical empirical dataset of train delays attributed to several extreme weather-related hazard events on the network can be useful to uncover interdependency relationships under extreme events and help to analyse and identify frequent and significant failure patterns for the railway network. An example of this is the work by McDaniels et al, (2007; 2008a) and Chang et al, (2009) who proposed a database for quantifying an interdependency failure from societal impacts. This database was then applied to interdependency analysis of several typical events such as the August 2003 blackout in North America, hurricanes in Florida (McDaniels et al, 2007) and the 2008 Chinese Winter storm (Rong et al, 2010).

The **Input-output based approach** was developed by the Nobel Laureate Wassily Leontief in 1973 who proposed the input-output economic model (Leontief, 1986), a static demand-reduction economy model based on the technological relationships of production. This can be applied to interdependency modelling of infrastructure networks by interpreting the output as a risk of inoperability, defined as the inability of the system to perform as it is designed to. Therefore, for a given hazard caused by a shock to one or more other infrastructure system or sectors of the economy, the model estimates the resulting disruption measured by the infrastructure inoperability.

Agent based approaches – This method approaches interdependency modelling in complex systems by assuming the behaviour of the system as a whole emerges from the interactions of autonomous agents, each interacting with one another based on a set of rules which imitates the way a real counterpart of the same type would react. By modelling infrastructure systems in this way, it is possible to study the behaviour or impact on the network as a result of disruption or cascade of failure to one of its agents.

Network based approach to modelling involves representing infrastructure systems as a graph network of nodes and edges. Nodes are used to represent the physical properties of assets while edges model the relationships between nodes. If the network structure of

an infrastructure system is known, its topology can be represented by a network model and the impact of failure to the network modelled by severing edge link between nodes and/or removal of nodes to ascertain the overall impact on the network. Across research literature, network-based approaches have become popular for modelling rail networks. This approach, based on the principles of graph theory models physical assets as nodes, with edges used to represent the dependencies and interdependencies that exist across the respective asset systems (Setola et al, 2016). In coming up with a model and methodology that can correctly replicate the behaviour of rail networks, it is necessary to have a proper understanding of how its complex system-of-systems interactions effectuates rail journeys and the systemic response to failure scenarios. To tackle this challenge, a number of existing research studies (Pagani et al, 2019; Pant et al, 2016; Johansson et al, 2011) have developed research models and methodologies which have been applied to rail networks at different scales.

These different modelling techniques can vary in their degree of abstraction, intricacy of systems and complexity of interactions which often determines their choice of use for specific research types (Eusgeld & Kroger, 2008). For example, agent-based modelling which assesses the effect of autonomous rule-based agents is often used in scientific, economics and informatics research (Barton & Stamber, 2000; Panzieri et al, 2004; Eusgeld & Kroger, 2008). Also, Leontief's Input-Output modelling approach (Leontief, 1986) which analyses economic disruption effects on interdependent systems has been used in economic forecasting as well as in estimating damage effects across infrastructure systems (Haimes & Jiang, 2001; Haimes et al, 2005; Joost, 2006). Network based approach has been used for vulnerability analysis across interdependent railway (Pant et al, 2016) and energy (Thacker et al, 2014) sectors. Depending on the complexity of the system under consideration, it is possible to combine one or more of these approaches to modelling a single network. For example, a combination of a network-based and input-

output based approaches can be used for modelling the topology of an infrastructure network and modelling economic disruption to the network in a single modelling exercise.

2.3 Rail system modelling

Modelling methodologies have become a favourable means adopted across several research literatures for studying interdependencies of critical infrastructure networks (Pederson et al, 2006). These cut across multiple dimensions including those of time – continuous vs. discrete modelling of time (Ossimitz & Mrotzek, 2008; Özgün & Barlas, 2009) and modelling techniques which include Agent Based modelling (Eusgeld & Kroger, 2008), Input-Output modelling, Petri Nets, System Dynamics, High Level Architecture, Critical Path Method, Hierarchical Holographic Modelling, risk based models (Pederson et al, 2006; Eusgeld & Kroger, 2008, High Level Architecture for complex distributed systems on military software systems (Department of Defense, 1997).

Due to their complexities, modelling methodologies have been adopted for studying rail networks across research literature. While several modelling methods exist, a number of rail related studies (Ilalokhoin et al, 2021; Pant et al, 2016; Johansson and Hassel, 2010) have adopted the network-based approach. This involves modelling of physical assets as nodes and edges to replicate the topology of the network. Johansson and Hassel (2010) discussed the modelling of rail networks in two parts – the functional and the structural modelling. The structural model of the network involves representing the physical characteristics of technical systems as a graph network. Physical components like substations, bridges are represented as nodes and edges to replicate the network's topology. Functional modelling, on the other hand can be engineering-oriented and represents the modelling of the functionality of assets across all the respective systems.

An example is the modelling of the power distribution from a traction power grid to a substation to facilitate the movement of trains on the track network.

Creating a structural model of the rail network comprises three parts. First, the modelling of the track system on which trains run. Next, the rail assets on the network are modelled together with their interdependencies in separate layers, with all the nodes and edges in the network graph mapped to a cartesian coordinate system and assigned point coordinates (x, y) to specify their location in space. All the modelled asset layers can then be merged to form an integrated rail network model which represent the relationship that exists between assets and the track network. Trains are then simulated on the network model traversing the track nodes and edges according to the methodology described in Chapter 4 to replicate their journey across actual multi-track pathways.

When simulating train journeys on a network model, the Dijkstra's shortest path algorithm (Ortega-Arranz et al, 2014) is a useful tool for finding the shortest path between a start node (also called “source node”) to all other nodes in the network graph. This algorithm starts at the source node and analyses the graph to find the shortest path between this node and all other nodes in the network, keeping track of all the shortest distance from each node to the source node and updating this until it finds a shorter path. When this happens, the node is marked as “visited” and therefore added to the path. This process continues until all the nodes in the graph have been added to the path which culminates in a path that connects the source node to all the nodes by following the shortest path possible to reach each node. Failure to the rail network is modelled as the removal of the directly disrupted node and/or edge from the network model which in turn results in the removal of all the affected network nodes and edges and trains across the network. The shortest path algorithm is therefore useful in rail systems modelling for finding alternative pathways following failure to a specific track node in the network which allows for the selection of an alternative path for rerouting a disrupted train through the network.

When passenger usage data is available, this can be integrated into the network model to allow for the estimation of the total passengers disrupted following the failure of an asset.

Other methods and models exist in practice which could be adapted to rail operational planning and modelling timetable and journey characteristics. These can broadly be categorised into aggregate models like the Network Evaluation MOdel (NEMO) which uses statistical data to model the operation of the rail network (Cui & Martin, 2011), and microsimulation models like Railsys, which simulate the actual operational behaviours of the rolling stock, timetable and infrastructure (Bendfeldt et al, 2000). Though in principle they could be used for simulation of physical network disruptions, in practice they are computationally expensive and require extensive recoding to represent the rerouting and timetable disruptions that occur during network disruption and they do not include disruptions to passengers.

A complete modelling of rail networks therefore needs to integrate the modelling of the complete system-of-systems architecture of the infrastructure network with the dynamic modelling of train movement according to established timetables. This integrated model can then allow for the quantification of disruptive effects from threats to the network.

3 Vulnerability and resilience of railway networks

3.1 Vulnerability

There is a lack of commonly accepted definition of transport system vulnerability (Mattsson and Jenelius, 2015). This notwithstanding, the definition by Berdica (2002) is often cited across several research literatures and it defines vulnerability in terms of susceptibility to incidents that can result in the reduction in network serviceability. While Berdica's definition relates specifically to road system vulnerability, this definition can be applied to other transportation modes. Similarly, Luathep et al (2011) discussed vulnerability analysis in terms of its principal focus in identifying the critical components of the network that result in the most adverse effect. All these definitions point to a central focus which is the emphasis placed on impacts on a system as a result of an initiating disruptive hazard event.

Vulnerability is defined here in terms of the susceptibility to loss or damage to a system when exposed to a hazard. Vulnerability analysis encompasses the estimation of the extent of the negative impacts from a hazard event. For large networks, this is the resulting systemic impacts of the disruption across the entire network. While the literature on vulnerability analysis across interdependent infrastructure networks is still growing, its application to rail networks is still in relatively small numbers. Some notable contributions in this area include the work by Xing et al (2017), Pant et al (2016), Johansson et al (2011), who have focussed on vulnerability assessment methodologies of rail networks with application to the networks in China, Great Britain and Sweden respectively.

In practical terms, rail networks, by the nature of their configuration, are vulnerable to a range of hazards including weather related natural hazards such as floods, wind, storms, heat and man-made hazards including malicious attacks, operational incidents. In recent years, these events have become more frequent, from targeted attacks at Lubyanka metro

station and Park Kultury metro station of Russia in 2010 which resulted in the death of about 40 people to the April 2017 St Petersburg metro bombing and the September 2017 Parsons Green London Underground metro bomb attack. Also, there is increased risk from extreme weather events and climate change with storm surges affecting sea defences (Armstrong, 2017; Network Rail, 2016) resulting in flooding of lineside assets, earthworks washout, damage to lineside trees and vegetation blown onto track leading to obstruction and disruption to train services.

A vulnerability assessment methodology for rail network modelling formulated by Pant et al (2016) is discussed here and it represents the operational functionality of an asset system as a state function, r_i which takes the binary values {0,1} with $r_i = 0$ representing complete loss of asset functionality and $r_i = 1$ representing an asset being in operational condition. In a railway network comprising a number of assets, there are therefore 2^a possible network states where $2^a - 1$ represents the failure state. In measuring the vulnerability of the network, it is possible to collate all the failure states arising from the failure of the asset, resulting in negative consequence in terms of asset failure and subsequent service disruption to trains. Network vulnerability can therefore be expressed in terms of a two-dimensional metric which represents (1) physical asset loss and (2) functional service loss and resulting disruptive consequences.

For a network state of operation given by the vector $\mathbf{r}^j = r_1^j, \ldots r_a^j$ for which r_i^j is either 0 or 1, the extent of physical asset loss on the network can be expressed in terms of

$$\Re(\mathbf{r}^j) = 1 - \frac{\sum_{i=1}^{a} r_i^j}{a} \tag{3.1}$$

where $\Re(\mathbf{r}^j)$ is a measure of the rail network's physical integrity following asset loss from a hazard event.

The magnitude of the functional loss of service disruption is measured as a proportion of the service levels pre and post asset failure. On train networks, this service level can be

quantified in terms of the performance reductions arising from delay to trains or the number of passengers disrupted as a ratio of the total numbers in a similar undisrupted day. This is represented mathematically as

$$\overline{\mathrm{R}}(\mathbf{r}^j) = \frac{s(\mathbf{r}^j)}{s} \tag{3.2}$$

where s refers to the pre-disruption service levels, $s(\mathbf{r}^j)$ refers to the post disruption service levels.

Overall network vulnerability metric, $V(\mathbf{r}^j)$ is the combined total of the physical loss to asset and the reduction in service functionality given by

$$V(\mathbf{r}^j) = 1 - \frac{\sum_{i=1}^{a} r_i^j}{a}, \frac{s(\mathbf{r}^j)}{s} \tag{3.3}$$

The limitation of the vulnerability assessment framework discussed above is its binary evaluation of failure states which in reality can be overly simplistic. This is because it is possible for rail networks to function in degraded modes. For example, a partial failure of an embankment slope close to a railway line may result in partial operability of trains network with line speed restrictions imposed along the affected route on the networks. While this may result in train delays and disruption across the network, it is not necessarily a complete failure state and the network can continue to function in this degraded state until full services are restored. In Chapter 4, these different failure modes are discussed and the theory behind their modelling and application to rail network performance are demonstrated for a practical rail network.

3.2 Resilience

Mathematically, resilience can be viewed as the opposite of vulnerability. The term resilience originates from the Latin words – *resilire, resilio* meaning *bounce,* and refers to the ability to cope with, and/or bounce back from mishaps or unanticipated disruptions. Its origin can be traced back to the field of ecology where Holling (1973) defined it as *"a*

measure of the persistence of systems and of their ability to absorb change and disturbance and still maintain the same relationships between populations or state variables". Its use is now prominent across different sectors like engineering seismic studies (Cimellaro et al, 2006), health (Alameddine et al, 2019), urban studies (Simonovic & Peck, 2013) to name a few. The increasing threat from natural and man-made hazards, with events such as Hurricane Katrina in 2005, the World Trade Centre attack (9/11) in 2001, several extreme weather and climate change events across many continents of the world have brought the attention of governments and decision makers to the need to withstand, recover from and maintain a level of service when subject to service disruptions. O'Rourke (2007) notes that these events have coincided with a notable shift in emphasis from critical infrastructure protection to that of resilience. While there is often a challenge in coming up with a universal definition for resilience (Kong et al, 2018), a widely accepted definition is that by Bruneau et al (2003) who described resilience as a function of system performance and adaptive capacity encompassing four dimensions – robustness, redundancy, resourcefulness, and rapidity

The robustness of a system refers to its inherent strength or resistance to withstand loss from a given threat without severe loss of function (O'Rourke, 2007). Redundancy refers to inherent system properties which allows a system to substitute and mobilise alternative pathways to ensure continuity or some level of service during disruptions (Kong et al, 2018). Robustness and redundancy dimensions go hand in hand, and their measure is a derivative of ex-ante resilience investment. Resourcefulness describes systemic performance following ex-post interventions and restoration measures. It refers to its capacity to identify and mobilise the necessary resources for restoration of service when disrupted (Bruneau et al, 2003). The time taken to restore service following disruptions is a measure of the rapidity of the system.

The work by Bruneau et al (2003) is often acknowledged as the pioneering framework on the concept of *Resilience Loss* also known as the *Resilience Triangle*, where they quantified the seismic resilience of communities due to earthquake events by measuring system performance as a point in a multidimensional space of performance measures. This approach to resilience assessment focussed on developing resilience metrics for the infrastructure system based on a two-system performance curve for disruption and restoration and checked against the expected performance curves, with the resilience of the system quantified as the area between both curves. In doing so they categorised a resilient system in a whole lifecycle context, as the total of the ability to reduce the failure probabilities (ex-ante), absorb the shock when it occurs (during the event) to ensure a reduced consequence, and recover quickly (ex post) following the shock. This illustration of the Resilience Triangle is expressed mathematically as:

$$R = \int_{t0}^{t1}[100 - Q(t)]dt \tag{3.4}$$

Where R = loss of system resilience & Q = system performance.

Chang & Shinozuka (2004) expanded on Bruneau et al's (2003) work to propose a probabilistic approach for measuring disaster resilience following earthquakes which led to the formulation of loss estimation models and methodologies to support decision-making for enhancing community resilience. Their research framework compared the resilience of a system with predefined system performance standards under four interrelated dimensions - technical, organisational, social, and economic aspects of community resilience.

Another interesting approach to resilience assessment was presented by McDaniels et al (2008) who used decision flow diagrams to study the robustness and rapidity properties of seismic events. This involved the use of qualitative methods involving interviews, interactions with managers and operators of infrastructure facilities to develop methods

which could be used for future planning. But this method relies on the accuracy of the information obtained from different human sources which can be subjective and requires a lot of effort to gather all the relevant data to produce the methodology.

Resilience in rail networks can take several forms. For example, this can involve the restoration of train services during perturbation by rerouting services to restore some form of operation. Also, several key assets like those which supply traction power to the rail network are designed to work in a degraded state based on the N-1 security criterion such that *"any probable single event leading to a loss of a power system element should not endanger the security of the interconnected operation, that is, trigger a cascade of trippings or the loss of a significant amount of consumption. The remaining network elements, which are still in operation should be able to accommodate the additional load or change of generation, voltage deviation or transient stability regime caused by the initial failure"* (IRGC, 2006). These systems allow for quick restoration of service through mobilising backups and alternative pathways to ensure continuity or some level of service during disruptions.

Research on resilience assessment of rail networks is growing, with a number of studies carried out in recent years. For example, the research by Tang et al (2021) investigated the resilience of rail mass transit systems and the effectiveness of bus-bridging services in enhancing network robustness with case studies of Singapore and Chongqing. Also, in their study of High Speed Rail networks, Li et al (2021) focussed on the key service feature of passenger flow and travel time as a key indicator of the network's functionality. Rungskunroch et al (2022) analysed the uncertainties of rail accidents and its impact on risk and resilience of the rail infrastructure to inform policy decisions on safety across the network while Neves et al (2021) presented a network vulnerability analysis for the Dutch rail network due to winter weather. Studies by Pagani et al., (2019), Adjetey-Bakun et al., (2016), Pant et al., (2016) have also contributed to research in this area in their

quantification of rail network disruptions in terms of passenger journey losses over a given period of time. While these studies have made substantive contributions to research knowledge of the resilience of rail networks, they are limited in their approach to analysing the dynamic knock-on effect of train disruptions on timetabling, train and passenger delays and how these propagate across the interdependent network. Also, these existing studies are limited in their approach to the study of the impact of system-of-systems interdependencies on the resilience of rail networks and their practical application to real-word networks, with a dearth in research literature of robust methodologies and models for resilience assessment of large, complex rail networks at regional and national scale (RSSB, 2016). While some previous studies have considered railway dependencies on electricity and telecoms systems, these were either represented in a notational way as networks with limited coverage (Adjetey-Bakun et al., 2016), and mostly as point assets (Pant et al., 2016), or as simplified networks that ignored several assets types within their systems (Johansson et al., 2011). In Chapter 5, a detailed approach to resilience assessment is presented for rail networks with application to practical case studies.

3.3 Climate change and extreme weather risks and adaptation on rail networks

A lot has been said and written about climate change and extreme weather changes in recent years. Today, it is widely acknowledged that the warming of the earth's climate system is unequivocal as evident from observed records over many years (IPCC, 2021) with projections of faster warming with the potential of crossing the global warming level of 1.5°C in the next decades if there is no action for a rapid and large-scale reduction in greenhouse gas emissions. The effect of climate change is widespread and includes sea level rises, warmer temperatures, and higher precipitation. There is already clear evidence of this happening with numerous flood events, extreme heat and coastal surges recorded more frequently across the world recently. For example, in the summer of 2021, Pacific

northwest areas of the U.S. and Canada experienced temperatures far above 40°C, levels that have never previously been observed, leading to deaths and hospitalisation (Philip et al, 2021). Similarly, across Europe, there were numerous extreme heat events with deadly wildfires across parts of Greece and Turkey (CNN, 2021). In the United Kingdom, the Met Office issued its first ever extreme weather heat warning in July 2021.

Rail networks, by their nature, can be significantly exposed to the impacts of climate change and extreme weather events. For example, an increase in the average design temperature of track assets can result in the change of their mechanical properties with the potential for malfunctioning and complete asset failure, risk of track buckling and emergency speed restrictions (ESRs) leading to disruptions and train delays. Across the UK, most railway assets show increased incident and failure rates when the temperature is above 26°C and increased track buckling incidents are often associated with temperatures over 30°C (Network Rail, 2014; 2015). Recent summers have seen continued high temperatures with significant consequences. For example, during the short-duration heatwave of 30th June – 1st July 2015 where a temperature of 37.5°C was recorded (at Heathrow Airport), there was a total of about 220,000 delay minutes resulting in about £16 million of economic loss to the national economy (Ferranti et al, 2018). However, despite this consistent increased in average temperature levels, the design standards for stress free temperature (SFT) in the UK remain unchanged for track assets with the potential for their continued design to stress levels which do not reflect the changing future projected risks. Other impacts of increased temperatures on rail networks include the expansion of swing bridges, overhead line wire sag and overheating of electrical equipment, passenger discomfort and heat stress on workers.

Increased precipitation due to climate change introduces the risk of flooding with surface water flooding from direct accumulation, river flooding because of excess runoff and riverbank bursts and ground water flowing as a result of increase in groundwater levels

(RSSB, 2016). This can result in earthwork failure, bridge scouring and flooding of track assets including electronic and track circuit failure which affects train reliability. Similarly, coastal and storm surge impact coastal assets, with erosion of earthworks, structures, tracks, and damage to sea walls. An example of this was the collapse to the sea walls at Dawlish and Dover in 2014 and 2015 respectively (Armstrong et al, 2017; Network Rail, 2016).

Considering the projected impact of climate change and extreme weather events on the railway network (IPCC, 2021), there is therefore a growing need for adaptation measures to mitigate against these risks. Climate change adaptation need to take a holistic approach that includes organisational governance, review of technical standards and specifications for critical assets, asset maintenance framework and economic investment for the formulation and sustenance of a long-term adaptation strategy. It is important to assess the level of intervention needed for climate change adaptation considering the risk and benefit of such interventions to the network. A useful toolkit for practitioners to aid the designing of climate change adaptation initiatives was developed by the United National Development Programme (UNDP, 2010). This includes six steps namely: (i) defining the problem, (ii) identifying the cause of the climate change induced problem, (iii) identifying and articulating the normative response and preferred solution to addressing the underlying problem, (iv) identifying key barriers to implementing preferred solutions, (v) designing project responses to overcome key barriers and (vi) reviewing the first five steps and completing checklist to ensure due diligence and effective implementation.

3.4 Quantifying impact of disruption on railway networks

The disruptive impact of a hazard event on systemic performance of the rail network can be quantified by finding the resulting direct and indirect damages. Direct damages refer to the immediate impact on asset systems which can be a loss of functionality or complete failure. Indirect damages refer to the indirect impacts from the directly failed assets. An

example is the train delays and disruption to passengers accrued following a damage to a substation asset.

3.4.1 Quantifying direct damages using asset performance fragility functions

At asset level, fragility curves can be used to estimate the probability of asset damage as a function of the hazard intensity. Fragility curves are essential for quantitatively assessing the physical vulnerability of an infrastructure asset and representing the likelihood of asset failure as a function of a given hazard intensity, z. The development of a fragility function is described by a lognormal probability distribution such that the loading condition associated with a specific asset failure is given as:

$$\Pr(s = 0|Z \geq z) = \Phi\left(\frac{1}{\beta}.\ln\left(\frac{z}{\theta}\right)\right) \quad (3.5)$$

where $\Pr(s = 0|Z \geq z)$ represents the probability that, for a hazard event, $Z \geq z$ will result in the failure of a railway asset; $\Phi(\,)$ is the standard normal cumulative distribution function, CDF; θ is the median threshold value of the fragility function, i.e., Z with the 50% probability of causing failure; β is the dispersion parameter obtained by finding the standard deviation of $\ln Z$. From the equation above, it can be deduced that it is possible to develop the fragility function for an asset by the estimation of just two parameters - β and θ. This simplicity makes the lognormal distribution a popular choice, with precedent of use in a number of research studies (Eads et al. 2013; Ghafory-Ashtiany et al. 2010; Bradley and Dhakal 2008; Porter et al. 2007; Ibarra & Krawinkler 2005). Several methods exist for estimating the fragility curve parameter data, θ and β, among this is the maximum likelihood estimation method described by the equation below which has precedence of use in rail and other transport related research studies as an appropriate fragility curve fitting technique for observed data (Anelli, 2020; Lamb et al, 2019).

If in a total of w hazard events there will be a total of g events that caused failure for certain hazard intensity, z, less than z_{max}, an estimate of the fragility function parameters can be obtained by maximising the logarithm of the likelihood function as follows:

$$\{\theta, \beta\} = \underset{\theta,\beta}{arg\,max} \sum_{i=1}^{m} \left\{ \ln \phi \left\{ \frac{\ln(z_i/\theta)}{\beta} \right\} \right\} + (w - g) \ln \left(1 - \Phi \left(\frac{\ln(z_{max}/\theta)}{\beta} \right) \right) \quad (3.6)$$

Where ϕ ( ) denotes the standard normal distribution PDF.

When an empirical dataset of observable rail asset damages from known intensities are available, the fragility function parameters can be quickly calculated using a simple software code supplement for analytical fragility function fitting (Baker et al, 2015).

3.4.2 Quantifying indirect damages using metrics of train and passenger delay minutes

The indirect impact on the rail network can be measured by metrics which reflect train punctuality and reliability. Punctuality is defined as a predefined service arriving, departing, or passing a predefined point at a predefined time (Rudnicki, 1997). The consistency of punctuality defines service reliability. Across most countries in the world, train punctuality is considered the most important determinant of railway service quality (NEA, 2003) and is measured based on the time of arrival of a train compared with the times published in the rail timetable, depending on whether they are local, Inter City or freight trains. In Europe, this ranges between 1 – 30 minutes. For example, in Great Britain, until April 2019, trains were said to be *"on time"* if they arrived at their destinations within 5 minutes of published time for trains services within London and regional services, and 10 minutes for long distance services. However, this has since been changed to record train punctuality by the minute, as this provides a more transparent indication of train delays.

The systemic performance measure used in Great Britain and adopted in this thesis is the metrics of *Delay Minutes* and *Passenger Delay minutes*. Delay Minutes are a set of regulatory metrics for measuring the punctuality of trains which is measured with reference to the time lost between two recording points or late departure from a recording point based on the actual times measured against the planned times from the rail timetable (DAB, 2019). These recording points, also known as Timing Point Locations (TIPLOC) are identified junction points and stations across the train path which correspond with the train schedule information on the rail working timetable. Passenger Delay Minutes on the other hand refers to the total train delays attributed to passengers using the train network. For each disrupted train, if the number of passengers on each train is known, it is possible to attribute the train delay minutes to passengers on the train to ascertain the passenger delay minutes.

However, there remains the challenge of estimating the number of disrupted passengers for each train journey. Generally, trip distribution models comprise two types depending on the data type used. These are (1) models based on aggregate data which use ticket sales information (2) models based on surveys which used data disaggregated at the level of interviews with system users. Research studies by Cordera et al (2018); Brzeziński et al (2018); Pant et al (2016); Wardman (1998; 2006) have developed methodologies for trip distribution. Cordera et al (2018) utilised boarding and alighting data of passengers at stations using ticket sales data for a regional railway line in Spain. Wardman (2006) proposed a trip distribution model using time series data for the United Kingdom in the 1990s, while more recently, Pant et al (2016) developed a model for rail trip assignment using a limited datasets of passenger journeys from the Office of Rail and Road (ORR) in Great Britain. Ghaemi et al (2018) also utilised daily passenger journey information between stations based on smart card transactions to develop a rail trip model on the Netherlands rail network. It is however important to note that the methodologies

discussed above for estimating trip distribution have their respective advantages and disadvantages. For example, while models which are based on ticket sales information may provide very useful information of actual passenger origin and destination, they may often be unable to provide detailed information about the actual journey pathway that a particular passenger takes as there may be multiple journey routes from an origin to a final destination. A practical example is the case of passenger journeys within the Greater London region of Great Britain which can often include travel between the mainline railway, metro and bus networks using the same ticket type. Also, the models which rely on surveys, although they may be able to capture actual train journey routes, are reliant on honesty of the responses and may be subject to human bias. A proper trip distribution modelling exercise should therefore take these drawbacks into consideration when attempting to correctly model passenger trip distribution noting that a combination of two or more approaches may be useful to provide a more accurate estimate.

In chapter 4, a mathematical formulation and modelling of the systemic performance metrics of train and passenger delay minutes is presented in elaborate detail culminating in the development of a model which can be used to estimate delays based on disrupted journeys from a real-world train timetable. This model is demonstrated for a number of flood hazard case study scenarios of the rail network in Great Britain.

4 A multi-track rail model for estimating journey impacts from extreme weather events: a case study of Great Britain's rail network

Abstract

Models that have been developed for analysis of the impacts of failure in railway networks have tended to make simplifying assumptions about train paths and delays and have not always accounted for the existence of multiple tracks on a route. In a step towards more realistic, yet computationally tractable analysis of the disruption of rail services, we present a multi-track rail model that simulates train journeys based on actual pathways and realistic routing decisions and allows for estimation of train delays, disruptions to passengers' journeys and spatial propagation of disruptions through the rail network. We use this model to analyse examples of weather-related disruptions on Great Britain's railway. Our model predicts delays with an average error of 7-8% for the windstorm and flood case studies considered. This new model should therefore enhance risk analysis for large rail networks, enabling the prioritising of interventions that could enhance network resilience.

4.1 Introduction

Rail networks are vulnerable to disruptions from natural hazards, including landslips on embankments and cuttings, flooding, coastal storm surges, bridge scour, heatwaves and strong wind. These failures can cause widespread disruptions to train operations far across the network, with significant economic consequences. For example, in 2014, storm surges resulted in severe damage to the Dawlish sea wall on the south coast of Devon in South West England leading to the loss of about 7,500 train services over a 60 day period and an overall economic loss of up to £1.2 billion excluding the cost of repair to the infrastructure (DMF, 2015). Also, in December 2015, severe rainfall resulted in widespread flooding, with sections of the West Coast Mainline of the national rail

network in Great Britain submerged under 2 metres of floodwater leading to several days of rail disruptions between London and Scotland (New Civil Engineer, 2015).

Many previous studies of railway systems have adopted network-based modelling approaches which have a long history of use in transportation research studies. Examples of these include the early research work in this area that presented a graph theoretic model of waterborne transport in Russian rivers in the Middle Ages (Pitts, 1965), to more recent research studies (Sen et al, 2003; Johansson et al, 2011; Pant et al, 2016; Pagani et al, 2019) that have all adopted this modelling technique for analysis of rail networks. However, previous studies have adopted single-track modelling approaches for representing rail routes, which is limited in the realism with which train disruptions can be represented. This limitation leads to inaccurate representation of train journeys along their actual route when this involves a multi-track network in real-world scenarios, with a direct effect on the correct estimation of the disruptive consequences of hazard events in terms of train delays, passengers disrupted and spatial representation of these impacts. These simplifications inherent in single track network models are understandable because access to complete multi-track data that show different route choices between the same pair of stations based on track speeds and operational rules may be limited due to commercial and security concerns. Moreover, once such data have been obtained, it is an extremely laborious exercise to correctly replicate the connectivity that exists across every part of a complex network.

An alternative approach would be to adapt models developed for rail operational planning, timetable and journey management. These can broadly be categorised into aggregate models like the Network Evaluation MOdel (NEMO) which uses statistical data to model the operation of the rail network (Cui & Martin, 2011), and microsimulation models like Railsys, which simulate the actual operational behaviours of the rolling stock, timetable and infrastructure (Bendfeldt et al, 2000). Though in principle they could be

used for simulation of physical network disruptions, in practice they are computationally expensive and require extensive recoding to represent the rerouting and timetable disruptions that occur during network disruption and they do not include disruptions to passengers.

To address these challenges and limitations, this research presents a novel methodology for multi-track modelling, timetable simulation and journey disruption modelling of rail networks at a national scale and demonstrates its use for the estimation of train delay and characterisation of passenger disruptions on the rail network in Great Britain. The main contributions of this paper include – (1) presenting a methodology for building a multi-track rail model that correctly simulates train journeys based on their actual routes on a multi-track network, as against frequently adopted single track models for rail research studies (Sen et al, 2003; Johansson et al, 2011; Pant et al, 2016; Pagani et al, 2019); (2) building a methodology and model, based on real world operational rules, that can be used to correctly estimate the disruptive impacts of weather-related hazard events in terms of train delays and passenger numbers; (3) using the model for spatial representation of disruption impacts on the network. We test the validity and applicability of our model by simulating real-life disruptions based on a number of case studies of observed events and compare the findings with the results from our network model.

4.2 Quantifying disruption on the rail network of Great Britain

Disruption to services on rail networks gives rise to delays and in some cases results in the complete loss of services. The causes of these delays can broadly be grouped into three primary reasons namely (1) operator causes arising from train faults and crew shortages; (2) infrastructure causes e.g. track and signalling faults; and (3) external causes e.g. suicide, vandalism and extreme weather events (Preston et al, 2009; Network Rail, 2017).

For this study we categorise train delays according to the rail industry standard classification for delay attribution in Great Britain, which are *direct delays, reactionary delays* and *reliability events*. A *direct delay* is defined as the delay to a train service which results from a causal incident that directly delays the train concerned, while *reactionary delays* are indirect delays occasioned by a prior delay to the same or any other train. A *reliability event*, on the other hand, refers to full or partial train cancellation, a train diversion from its booked route or failure to call at a scheduled timetable stop, including when a train runs through a station it is booked to call without stopping (DAB, 2019).

In Great Britain, Delay Minutes are a set of regulatory metrics for measuring the punctuality of trains and refer to the time lost either between two recording points or late departure from a recoding point based on the actual times measured against the planned times from the Working Timetable (DAB, 2019). Delay Minutes are closely linked with the rail Public Performance Measure (PPM) which until April 2019 was the industry standard metric for rail performance. PPM refers to the percentage number of trains arriving at their terminating station '*on time*' compared with the total number of trains planned. Prior to April 2019, a train service was defined as being '*on time*' if it arrived at its scheduled destination within five minutes of the planned arrival times for London and southeast services, or 10 minutes for long distance services. But this can be misleading as it fails to measure actual train arrival times to the minute. Also, it does not reflect the period of the day during which the journey takes place as it gives the same weighting to services irrespective of whether they run during peak or off-peak periods. Furthermore, when disruptions happen, because planned train services are confirmed between Network Rail (who own and operate most of Britain's mainline rail infrastructure) and the Train operators at 22.00hrs the day before (ORR, 2019), when a potential disruption event is envisaged, an amended timetable with fewer train services and times can be implemented prior to the event and the PPM figures for that day measured against this new plan. This

could result in higher PPM values than if they were based on the normal timetable which can be misleading. Since April 2019 Network Rail has adopted an on-time, to-the-minute recording of arrivals of some train services which reflects a more accurate measure of train punctuality.

When a hazard event occurs, this can result in either a Section Loss or Line Speed Restriction (LSR), which leads to delays, cancellations and/or rerouting of train services. Delays to primary routes if not resolved quickly can result in knock-on effects or reactionary delays to other services across the network with the potential for these to continue long after the original disruption event has been resolved. This can be particularly challenging for busy networks as contingency plans need to be triggered very quickly to regularise services, which can take the form of (1) cancelling trains so that there is space on track for delayed trains to complete their journeys quickly; (2) missing stops to make up time or (3) cancellation of all trains in the affected areas for an hour to get trains running on time again (Network Rail, 2017).

On the rail network in Great Britain, Network Rail uses a system called TRUST (Train Running System TOPS [Total Operation Processing System]) to record the details of train operational data and scheduled train times, supporting the logging of delays and its associated attribution process. The TRUST system comprises four essential parts (DAB, 2019):

- The Train Plan
- Record of the times at which a train arrives, departs, or passes specific locations
- The cause of train delay and reliability event
- Incidents that can be attributed to the ‘responsible’ organisation and to which the train delays and reliability events can be allocated

Delay minutes are calculated on TRUST by recording the 'Lateness' of a train at a particular point calculated as the difference in time between which a train actually arrives at, departs or passes a *recording point* with that shown in the Train Timetable. Reliability events due to full or partial cancellations are also recorded in TRUST with trains that are diverted to an alternative destination recorded as diversions. Where a train fails to call at all its scheduled location, this is recorded in TRUST as a *failure to stop* report.

When a *reliability event* occurs, a cancellation penalty is recorded and converted to delay minutes. A cancellation penalty is issued by Service Group, which means that for certain kinds of delay, multiple Service Groups can be affected by the same incident. Table 4.1 shows a truncated list of cancellation penalty minutes for *reliability events* by Service Groups across the respective regions in Great Britain. The cancellation minutes for a particular Service Group reflect the average time in minutes that a passenger has to wait to board the same or alternative train to their destination following a cancellation of a train service. Therefore, at stations where there are more frequent trains going to a specific destination, the minutes attributed to a specific cancellation event will normally be smaller compared with areas with less frequent trains.

Service Group Type	Service Group Name	Cancellation Minutes
All Trains	North Trans Pennine	46
All Trains	South Trans Pennine	87
All Trains	Preston - Scotland	110
Off-Peak	Southend & Southminster	30
Peak	Southend & Southminster	19
Off-Peak	Great Eastern Outers	32
Off-Peak	Anglia Inter City	45
Peak	Anglia Inter City	29

Table 4.1 A truncated list, showing examples of cancellation Penalty minutes for trains across different parts of Britain

4.3 Methodology

4.3.1 Building the multi-track model

In Figure 4.1, we present an illustration of the process adopted in building the multi-track model and simulating rail journeys according to their real-world track pathways.

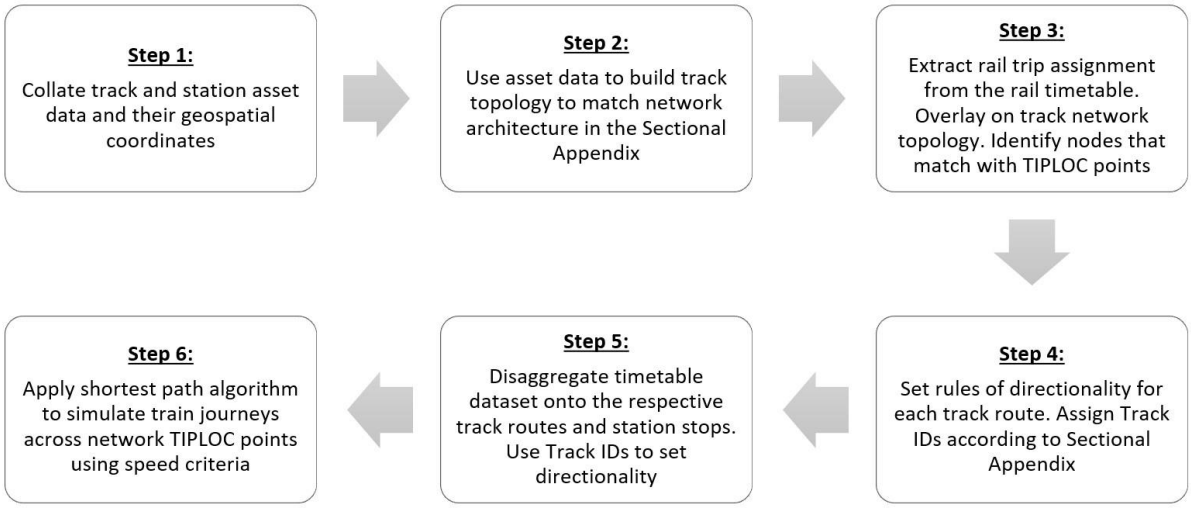

Figure 4.1 An Illustration of the methodology for model development and rail journey simulation

First, we obtain the track geospatial asset dataset from Network Rail's RINM (Rail Infrastructure Network Model) database, which is a repository for asset geospatial data for the entire rail network in Great Britain (RailEngineer, 2015). This includes a total of 2,567 rail stations, 49,787 track sections and 45,228 rail nodes and junction assets also known as switches & crossings (S&C), which we use to build the topology of the track network. To do this, we start by disaggregating the entire track network into a reduced abstract structure of nodes and edges which captures basic information of its parts and serve as a means of representing connections or interactions across its several asset groups (Newman, 2010). We build the topology of the network to represent its actual track network architecture as published in the National Electronic Sectional Appendix, also known as *Sectional Appendix* (Network Rail, 2020). The *Sectional Appendix* is Network Rail's official document that contains detailed information of the railway's capability, its track network and their geographical and functional characteristics. It is updated regularly

through Weekly Operation Notices (WON) to capture track renewals and enhancement upgrades to the rail network. The functional characteristics from the *Section Appendix* that we identify and assign to the nodes and edges include the: (1) Track ID - which gives the direction of travel, delineated into *'Up'* and *'Down'* lines depending on their direction of travel from a major city; (2) speed – which allows us to segregate tracks into '*Fast'* or '*Slow'* lines; (3) junction details; (4) stations and other assets along the route. By doing this, we accurately represent the topology of all the 21,802 miles of track network nationally correct to its as-built operational status as of July 2019 when this modelling exercise was carried out. A map of this shown in Figure 4.2.

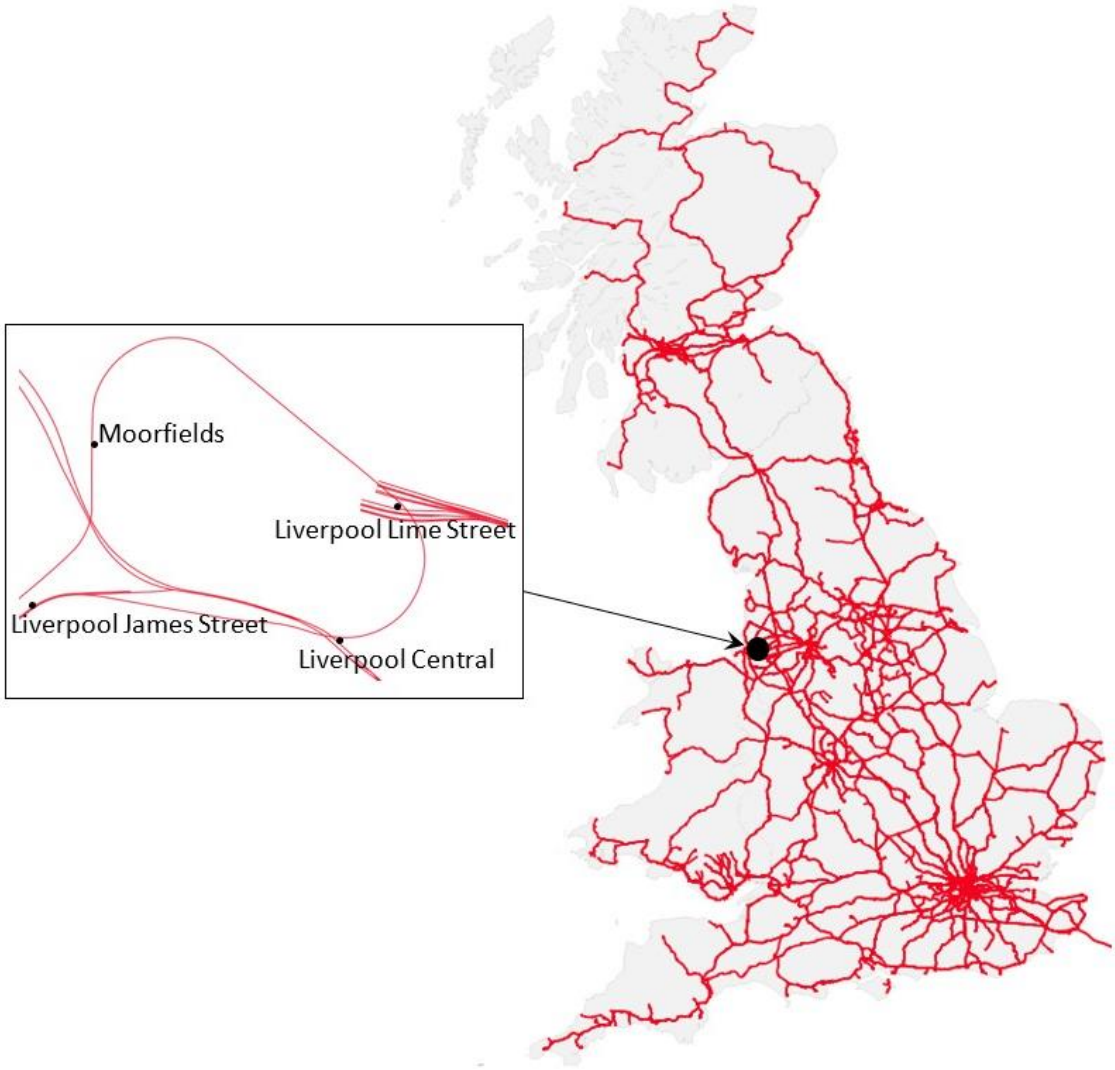

Figure 4.2 Map representation of a multi-track model for Great Britain's rail network

4.3.2 Rail timetable simulation & journey path allocation

Once the network topology with operational attributes is built, the next step is to correctly simulate actual passenger train journeys on the network model. In Great Britain, Network Rail and the Association of Train Operating Companies (ATOC) are responsible for the bi-yearly May and December passenger train timetable. The May 2019 train timetable dataset is used for this research and is obtained from the Rail Delivery Group (RDG).

To correctly simulate the train journeys on the train network model, we start by extracting the rail trip assignment information from the timetable dataset resulting in a 145,334 x 16 journey matrix, with the rows representing the individual train journeys and the columns representing the journey characteristics. A truncated snapshot of this output file is shown in Table 4.2. The 145,334 extracted journeys from the timetable dataset comprise mainline rail passenger services only and exclude all regional tram services, metros, London Underground services and freight trains.

Journey details													
Start date (dd/mm/yy)	End date (dd/mm/yy)	Max line Speed (mph)	Train _path	Start _time	Departure_ time	Train _id	S	M	T	W	T	F	S
19/12/18	17/05/19	125	['PLYMTH', 'TOTNES',..]	['1325', '1349',..]	['1325', '1351',..]	C10865	0	1	1	1	0	1	0
19/12/18	17/05/19	100	['BRSTLTM', 'BRSTPWY',..]	['0520', '0529',..]	['0520', '0538',..]	C10866	0	0	1	1	1	1	0
19/12/18	17/05/19	125	['RDNGSTN', 'OXFD',..]	['1345', '1411',..]	['1345', '1413',..]	C10867	0	1	1	1	1	1	0
19/12/18	17/05/19	125	['PLYMTH', 'LISKARD',..]	['0628', '0649',..]	['0628', '0651',..]	C10868	0	0	1	1	1	1	0
19/12/18	17/05/19	125	['EDINBUR', 'DUNBAR',..]	['1307', '1330',..]	['1307', '1332',..]	C10903	0	1	1	1	1	0	0
19/12/18	16/05/19	125	['GLGC', 'MOTHRWL',..]	['0900', '0914',..]	['0900', '0915',..]	C10904	0	1	1	1	1	0	0
19/12/18	16/05/19	100	['NTNG', 'BESTON',..]	['1907', '1912',..]	['1907', '1912',..]	C10905	0	1	1	1	1	0	0
19/12/18	16/05/19	125	['MNCRPIC', 'CREWE',..]	['0511', '0542',..]	['0511', '0547',..]	C10906	0	1	1	1	1	0	0

Table 4.2 An extract of the journey trip assignment data from the rail timetable – (train_path, start_time & departure_time columns are truncated for brevity)

For each journey type denoted by a unique *train_id*, the train service calls at all its scheduled intermediate stations stops as defined in the train path and at the specified times defined by the start time and departure time columns of Table 4.2. The *train path* (Train_path column in Table 4.2) refers to Timing Point Locations (TIPLOC) which generally corresponds to known stations and important junction points along the network. TIPLOCs are populated with train schedule information, which comprises train arrival and departure times through particular sections of the track network and matches the information published in the Working Timetable (WTT). The *train_path* lists all the TIPLOC points for each journey and this column is truncated in Table 4.2 for brevity. We put together a geospatial representation of all the railway TIPLOCs nationally and overlay these on the network model such that the coordinates of the TIPLOC matches with the corresponding nodes on the network model to facilitate an accurate simulation of train journeys through their allocated pathways.

When carrying out the journey path simulation, it is important for train journeys to correctly traverse the right nodes and edges in accordance with the established rules of the route set out in the *Sectional Appendix*. Our approach to this is four-fold. The first step is to ensure that the right TIPLOC codes are allocated to the originating, intermediate and destination junction points and stations for each train service and that their geospatial information match the corresponding nodes on the network model. Secondly, we set rules for directionality for all the edges in accordance with the *Sectional Appendix*. This means that edges are identified as *Up* or *Down* rail lines depending on their direction towards or away from a major city respectively. Next, using the train speed from Table 4.2, the unique Track ID from the *Sectional Appendix* and the train timetabling TIPLOC dataset, we ascertain if the train travels on the Fast (Main) or Slow (Relief or Suburban) line. It is important that trains are allocated according to their actual paths using the published speeds and the respective track IDs according to how they are represented in Sectional

Appendix. The location along the network where they transverse from one line to another using the switches and crossings are as stipulated by the Sectional Appendix and this line architecture form the basis for the meticulous modelling of the TIPLOC points on the network model. While the Sectional Appendix provides details of locations of where track crossovers points are located as well as the route availability, the timetable dataset is used to model train directionality and the journey pathway across the entire tract network between Fast and Slow lines across the respective TIPLOC points set in the working timetable. Validation of the train path is done by comparing the entire nodes and edges traversed for each journey with the actual journey pathway set in the train timetable dataset. Finally, we apply the shortest path algorithm with least time criteria (Ortega-Arranz et al, 2014), noting that trains on the Main lines will run fast between stations and make fewer stops between destinations compared with trains on the Slow Suburban lines. The train stations called for each journey are recorded until a train reaches its destination. Applying the same principle to every train journey, we allocate the entire train timetable information onto physical routes and stops on the spatial network and this is validated by comparing with the path defined in the Train timetable dataset and the Sectional Appendix.

4.3.3 Passenger allocation model and estimation

When a complete dataset of passenger journey characteristics and travel patterns is available, it is possible to quantify the number of passengers affected by a disrupted train service. A good example is discussed in (Ghaemi et al, 2018), where the authors were able to obtain passenger disruption data on the Netherlands rail network using daily passenger journey information between stations based on smart card transactions. In Great Britain, extensive work has been carried out on passenger travel demand and forecasting (Worsley, 2012). However, there are often challenges in obtaining access to this information due to a number of issues, including commercial sensitivity and security.

For this study we have been able to overcome this challenge by obtaining access to the Model of Inter-Regional Activity (MOIRA) which we use for estimating passenger disruption information. MOIRA is a frequently used rail demand forecasting models on Great Britain's network and it relies on an elasticity-based approach for modelling how planned timetable changes affect passenger flow and revenue using ticket sales information from the Latest Earnings Network Nationally Over Night (LENNON) ticketing and revenue database to allocate passengers to trains (Worsley 2012). Like most models that rely on an elasticity-based approach, MOIRA uses an empirical historic data of observed demand for predicting passenger demand forecast on the rail network. Due to its commercially sensitive nature, it is only privately available to those who have contributed to its development and it is the responsibility of the Association of Trains Operating Companies (ATOC), managed by the Rail Delivery Group (RDG). While MOIRA provides a good estimation of passenger trip distribution across the mainline network in Great Britain, it is important to understand some of its shortfalls when considering its use for modelling passenger disruption. First, it can often present incomplete information in certain areas especially around the Greater London region where it does not capture important interchanges with the London Underground metro services. There is also often a challenge in ascertaining from the model the actual path travelled by a passenger especially where this involves interchanges. Also, because it does not give detailed dynamic overview of passenger travel data on the network, this can result in a challenge when attempting to extract from the model what alternative routes were taken by passengers following a disruption event.

For this study we extract a static MOIRA output, which comprises details of passenger loads (or numbers) by stop from origin to destination for all trains according to the national rail working timetable for a given 24-hour period during a Monday working weekday. We then map this dataset onto our multi-track model stations and routes. A total

of 23,547 unique journeys were extracted for this period and in Figure 4.3, we present a spatial representation of passenger density per station across the network nationally for Monday morning peak travel between 07.00 – 08.00hrs.

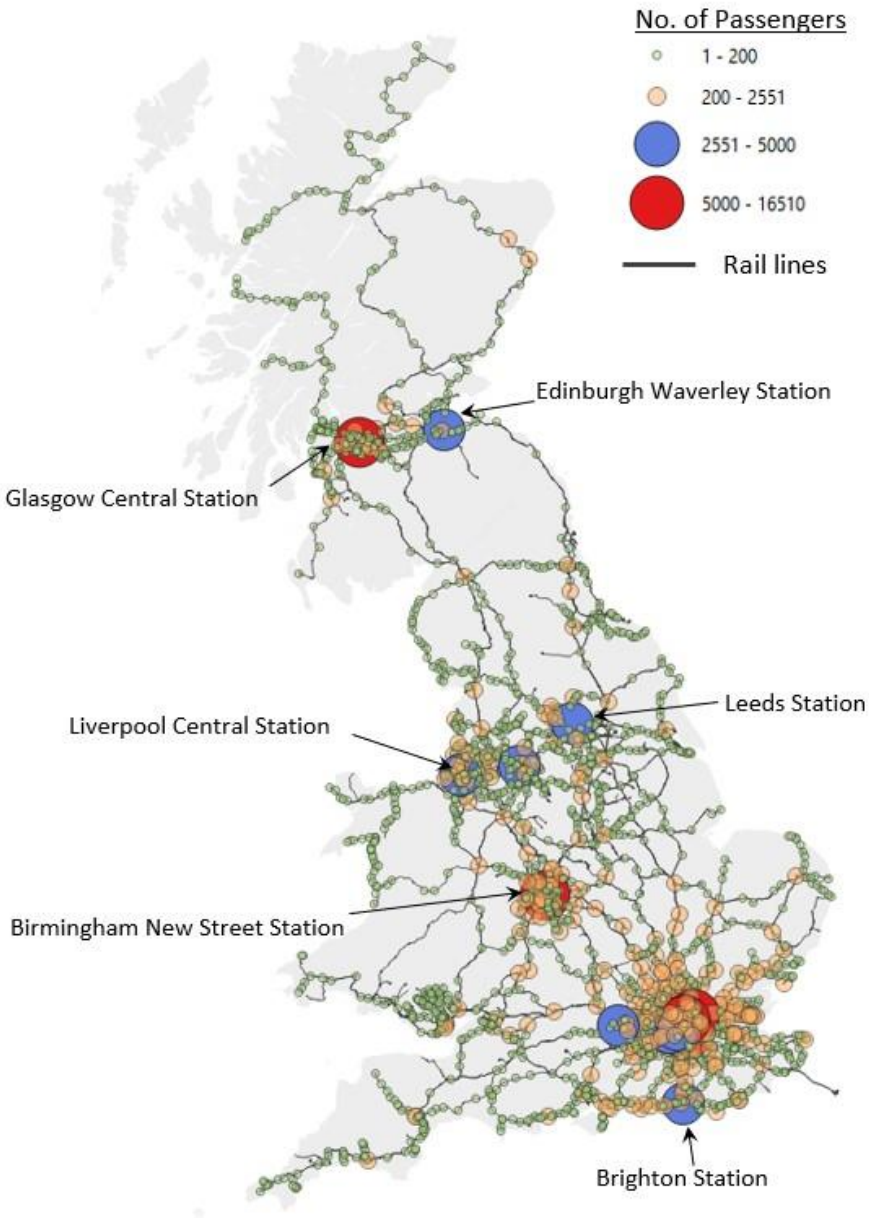

Figure 4.3 Map representation of the clusters of passenger journeys during the morning (AM) hourly peak travel across all stations in Great Britain's railway network (data source: MOIRA)

4.3.4 Disruption modelling and impact quantification

Following the journey assignment to track nodes and edges, we replicate real-world rail operational rules in the network model to allow us to correctly assess the impact of disruption on train services and passengers. Figure 4.4 and Figure 4.5 show the sketch of

a multi-track railway line with two lines running in each direction of travel. Following disruption to the Down Fast line, services can be rerouted via the Down Slow line, albeit with possible service delays and cancellations. When the same scenario is considered on a single track model, it leads to all the UP and Down routes becoming entirely unavailable because there is no distinction between both lines on the single track model.

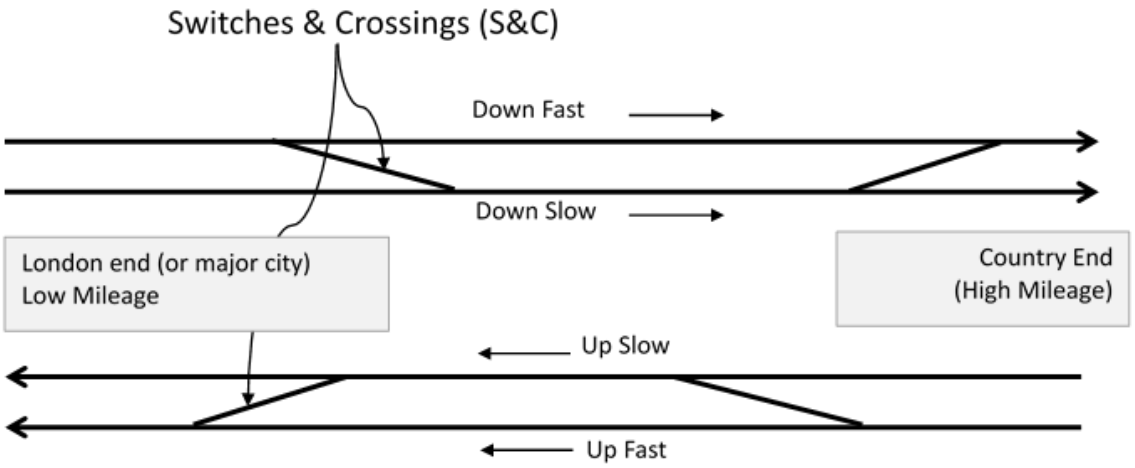

Figure 4.4 Sketch showing a multi-track representation of a railway line (pre-disruption)

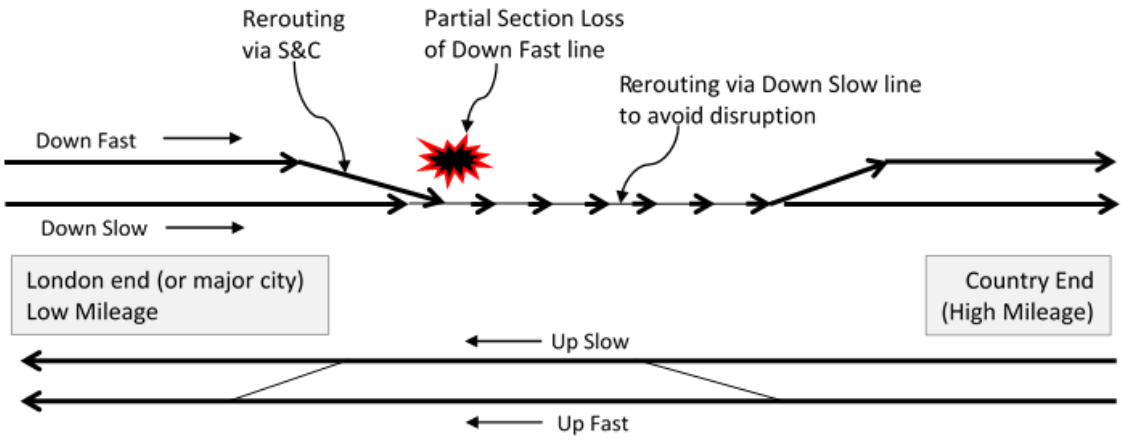

Figure 4.5 Sketch showing the disruption to a section of multi-track railway line

4.3.4.1 Assumptions

In carrying out disruption modelling and impact quantification on the network, we have assumed that:

(i) If all trains run according to the scheduled timetable, there will be no conflict at stations and junction points.

(ii) Our multi-track network model is based on a fixed-block signalling system which means that only one train can occupy a 'block section' at any particular time as it helps to guarantee a safe distance between trains (D'Ariano et al, 2008). Therefore, when a section of the track is occupied by a delayed train, it is not possible for a train to overtake the delayed train on the same line.

(iii) Signalling headways in the Working Timetable remain unchanged. Signal headways refer to the time between two trains on a particular route on the rail network.

(iv) When a disruption results in delay to passenger train services, we quantify the knock-on delays on other parts of the network on the assumption that the train movement priority specified in the published rail Timetable is maintained throughout the duration of the disruption. While it is possible in real-world operational conditions for a Traffic Controller or Signaller (as they are often referred to in operational rail terminology) to implement a progressive recovery action to regularise the service and limit the impact of the delay, our methodology is limited to quantifying the delay impact from hazard events prior to the implementation of any service restoration or regularisation strategy.

(v) The train dwelling times at stations remain unchanged from what is allowed for in the working timetable throughout the period of the disruption.

(vi) It is not possible to introduce additional trains to the network. This assumption is true for critical parts of the rail network in Great Britain where during peak time the network runs at close to 100% capacity (Network Rail, 2019).

We classify the disruption consequence from exogenous threats to the rail network as one of two possibilities – either a Section Loss or Line Speed Restrictions (LSR). A Section Loss, which can either be a partial or full Section Loss is occasioned by the loss of part

or an entire section of the train network, leading to the restriction of rail services along the affected route. Line Speed Restrictions on the other hand can take different forms – either temporary or emergency speed restrictions and may be planned or unplanned. For this study, our focus is on the impact from emergency line speed restrictions, which are restrictions applied over an area of the rail network in response to hazard events, allowing for the continuous running of rail services but at a reduced speed and resulting in train delays.

A route contains several trains passing through it, and there are several routes passing through a given network node. Broadly, two types of routes are associated with nodes: (1) Primary route – which is the route passing through the node for which the trains will get first priority over all other trains from other routes. When a disruption occurs resulting in the removal of a node from the network graph, the primary route is the first route disrupted which should have travel priority through this node but couldn't anymore as a result of this node removal. The primary route at a node may be different for different disruptions depending on which route the disruption first occurred on; (2) Secondary route – which represents all other routes and the respective trains passing through the nodes. When a disruption occurs, the first step in the delay calculation process is to identify the location(s) affected. We identify the delay attributed to the primary route as the primary delay and identify the secondary delays on secondary routes as well as the delay associated with cancelled trains. Due to the detailed network characteristics of a multi-track railway model, it can be a very complex exercise to correctly estimate how train delay on a primary route cascades to secondary routes and other parts of the network. We address this complexity by introducing the concept of a *delay threshold* at nodes and junctions, measured per hour based on the rail working timetable and find the value for *delay threshold* for all nodes on the rail network for each of the train journeys considered. The *delay threshold* is defined as the time in minutes beyond which knock-on effects of

delays are (1) cascaded to other trains on the same route, (2) cascaded to other trains on an adjoining secondary route or (3) lead to cancellation of services across the network.

4.3.4.2 Delay threshold for reactionary delays, d_{tr}

This refers to the *delay threshold* in minutes beyond which a primary delay $d(p)$ results in knock-on or reactionary delays to be cascaded to other trains along the same route or to trains along secondary routes. The methodology for delay estimation discussed in this section is used to estimate delays for each specific train as well as the aggregate of the reactionary delays associated with the initial delayed train. The correct modelling of this initial delay incurred and delay threshold, d_{tr} at which the delay is cascaded across the network is therefore important in correctly estimating the total delays to the entire network.

When a particular hazard event delays an affected train, x; pending any recovery action, we assume that the next train $x + 1$ will be subject to delays when $d(p) > h_o$, where h_o refers to the allowable operational headway in minutes (this is the distance between successive trains divided by the train speed) in the system which is determined by the signalling system. The headway is defined as the allowable safe distance between trains which is necessary to keep them safely separated without the need to reduce train speed (MTI, 2015). The value of h_o for each affected route is obtained from the rail working timetable. The value of d_{tr} is obtained by finding $d(p) - h_o$ and the threshold for cascade of knock-on delays is reached when the value of $d(p)$ exceeds h_o, following which the resulting delays are cascaded to other trains on the route. The delay threshold for reactionary delays (d_{tr}) is measured at junction nodes through which there is one primary route and one or several secondary routes, by obtaining the minimum non-disrupted time difference of a fixed time block between the times the primary route trains pass through the junction and the times when the next secondary trains pass through the

junction. If in a fixed time block T the primary route (p) trains through a node and is followed by all secondary routes (s) trains as per the generalised time sequence

$t_0(p) < t_0(s) < t_1(p) < t_1(s) < \cdots < t_k(p) < t_k(s), where\ t_j(s) - t_j(p) \leq T\ \forall\ j \in \{0,..,k\}$, then

$$d_{tr} = \min_{j\in\{0,..,k\}} \left(t_j(s) - t_j(p)\right) \tag{4.1}$$

Where $t_0(p),\ t_1(p) \ldots t_k(p)$ and $t_0(s),\ t_1(s) \ldots t_k(s)$ represents the train times in sequence on the primary and secondary route respectively starting from the first disrupted service to the *k* disrupted service. We note that not all nodes necessarily have secondary routes and trains through them and, if they have secondary route trains, the frequency of the trains passing the node may be much lower than the primary route trains. This means that there may not be any secondary route trains between consecutive primary route trains.

In the event of speed restrictions, the trains on the network will be delayed, affecting all primary and secondary routes. The delay times along the route are estimated by summing up the delays associated with each train along the route, and all nodes on the route are allocated the value of this delay times. Hence, the delay associated with a primary route (p) with trains arriving at times $t_0(p), t_1(p), \ldots, t_k(p)$ before disruptions and at section loss or speed restrictions induced delayed times $\tilde{t}_0(p), \tilde{t}_1(p), \ldots, \tilde{t}_k(p)$, where $\tilde{t}_j(p) \geq t_j(p) \forall\ j \in \{0, \ldots, k\}$ after disruption is estimated as:

$$d(p) = \sum_{j=0}^{j=k} \left(\tilde{t}_j(p) - t_j(p)\right) \tag{4.2}$$

Similarly, delays on the secondary routes can be estimated in terms of the pre- and post-disruption time difference of same trains on such routes.

$$d(s) = \sum_{j=0}^{j=k} \left(\tilde{t}_j(s) - t_j(s)\right) \tag{4.3}$$

4.3.4.3 Delay threshold for cancellations, d_{tc}

This refers the *delay threshold* in minutes beyond which train services will be subject to cancellation on a specific route. The value of d_{tc} differs per route and the time of the day for peak and non-peak travel times. It is obtained for this study by comparing the

calculated value of the delay at each node in the network model with the cancellation minutes per Service Group obtained from Table 4.1. The cancellation minutes by Service Group for each route, detailed in Table 4.1 are used to model the limiting value for cancellations, d_{tc} for each hazard disruption event. Therefore, when the calculated value of delay minutes exceeds the assigned Service Group cancellation, this results in a fixed cancellation delay in minutes $d(c)$ equal to the corresponding cancellation minutes obtained from Table 4.1.

4.3.5 Delay estimation algorithm

In the event of a network wide disruption, we collate a set of all the affected l primary routes $P = \{p_1, p_2, \dots, p_l\}$, m secondary routes $S = \{s_1, s_2, \dots, s_m\}$, and n cancelled routes $C = \{c_1, c_2, \dots, c_n\}$. The delay minutes on these routes are estimated respectively and collated in sets as $D(P) = \{d(p_1), d(p_2), \dots, d(p_l)\}$, $D(S) = \{d(s_1), d(s_2), \dots, d(s_m)\}$, and $D(C) = \{d(c_1), d(c_2), \dots, d(c_n)\}$.

Total delays on primary, secondary and cancelled routes are estimated as:

$$t\big(D(P)\big) = \sum_{i=1}^{i=l} d(p_i) = \sum_{i=1}^{i=l}\sum_{j=0}^{j=k}\big(\tilde{t}_j(p_i) - t_j(p_i)\big) \tag{4.4}$$

$$t\big(D(S)\big) = \sum_{i=1}^{i=m} d(s_i) = \sum_{i=1}^{i=m}\sum_{j=0}^{j=k}\big(\tilde{t}_j(s_i) - t_j(s_i)\big) \tag{4.5}$$

$$t\big(D(C)\big) = \sum_{i=1}^{i=n} d(c_i) \tag{4.6}$$

In Figure 4.6, we present a step by step procedure for Delay Minutes estimation, which is explained as following:

1) Establish the hazard consequence – whether it is a Section Loss or Line Speed Restriction.

2) Obtain the geospatial coordinates of the primary route p, collate all disrupted edges and nodes into a failure database.

3) Line Speed Restriction: Where the consequence of the disruption is a line speed restriction,

   a) Using Equation 4.1, find the value of d_{tr} for all affected junction points along the affected route.

   b) Using Equation 4.2, obtain the primary delay, $d(p)$ accrued.

   c) If $d(p) \leq d_{tr}$, the delay is limited to the primary route only.

   d) If $d(p) \geq d_{tr}$, knock-on delays will be cascaded onto secondary routes and may result in conflict at junctions. Using Equation 4.3, obtain the delay to secondary routes.

   e) Conflict resolution at junction points: Where delays on a line results in conflicts at junction points, we assume that there is no priority movement authority at the junction points and that trains will navigate through these junctions in the order specified in the rail Working Timetable. Therefore, any delays accrued at the junction from the $d(p)$ are cascaded to all trains which navigate through the affected junction until a recovery action or regularisation of service is implemented.

   f) Cancellations (reliability event): Find d_{tc}. When the value for d_{tc} on a line is reached, this will lead to a reliability event with a cancellation penalty applied to all affected trains based on the Service Group affected (Table 4.1).

   g) Using Equations 4.4 – 4.6, obtain the total delays accrued as a result of the LSR.

4) Section Loss:

   a) Full Section Loss: Where a full Section Loss occurs with no option for rerouting, use Equations 4.4 – 4.6 to estimate the total delay minutes accrued.

   b) Partial Section Loss and Rerouting Options: When a partial Section Loss occurs or where there is an option for rerouting during a full Section Loss, we apply following steps:

      i) Reroute the affected services to avoid the disrupted section of the track such that the train service calls at all possible stations along its original route. This

is done by designating the start and end of rerouting as the junction nodes preceding and after the disrupted section respectively. Rerouting can only happen via legitimate routes set in the Sectional Appendix.

ii) Using the Dijkstra's shortest path algorithm with lest time criteria, find the rerouted path between the affected junction nodes.

iii) For all rerouting scenarios, obtain the d_{tr} for the new route. When this is exceeded, rerouting will introduce knock-on delays on the new route. Use Equation 4.3 to estimate this delay in minutes.

iv) Find d_{tc} for the new route. Rerouting on routes which have been signalled to full capacity will almost invariably lead to a cancellation of service to allow for the rerouted service. Obtain cancellation delay minutes using Equation 4.6.

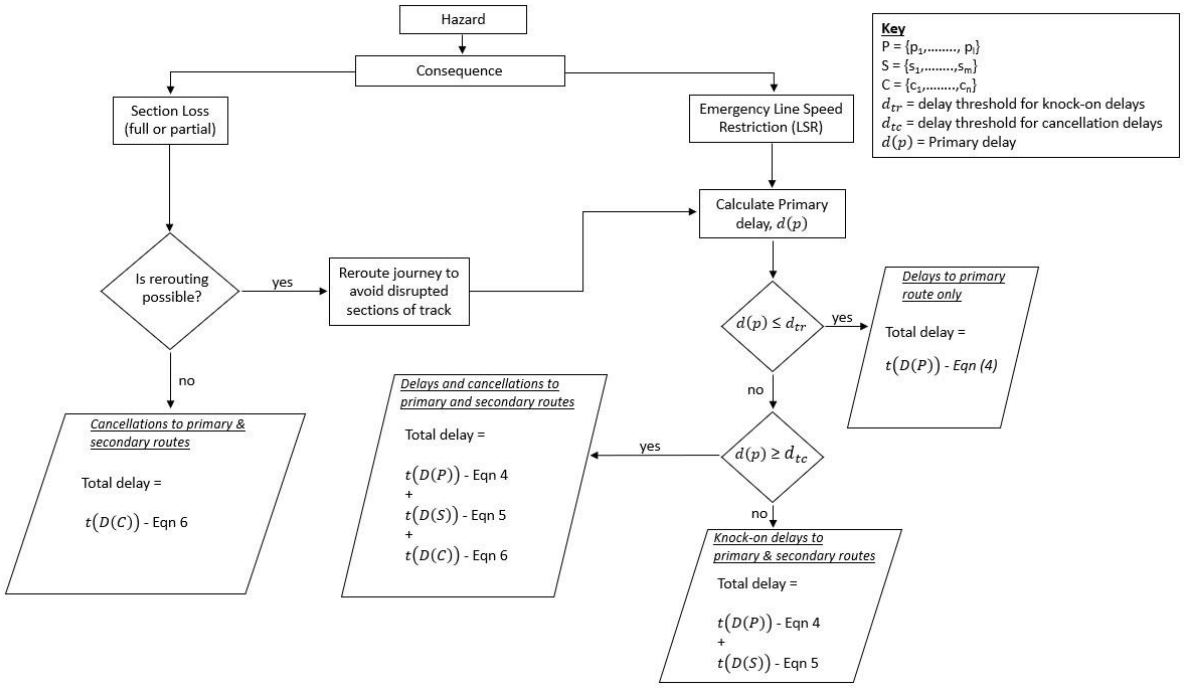

Figure 4.6 Flowchart of the algorithm developed in this study for estimating train delay minutes following disruptions from hazard events

4.4 Practical application to case studies on Great Britain's rail network

In this section we demonstrate the practical application of our methodology using six case studies of weather related hazard events across Great Britain's national rail network. We obtain access to a large dataset of all the extreme weather-related disruptions on Britain's railway from 2006 to 2019. The hazards are categorised into nine different types namely

– adhesion, cold, flood, fog, heat, lightning, snow, subsidence and wind. In Figure 4.7, we present the yearly aggregate of all the weather-related hazards on Britain's rail network for 2006 – 2018 financial years. We have omitted the data for 2019 because the financial year of 2019 ends in March 2020 and the results we presently have for 2019 are not representative of the entire year running through until March 2020.

We find that, even though they represent only a third of the recorded weather-related hazard types on the rail network nationally, wind, snow and flood hazards were responsible for about two-thirds of all the recorded weather-related delay minutes. Also, from Figure 4.7, the total of 21,077,876 recorded delay minutes for 2006 – 2018 were found to be as a result of 277,783 separate weather-related events. Of these, about a third of the total delay minutes – 7,055,281 were accrued from 654 or 0.235% of these recorded events. Even so, 477 of these 654 separate events were as a result of snow, flood and wind hazards which accounted for 77% or 5,430,221 of the largest recorded delay minutes on the rail network. The significant statistical relevance of the impact of these three weather-related hazards has therefore informed their choice of use for this study.

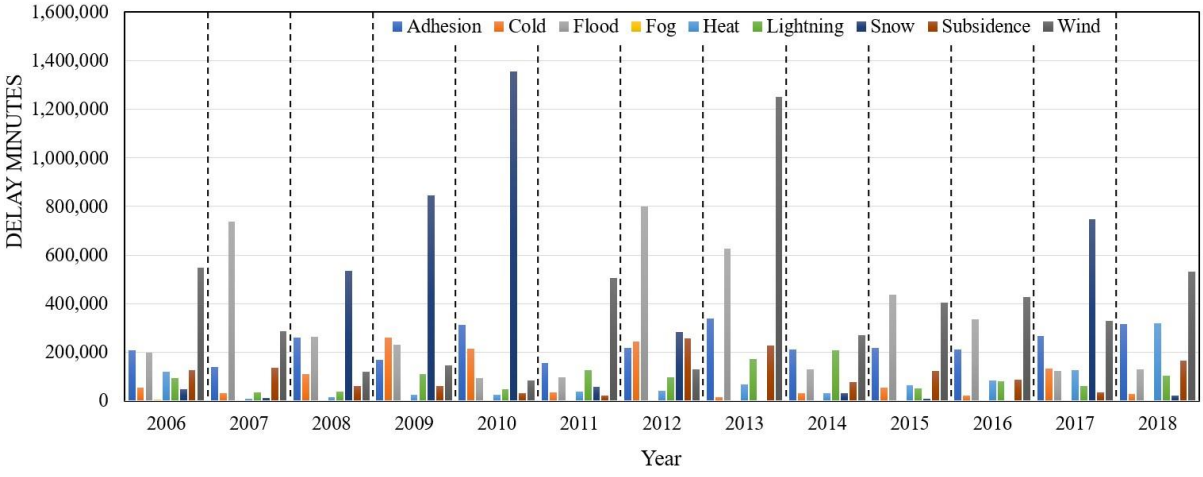

Figure 4.7 Delay minutes on Britain's railway from 2006-2018 (Source: Network Rail)

From the dataset of weather-related disruptions, we selected have six hazard events. The hazard types considered and the delay attribution STANOX locations are shown in *Figure*

4.8. A STANOX location code is a unique code for describing specific locations along the railway network on the rail network in Great Britain. The six case studies are selected to represent key critical routes and a representative geographical spread across the rail network nationally.

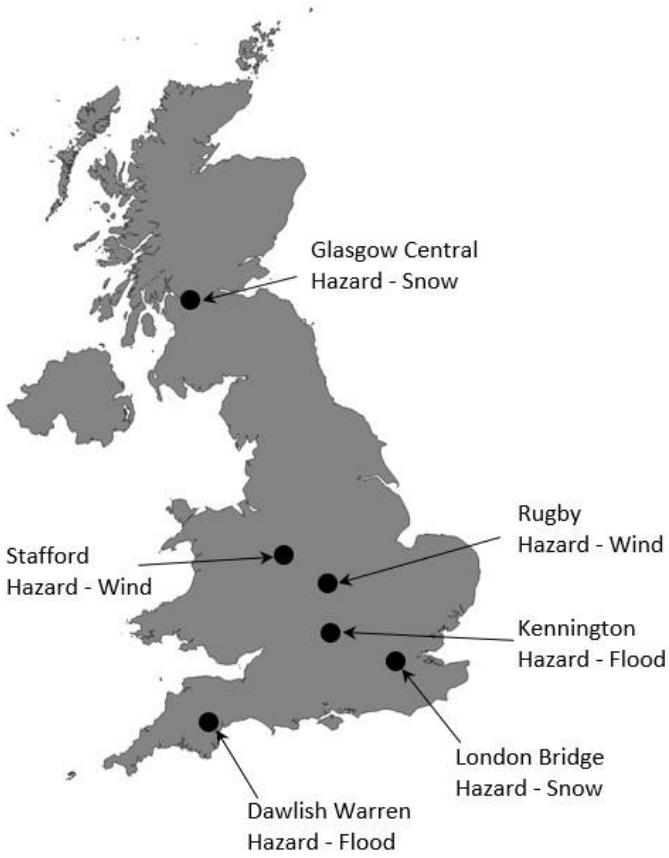

Figure 4.8 Map representation of the case study locations and hazard events considered in this study

4.5 Presentation and discussion of results

4.5.1 Comparison with empirical data

We adopt the methodology and algorithm discussed above and use our model to estimate the delay minutes accrued and passenger numbers disrupted for all the six case studies. The results of these, presented in Table 4.3 show the comparison between the calculated delay minutes from our model and the observed records from the TRUST empirical delay minutes dataset. The results presented in the table are the aggregate delays arising from the initial delay and the subsequent reactionary delays, however it is possible to estimate

delays attributed to specific trains in the simulation. Spatial maps of all affected rail journeys and passengers disrupted for two of the six case studies are presented in Figures 4.8 and 4.9. When the results from our model are compared with that from the empirical dataset, they show an average of 7% and 8% margin of error for the wind and flooding case study events respectively, whereas for the snow case study events this margin is higher, rising to an average of about 27%. The higher margin for snow events can be attributed to a number of reasons. First, while the consequences of certain hazard events like flooding can be localised and straightforward to attribute to a particular location, others like snow, which affect large, multiple areas at the same time can present challenges in attributing to a specific location. A practical example of this is the case of Storm Emma which happened in late February 2018. Even though this hazard event was reported widely in the media (The Guardian, 2018) to have affected several parts of the country, the delay dataset from Network Rail attributed the resulting delay for most of the Scotland area to Glasgow Central station. Therefore, in attempting to replicate this hazard scenario in our network model, we have removed only the assumed affected nodes and edges for the Glasgow Central STANOX section which results in an underestimation of the calculated delay minutes. Secondly, it is acknowledged that the process of recording delay minutes in TRUST introduces a number of anomalies, duplicate entries of delays and reporting errors (DAB, 2019) which can result in exaggerated differences for big weather events like snow. Therefore, with the right methods of attributing and recording these kinds of disruptions which have the propensity to affect large areas at the same time, the delay minutes recorded in TRUST can be attributed with a higher margin of accuracy so that they compare favourably with the results from our model.

s/no	TRUST[a] Incident ID/date/ duration	Hazard/ STANOX[b]	Hazard Consequences	Results					
				No. of disrupted passenger train services	Passenger numbers disrupted	Recorded delay minutes (Min_{REC})	Calculated delay minutes (Min_{CAL})	% difference between (Min_{REC} & Min_{CAL})	Average % difference between (Min_{REC} & Min_{CAL})
1	4833343 02/02/09 – 24hrs	Snow/ London Bridge	Full section loss, no trains via London Bridge station	1,902	568,611	68,351	52,777	23%	27%
2	841442 02/02/09 – 24hrs	Snow/ Glasgow Central	Storm Emma resulting in full section loss	885	905*	57,962	40,614	30%	
3	587033 29/11/18 – 8hrs	Wind/ Stafford	Blanket 50mph (LSR)	197	16,170	6,688	6,832	2%	7%
4	7085151 23/02/17 – 6hrs	Wind/ Rugby	Blanket 50mph LSR	170	11,644	4,572	5,097	11%	
5	8403962 02/03/18 – 10.45hrs	Flooding/ Dawlish Warren	Full section loss	99	33,414	5,471	5,871	7%	8%
6	429202 25/07/07 – 24hrs	Flooding/ Kennington	Full section loss	241	46,686	12,628	11,484	9%	

Table 4.3 Summary of results of disruption case studies

4.5.2 Spatial and temporal assessment of network-wide delays

In addition to estimating delay minutes and the numbers of disrupted passengers, an important output from our model is its ability to present a spatial representation of journey impacts on the network which can inform a systemic understanding of the impact of disruption to train routes, junctions, stations and passengers for each hazard type. These outputs are shown in Figure 4.9 and Figure 4.10 for two of the six case studies considered.

In Figures 4.9(i) and 4.10(i), we present the output of the delay minutes accrued across the disrupted rail routes which shows a number of significant insights and research contributions. First, it shows the extent to which localised disruptions can affect large sections of the rail network beyond the point of disruption. For example, in Figure 4.10(i), the flood hazard event at Kennington in Oxfordshire results in disruption to train services as far as Edinburgh. Secondly, because we have modelled all the multi tracks that make up the rail network and simulated train journeys through their actual pathways, we are able to show the impacts of train delay with better granularity than a single track model. This is illustrated by the different colours in Figures 4.9(i) and 4.10(i) which demonstrates how multi tracks along the same route accrue different delay minutes depending on the journeys they facilitate on the rail timetable, allowing for a more accurate understanding of the true impact of disruption to the network than is possible with a single track model. Thirdly, by attributing the rail journeys to their respective multi-tracks, our model can be used to obtain the values of actual rail tonnages and track asset utility information based on different rail timetable scenarios which can inform asset management and maintenance decision making by Infrastructure Managers.

Figures 4.9(ii) and 4.10(ii) show a plot of the passengers disrupted by each hazard event. For example, the snow hazard at London Bridge resulted in the most severe impact to passenger travelling to and from the east of London Bridge around the Lewisham and Catford axis of London (Figure 4.9(ii)). In the case of Flooding at Kennington, the most

disruptions were to passengers at London Paddington and at Oxford stations (Figure 4.10(ii)). The passenger delay data refers to the station that the passengers were located or travelling via when the disruption occurred. Unlike the train delay minutes presented in Table 4.3, there was no real-world validation data available to calibrate our output results for passenger delays. Nevertheless, the results and findings are important and provide valuable dataset which can inform resilience scenario planning and decision-making during disruptions, for example in the planning of rail replacement buses and alternatives to be provided for disrupted passengers.

Another important output from our model is the time-series plot of passenger disruptions for each hazard event shown in Figures 4.9(iii) and 4.10(iii). These show the variation in passenger disruptions for different times of the day. We deduce from these plots that for the snow hazard event disruption at London Bridge (Figure 4.10(iii)), a significantly higher number of passenger journeys were disrupted at peak travel times in comparison with the flooding disruption event at Kennington (Figure 4.10(iii)). Also, the highest passenger disruptions occurred during the morning peak travel times in the case of London Bridge, while they occurred during the evening peak travel times in the case of Kennington in Oxfordshire. All case studies considered in this paper show a spike in the number of disrupted passengers during peak time travel, however for the case studies plotted in Figure 4.9 and Figure 4.10, these were mostly influenced by travel originating from and towards London. Such an output can inform which routes and locations will be the most affected during peak travel times and when to schedule maintenance in order to avoid the highest disruptions to peak travel along the network. In Figures 4.9(iv) and 4.10(iv) we present a time-series plot of the aggregate train delay minutes. Similar to the passenger disruption plots, these show the variation in calculated delay minutes across the entire delay period with noticeable increase in delay minutes during morning and evening peak travel times for the hazard event at London Bridge compared with the

Kennington case study where the morning peak is more prominent than in the evening peak, influenced by travel into London.

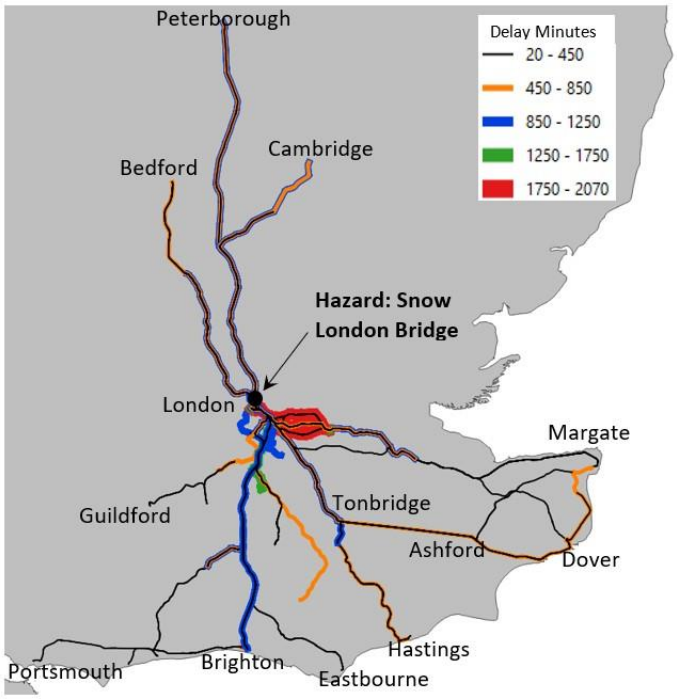

Figure 4.9 (i) Spatial plot showing disrupted train routes
Number of disrupted services = 1,902 trains
Total delay = 52,777 minutes

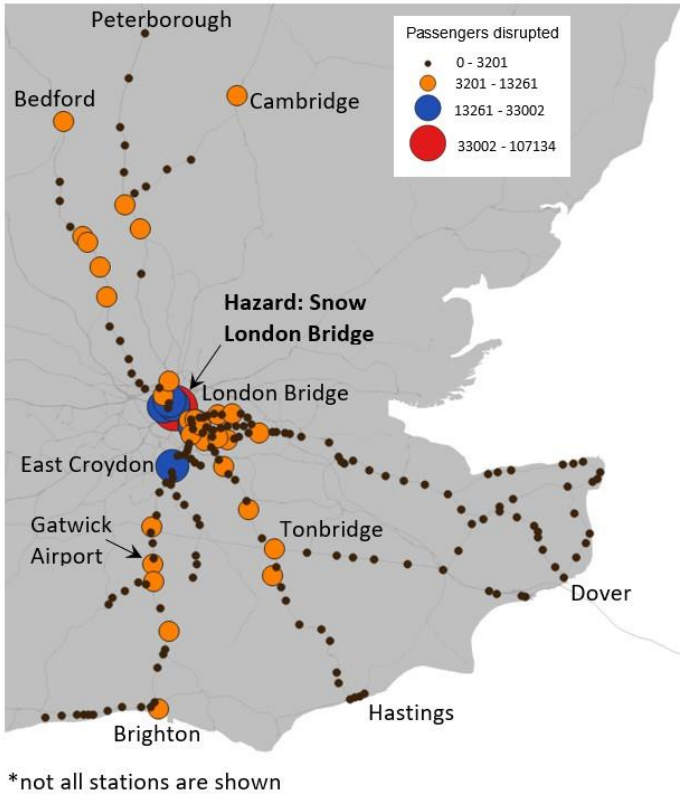

Figure 4.9 (ii) Spatial plot showing disrupted passenger numbers
Total number of disrupted passengers = 568,611

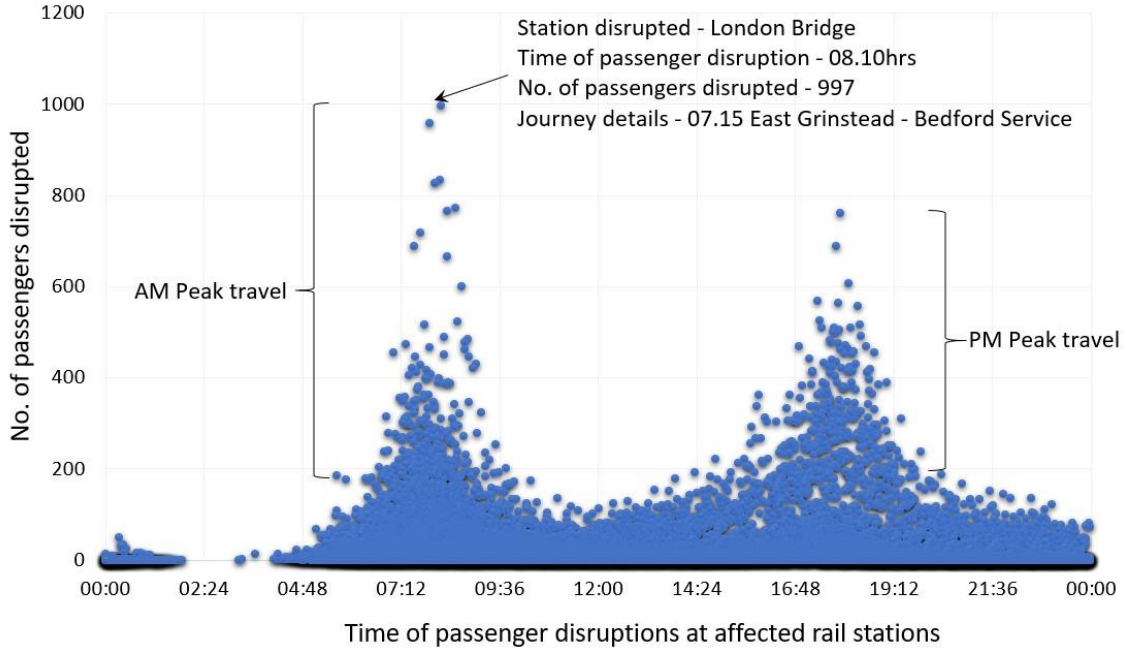

Figure 4.9 (iii) Time series plot of passenger disruptions

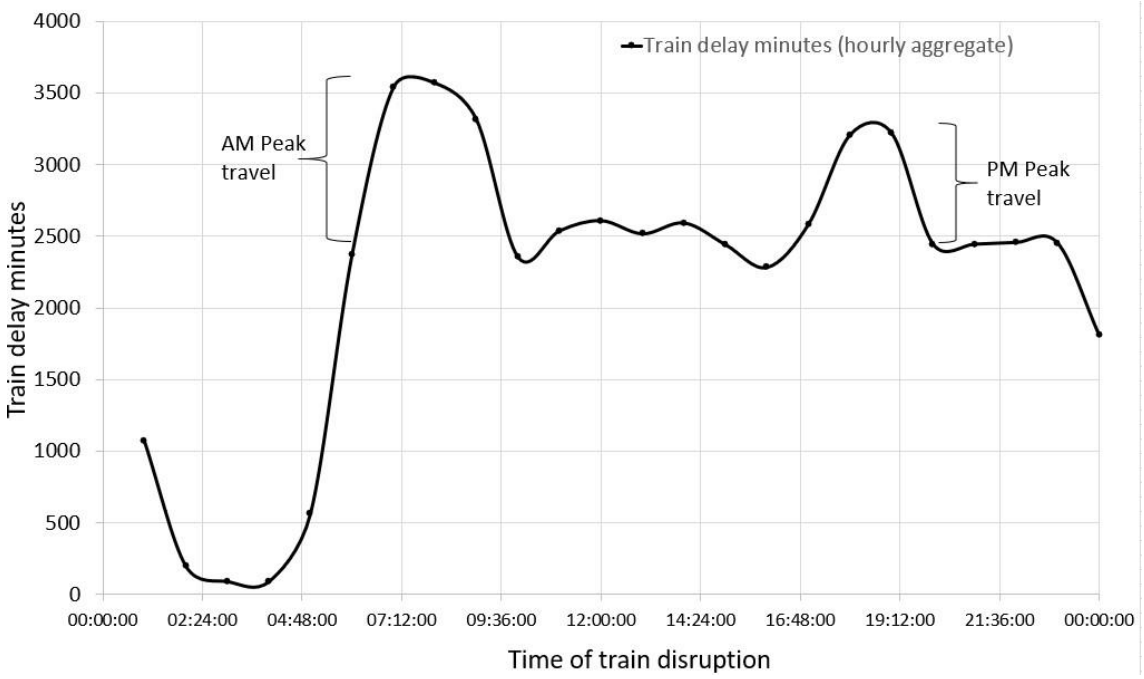

Figure 4.9 (iv) Time series plot of aggregate hourly train delay minutes

Figure 4.9 (i – iv): Results of case study 1 - snow at London Bridge, duration of disruption 24 hours, showing:

(i) Map representation of the concentrations of delay minutes estimated for different disrupted trains along routes affected by the hazard event;

(ii) Map representation of the locations and concentrations of passenger journey's disrupted at stations affected by the hazard event;

(iii) Time series plot of the evolution and distribution of passenger disruptions across morning (AM) and evening (PM) peak times and off-peak times; and

(iv) Time series plot of the aggregated hourly delay minutes over the duration of the disruption of the hazard event

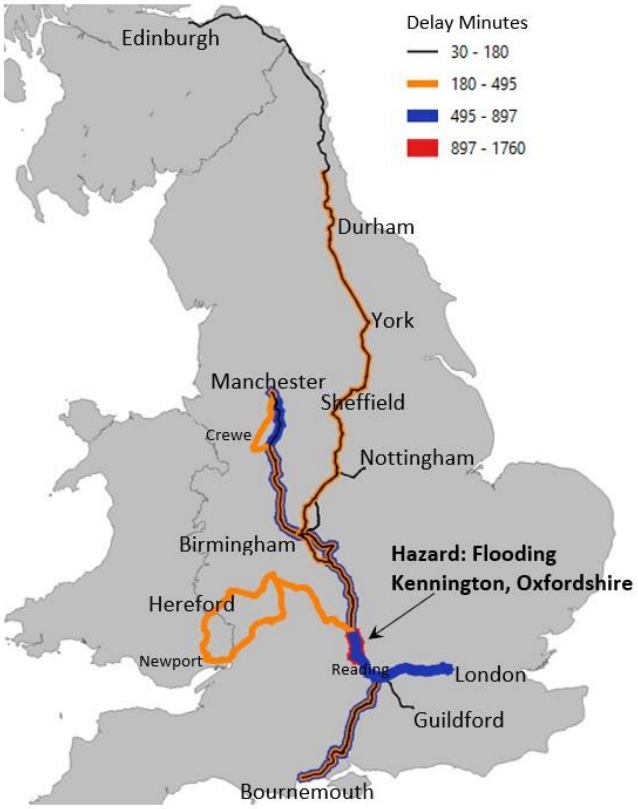

Figure 4.10 (i) Spatial plot showing disrupted train routes
Number of disrupted services = 241 trains
Total delay = 11,484 minutes

Figure 4.10 (ii) Spatial plot showing disrupted passenger numbers
Total number of disrupted passengers = 46,686

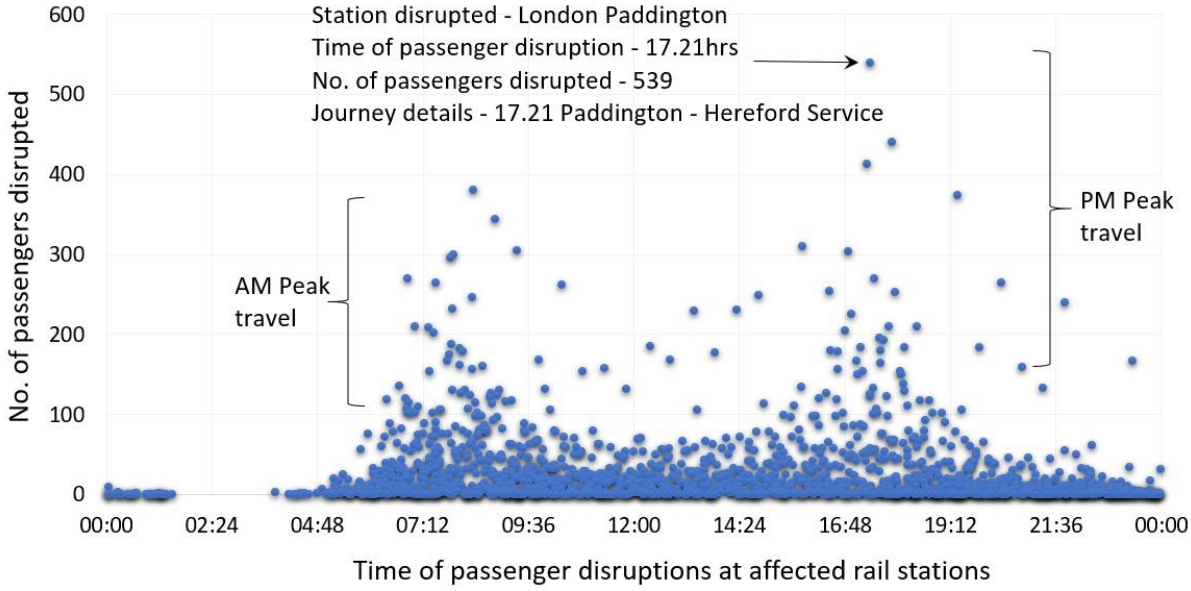

Figure 4.10 (iii) Time series plot of passenger disruptions

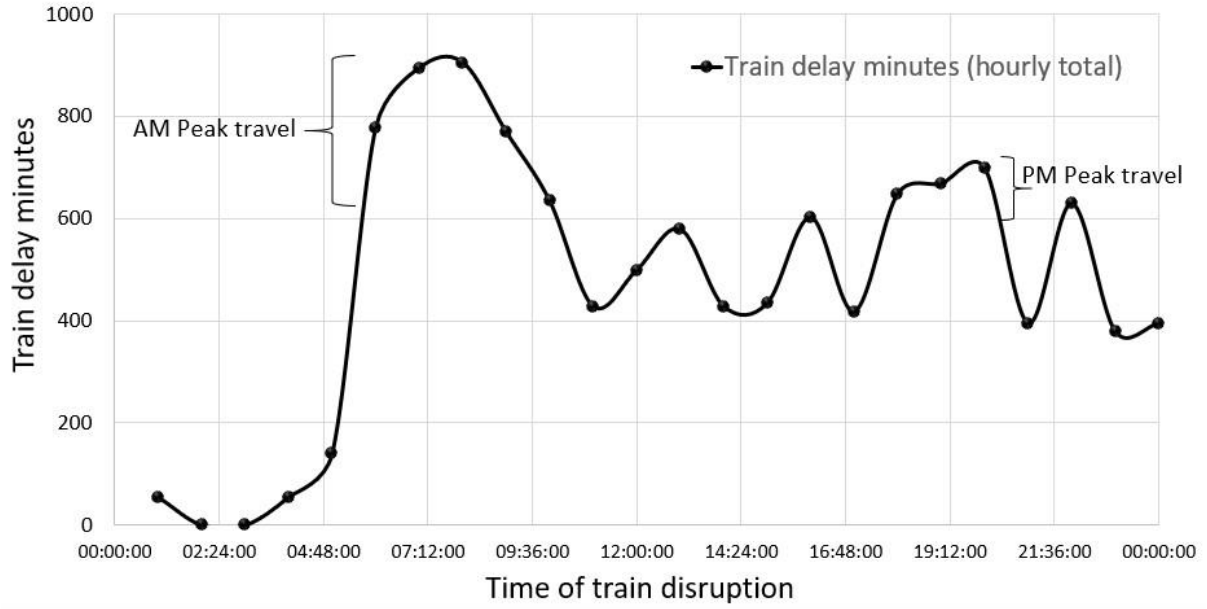

Figure 4.10 (iv) Time series plot of aggregate hourly train delay minutes

Figure 4.10 (i – iv): Results of case study 6 – flooding at Kennington, Oxfordshire, duration of disruption 24 hours, showing:

- *(i) Map representation of the concentrations of delay minutes estimated for different disrupted trains along routes affected by the hazard event;*
- *(ii) Map representation of the locations and concentrations of passenger journey's disrupted at stations affected by the hazard event;*
- *(iii) Time series plot of the evolution and distribution of passenger disruptions across morning (AM) and evening (PM) peak times and off-peak times; and*
- *(iv) Time series plot of the aggregated hourly delay minutes over the duration of the disruption of the hazard event*

4.6 Conclusion

In this paper we have presented a methodology for multi-track and disruption modelling and demonstrated its use for risk analysis of several failure case studies on the rail network in Great Britain. We have combined an accurate dataset of the track network with practical knowledge of the processes that lead to train delays and passenger disruption to build a realistic model of rail journey disruptions due to natural hazards, which is computationally tractable for use in testing very large numbers of possible failure events such that computation of the impact of train and passenger delays across a large scale national rail network can be estimated in minutes in a single simulation run on our model.

This model has been used to calculate the resulting delay minutes from disruption to passenger train services and to characterise the number of passengers disrupted for each hazard event. By doing this we have been able to demonstrate the use of our model to estimate multiple impacts for each hazard type as well as present a spatial representation of these impacts across the rail network, making a significant improvement on some of the existing models (e.g. TRUST and MOIRA) used on the rail network in Great Britain. For example, TRUST can only record ex-post delay minutes for each hazard event. MOIRA on the other hand, produces output of passenger disruption. In comparison with both, our model can estimate ex-ante train delay minutes and passenger disruption information for each hazard event in a single model simulation as well as produce a visual spatial plot which shows the systemic impacts from these disruptions at regional and national scales. In this study, we have also addressed the limitations in previous rail research studies of the use of single-track modelling approaches for representing rail routes, which is limited in the realism with which train disruptions can be represented and can lead to inaccurate representation of train journeys in real-world case studies where it involves multi-track scenarios. This multi-track model therefore provides researchers and infrastructure managers with useful tools to predict the impact of hazards and inform planning and decision making with regards to infrastructure resilience.

Multi-track models present an opportunity to correctly route rail journeys through their actual pathways and replicate the behaviour of the rail network in a theoretical model. We have successfully demonstrated this by analysing actual observed disruptions scenarios and compared the outputs with those obtained from our network model. We find that these give results which compare with observed values with low margins of error. Our approach also provides researchers and infrastructure managers with a sound basis for ascertaining the criticality of routes across the entire rail network based on the

delay minutes accrued and number of passengers affected which can inform scenario planning and resilience decision making.

5 A model and methodology for risk and resilience assessment of interdependent rail networks – case study of Great Britain's rail network

Abstract

Rail networks entail multiple interdependencies which can initiate or propagate network failures with serious consequences for the movement of trains and passengers. In this study, we present a rail infrastructure system-of-systems model which can be used to simulate disruptions to the network's operations and propose a performance metric based on train and passenger delay minutes. We demonstrate the applicability of our model by evaluating the resilience of the southern region of Great Britain's rail network in scenarios of failure initiated in the traction power supply system. The results highlight the sensitivity of the rail network to a small number of traction assets concentrated in the London area, where we find that failure of one of the region's most critical electricity traction power grid could disrupt 75% of all trains in the southern region and 25% of all trains nationally. Our analysis demonstrates how the resilience of the rail network is influenced by the speed of backup restoration following a failure event as well as the network's vulnerability to failure at peak travel times with a delay during peak travel resulting in about 63% increase in passenger delay minutes compared with off-peak travel times for the same duration.

Keywords: risk, resilience, critical infrastructure systems, rail networks, systems-of-systems, interdependencies, rail disruptions, hazards, traction power systems

5.1 Introduction

The resilience of critical national infrastructure networks, which includes transport, communications, and energy assets required for the smooth functioning of modern society has been the subject of significant research and policy interest (PCCIP, 1997; EPCIP, 2008, UN, 2015; Thacker et al, 2017). In recent years, attention has been paid to the changing nature of the threats to these systems, cascading of network failures, and society's exposure to their outcomes (Hall et al, 2016; House of Lords, 2015; Cabinet Office, 2011). For example, in England, on the 9th of August 2019, two electricity generators ceased operating at the same time as a result of lightning strike to an overhead transmission line, resulting in disruption to power supply from the National Grid with large parts of England and Wales left without electricity (FT, 2019). This loss of generation caused the frequency of power supply to the rail network to drop below its nominal 50Hz to below 49Hz for approximately 33 seconds, resulting in trains ceasing to function and requiring technician assistance to restart, with significant delays to railway services (FT, 2019; ORR, 2020). Also, in 2014, extreme weather events resulted in the collapse of the Dawlish sea wall which supports the railway line into Devon and Cornwall in Great Britain, severing all rail services to this part of the country for several weeks, resulting in loss of power and damage to properties (Armstrong et al, 2017). The following year, storm hit the Dover sea wall on the Kent coast resulting in major disruptions to the UK's High Speed Rail link and closure of the link between Folkestone and Dover Priory for about nine months (Network Rail, 2016). These examples illustrate the increasing threat of disruptions across multiple critical infrastructure systems and their wider, far reaching socio-economic impact.

While the lack of universality in the definition of resilience in research literature has been acknowledged (Kong et al., 2018), our approach in this paper to assessing the resilience of rail technical systems involves adopting two important dimensions of systemic

performance. These are systemic robustness - defined as the ability to withstand disruption from an external shock event without severe degradation in asset and service performance; and systemic recovery - which describes the pattern and speed of recovery to full operational functionality (O'Rourke, 2007). We define *disruption* as either a delay or cancellation to a particular service following an external shock event. Many Railway Authorities across the world adopt train punctuality as a prime system performance criteria for measuring the network's robustness and recovery (NEA, 2003). Train punctuality is defined as a train service arriving, departing, or passing a point on the network at a predefined time with train delay minutes measured in terms of its exceedance from a predefined timetable (Rudnicki, 1997). Whilst train punctuality is an obvious system performance metric, it does not weight train delays along with the numbers of passengers disrupted, which would be a more comprehensive system performance criteria. For example, by relying on the performance of train delay minutes only, it assigns the same performance weighting to a disruption involving a very busy 12-carriage peak time train service in a major city like London and a single carriage train service in a remote part of the country as long as they accrue the same number of delay minutes, thereby ignoring the salient contribution of passenger weighting to route criticality.

A number of existing studies (Pagani et al., 2019; Adjetey-Bakun et al., 2016; Pant et al., 2016) quantified disruptions in terms of passenger journey losses over a given time period whilst mostly overlooking the dynamic knock-on effect of train disruptions on timetabling which can propagate far across the network. While the work by Adjetey-Bakun et al. (2016) considered the recovery aspects of resilience, others (Pagani et al., 2019; Pant et al., 2016; Johansson et al., 2011) focussed on network robustness. There are few risk assessment methodologies which study the impact of system-of-systems interdependencies on the resilience of rail networks. Those with practical application to real-word networks are particularly rare, with a dearth in research literature of robust

methodologies and models for resilience assessment of large, complex rail networks at regional and national scale (RSSB, 2016). While some previous studies have considered railway dependencies on electricity and telecoms systems, these were either represented in a notational way as networks with limited coverage (Adjetey-Bakun et al., 2016), and mostly as point assets (Pant et al., 2016), or as simplified networks that ignored several asset types within their systems (Johansson et al., 2011).

We seek to address these research gaps by developing a modelling framework that contains several elements that we consider to be important for the proper representation of rail network resilience. These include: (i) the detailed representation of realistic spatial and operational interdependence of electricity, signalling and telecommunications systems that support a functioning rail network, to understand the cascading failures notably through the electricity traction system; (ii) a full representation of the geographical complexity of failure impacts on large-scale multi-track rail networks, including time-table disruption and its effect of passenger journeys in terms of passenger-delay-minutes; and (iii) representation of resilience in terms of the effectiveness of time taken to undertake post-disruption actions such as providing back-up supply, repairing failed assets and regularising train services. Methodologically, our study contributes to the growing literature on interdependent infrastructure systems risk and resilience modelling (Ouyang, 2014; Hosseini et al., 2016; Bešinović, 2020), where lack of access of precise interdependency data integrated with simulation modelling is often seen as a major gap in most studies. The study also has value for railway asset owners and operators by showing how theoretical ideas emerging from resilience engineering can inform real-world resilience planning, which is often missing in translating large-scale interdependent systems research into practice (Hickford et al., 2018).

Firstly, we describe the methodical process for building a topological model of the entire rail network complete with all its interdependencies. Secondly, we discuss the building

of a journey assignment and disruption model which allows train journeys to be correctly assigned to their actual multi-track routes based on a real-world operational timetable. Next, we combine both models into a single integrated rail infrastructure network model which allows us to correctly simulate failure propagation and evaluate the systemic performance of train and passenger delays in a single model. Finally, we integrate the failure propagation analysis with recovery decisions towards quantifying resilience outcomes for different failure and recovery scenarios. We then demonstrate the application of our model and methodology to Great Britain's rail network by evaluating the resilience of the southern region network to threats on its traction power system.

5.2 Resilience assessment methodology

In Figure 5.1 we present an illustration of the resilience assessment framework developed for this study. The framework, which is divided into three distinct steps, provides a methodical workflow that can be adopted for the resilience assessment of rail networks, each of which is described in the subsequent sub-sections.

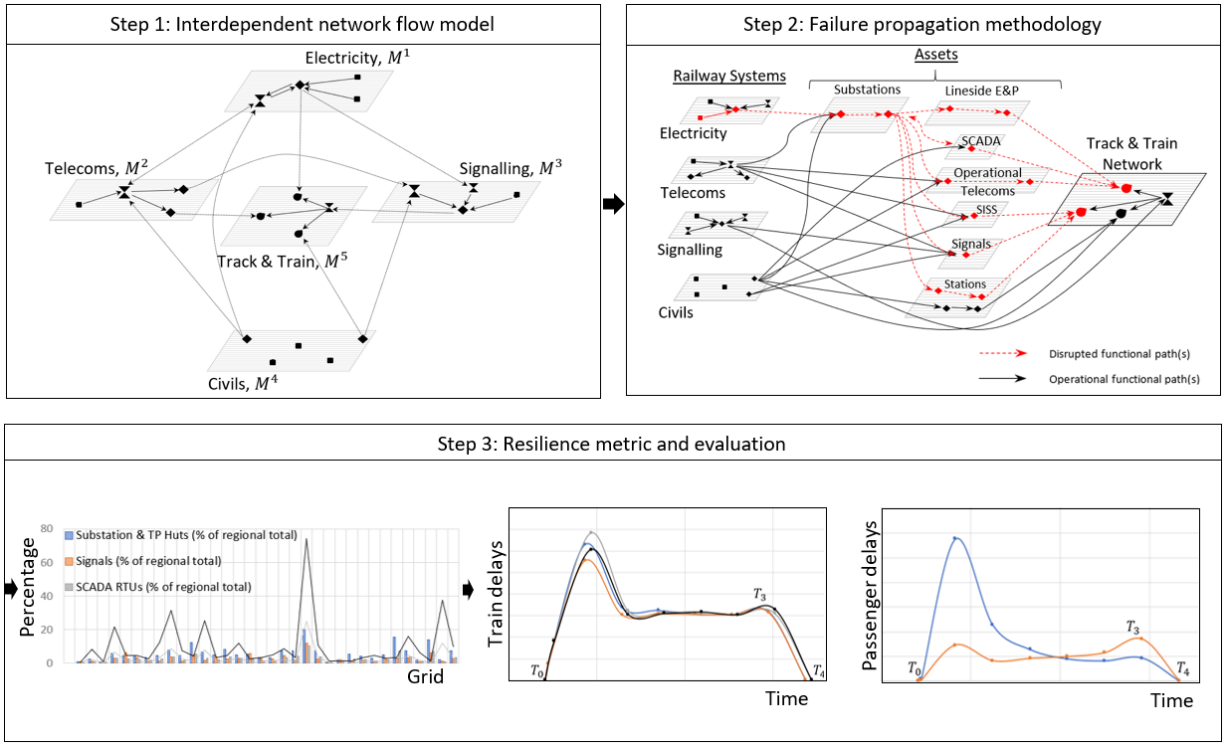

Figure 5.1 Resilience assessment framework for technical systems of rail networks

5.2.1 Interdependent network flow model

The first step in our methodology is the presentation of a network-based approach for building the spatial and topological model of the rail network. We start by identifying the respective infrastructure systems which make up a typical rail network. These include electricity, permanent way, signalling, civils and telecommunication systems. Assuming that these are represented by g number of systems, the rail network can be denoted by the set $M = \{M^1, \ldots, M^g\}$ where each system, $M^i \in M$ is a graph comprising nodes and edges such that $M^i = (N^i, E^{i,i})$. We denote $N^i = \{n_1^i, \ldots, n_z^i\}$ as the set of z nodes and $E^{ii} = \{e_{jv}^{i,i} = (n_j^i, n_v^i) \subseteq N^i \times N^i\}$ as the set of edges which defines the connectivity that exists across nodes in the system M^i. This means that the edge element $e_{jk}^{i,i}$ connects the nodes n_j^i and n_k^i in M^i. Next, we represent the interconnectivities that exist across the respective infrastructure systems in our network model by the set $E^{i,u} = \{e_{jv}^{i,u} = (n_j^i, n_v^u) \subseteq N^i \times N^u\}$ and create the rail network graph by combining all the node and edge sets to form a system-of-systems such that $M = (N, E)$, where $N = \{N^1, \ldots, N^g\}$ and $E = \{E^{i,j} \forall i, j: 1, \ldots, g\}$.

All the nodes and edges in the network graph M are mapped to a cartesian coordinate system with nodes assigned point coordinates (x, y) to specify their location, while the edges represent line geometries connecting node points.

The operational functionality of the rail network relies on resource flows across its respective assets. Resource flow is defined here as the service provided by one asset to another or group of assets to facilitate operational functionality. For example, the flow of electricity from substations to conductor rails, command and control from lineside signals to trains, data communication transfer via Fixed Telecoms Networks (FTN) or wireless data links to substations. We classify all nodes in the network model as source, intermediary or sink nodes depending on their role in facilitating resource flows (Thacker

et al. 2017a) with flows originating from source nodes and terminating at sink nodes via intermediary nodes, creating functional paths. All the edges in the graph are modelled as directed edges and depending on the systems considered, could represent unidirectional or bidirectional flows. Nodes are also assigned attributes in the network model depending on their roles in facilitating resource flows. We make a distinction between bi-directional flows along the same edges and treat them as separate, i.e. $e_{i,j} \neq e_{j,i}$.

We represent the set of all source nodes in the graph M as O and the sink nodes as D. For a given source node $n_o \in O$ and sink node $n_d \in D$, the functional path $F(n_o, \ldots, n_d)$ represents the set of all nodes and edges that facilitate an uninterrupted route from the source to the sink. By mapping all functional paths between all sources and sinks in our model, we are able to create a set of all functional paths of resource flows $F = \{F(n_o, \ldots, n_d)\ \forall n_o, n_d \in O, D\}$.

The resource flows across the different systems that make up a typical rail network are shown in Figure 5.2 and this illustrates the directionality of resource flow across the system-of-systems and how it eventually facilitates train journeys on the track network. For example, $F = \{n_2^1, n_{11}^3, n_{10}^3, n_{20}^5\}$ represents the resource flow paths from the electricity system to signalling systems for the facilitation of train services on the track and train system.

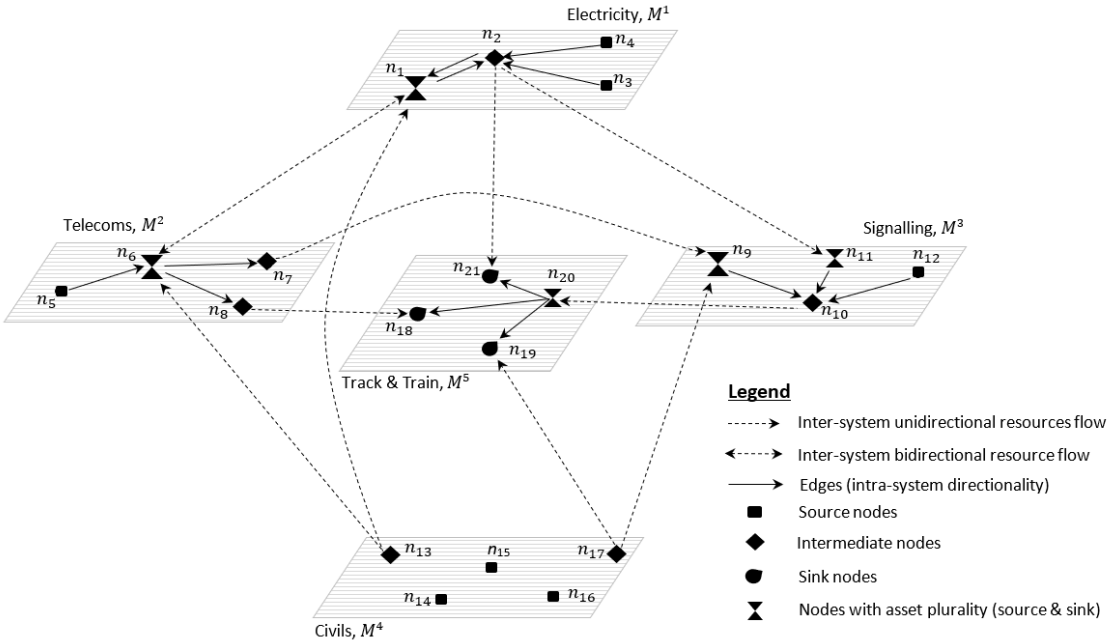

Figure 5.2 System-of-systems representation of the rail network showing resource flows across its different systems

Flows of trains within the rail network are a particular version of source-sink relationships, whereby origins are sources and destinations are sinks, along with a series of intermediate station stops. The routing of trains along origin-destination paths is governed by timetables. These flow patterns, and the implications of disruption to them, was proposed in the multi-track journey disruption model developed by Ilalokhoin et al., (2021) and presented in Chapter 4 of this thesis. This multi-track journey disruption model involves building the topology of the railway based on its network architecture and using a rail timetable to develop a rail trip assignment model which allows for the correct traversing of train journeys through their actual track routes and passengers assigned to trains on the network. We build both models to a common cartesian coordinate system which allow for the merging of the rail infrastructure network model with the multi-track journey model to form an integrated rail infrastructure network model based on their common track systems geospatial attributes.

5.2.2 Failure propagation methodology

We model failure as the interruption to functional paths of resource flows and this is initiated when a set of nodes and edges are physically disrupted or can no longer operate

due to an external shock event. A practical example is when a security breach in the Supervisory Control and Data Acquisition (SCADA) system results in disruption to telecommunication data flow from the Master Terminal Units (MTU) to Remote Terminal Units (RTU) at trackside electrical substations, leading to the interruption of communication and power supply from substations to track conductor rails and eventual disruption to train services. We denote the collection of all disrupted functional paths of resource flows between sources and sink nodes by the set $\bar{F}$, which are obtained from the set of the previously mapped functional paths. Depending on the linkages that exist between the respective asset systems in M, the failure to a single asset's functional path can result in disruption to several other functional paths across the network. This is referred to as a failure cascade across networks. To represent failure cascades, we assemble the set $\bar{F}$ in an ordered sequence of disruptions of assets and the functional paths that exists across different nodes in the network graph. Following an external shock event, the directly failed nodes are collated in the set of $\bar{A_0}$ whose failure in turn triggers an ordered failure to functional paths. Assuming there are q ordered sequences of failure cascades, the sets $\bar{F}_1, \ldots, \bar{F}_q$ denote the collection of indirectly failed assets disrupted in the ordered sequence, and the total failure as a result of these is the union of the set, such that $\bar{F} = \bar{F}_1 \cup \ldots\ldots \cup \bar{F}_q$. The complete set of all failed assets, either directly or indirectly are given by the set $\bar{A} = \bar{A_0} \cup \bar{F}$. In Figure 5.3 we describe an example of an ordered sequence of cascading failure following disruption to the electricity system. It shows that an external shock event results in the failure of node n_4 on the electricity system which in turn triggers a series of cascading failures, disrupting several functional paths through node n_2 in the electricity layer and affecting intermediary nodes across several sub-systems. This then leads to the failures of sink nodes n_{31} and n_{34} on the track and train network. The failure path is shown in red.

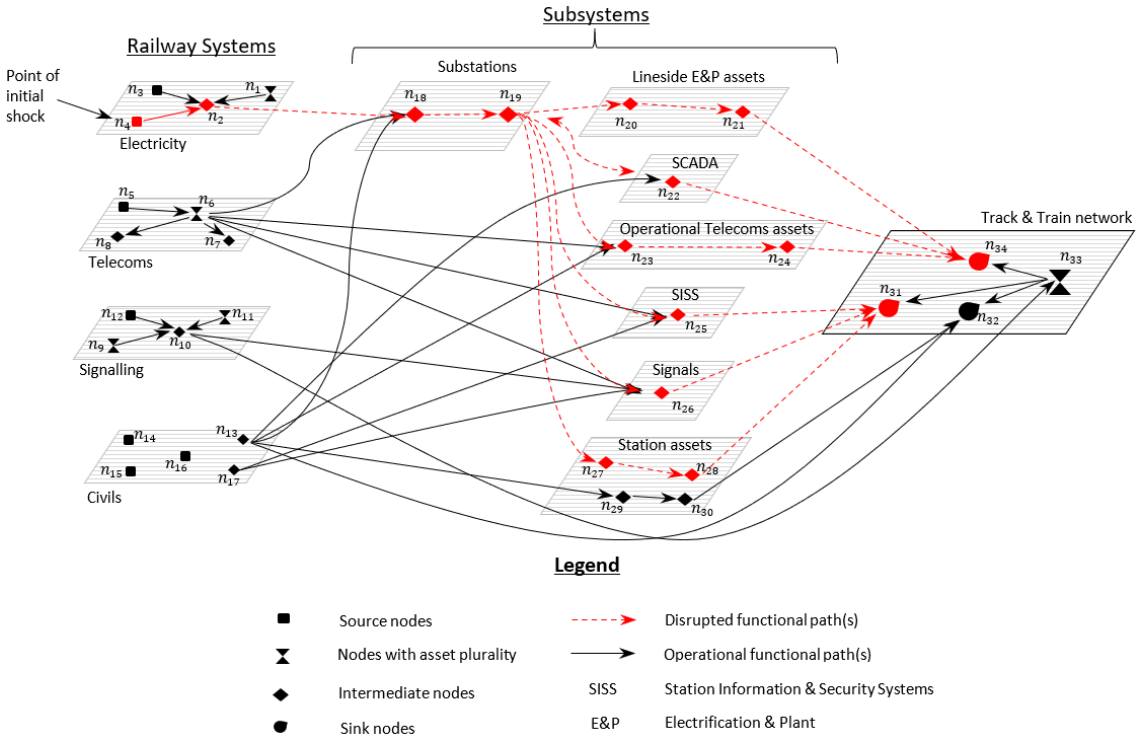

Figure 5.3 System-of-systems representation of the failure cascades across the rail network showing functional paths for each system disrupted due to failures originating in the electricity system

5.2.3 Resilience metric and evaluation

At the pre-disruption state, the total train delay minutes accrued is zero and the rail network is assumed to operate according to the set timetable. Following an external shock event, the disruption in asset functionality that follows results in the degradation of network performance and an increase in delay minutes, the magnitude of which is determined by the network's capacity to cope with disruption. Resilient critical infrastructure networks provide some level of service even in a degraded state (IRGC, 2006) as well as have the capacity to mobilise backups and alternative pathways to ensure continuity or some level of service during disruption. Figure 5.4 shows the evolution of the post-disruption delay minutes, with the sequence of different resilience strategies that help train services to recover from the initial disruption. At the onset of disruption at time T_0, the first resilience action on the network is the mobilising of backups which comes into effect at time T_1. The time taken to regularise services depend on the level of service displacement as well as a number of factors, including the reserve network headway

capacity, inbuilt timetable recovery times, network constraints, train stabling facilities, train staff and crew availability and passenger demand profile (MTI, 2015). Depending on the magnitude of the disruption, train delays can continue to accrue until services are regularised.

The strategies for service regularisation often require the implementation of service recovery protocols and/or physical interventions. These protocols include (i) do nothing option, (ii) de-training, (iii) holding some or all trains on the line, (iv) taking some or all trains out of service, (v) service diversion, (vi) running shuttle services and (vii) trains running fast through certain stations (Schmöcker et al, 2005). Therefore, when backups are mobilised, it does not necessarily result in an instantaneous reduction in the rate of increase in delay minutes, but is instead preceded by an initial further increase in delay minutes because the initial measures instituted to regularise train services can often result in further disruption in the short term. This is represented by the first parabolic section of the resilience graph in Figure 5.4 between T_1 and T_2. Eventually, the combination of the backups and train service regularisations result in the reduction in the rate of increase in delay minutes and the stabilising effect from this is represented in the section between T_2 and T_3 in Figure 5.4.

Following the completion of asset repair at T_3, service recovery to pre-disrupted levels is restored at T_4.

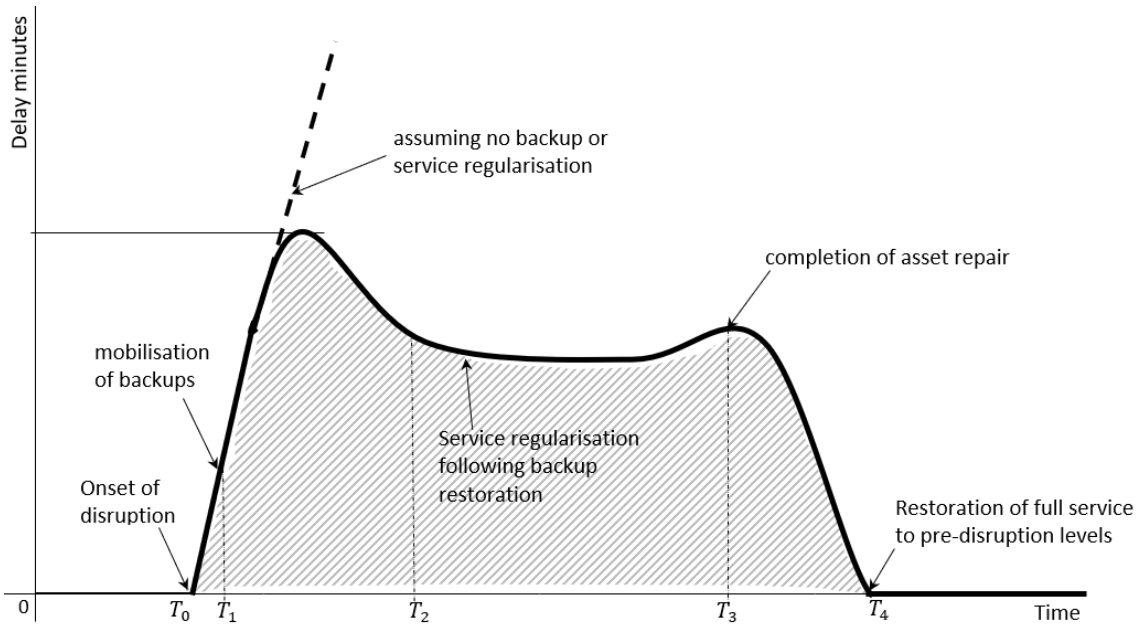

Figure 5.4 Network performance and resilience quantification using delay minutes

Recovery time is defined as the time taken to restore the network to its pre-disrupted state and is estimated for each external shock event and failure scenario. This timeframe, shown in Figure 5.4 as the time taken from T_0 to T_4, depends on a number of factors, which include the availability of resources - repair crews and replacement parts, money, time taken to travel to the damaged asset, repair timescale and time taken to regularise services. Modelling the constraints of availability of resources, money and the time taken to arrive at the failed asset is beyond the scope of this study as it requires the coupling of complex resource schedules, finance and road network modelling at national scale. However, Railway Undertakings have specialist maintenance delivery units which are equipped with dedicated and funded repair teams to carry out prompt repairs to critical rail assets to facilitate the restoration of train services to pre-disrupted levels (ORR, 2018). The time taken to repair the failed asset will depend on the location and type of asset damage, with historical outage and repair data serving as a useful source of empirical repair timescales for different categories of assets (Kelly-Gorham et al., 2019; Cadwallader, 2012).

We estimate delays to train services using the integrated rail infrastructure train and passenger journey assignment model described in Ilalokhoin et al. (2021), whose main

steps and equations are discussed below. We classify train delays into three different types - direct delays, reactionary delays and reliability (cancellation) events (DAB, 2019). Direct delays are those which result from the failure to assets in the set of $\bar{A}$, while reactionary delays occur as a result of knock-on effects to secondary trains affected by direct delays. When a failure event leads to train cancellations, diversions or failure to call at a scheduled stop, this is referred to as a reliability event (DAB, 2019:17). When an external shock event results in asset failure, this can result in a change in train running times which leads to train delays. These delays can be further aggravated by the increase in train dwell times at stations especially during peak times when increase in passenger numbers and change in behaviours influence boarding and alighting times (Kariyazaki et al., 2013).

The track nodes in the set of $\bar{A}$ include the primary delay nodes and represent the points on the rail network where delays are initiated. The total delay minutes attributed to $\bar{A}$ are obtained by collating the set of all the affected primary routes $P = \{P_1, P_2, \dots, P_l\}$, secondary routes $S = \{S_1, S_2, \dots, S_m\}$, and cancelled routes $C = \{C_1, C_2, \dots, C_r\}$ for all trains services affected between times T_0 to T_4 in Figure 5.4. A route (P_i or S_i) refers to a train's journey path and is the collection of nodes and edges on the track and train network traversed between the origin station where the train journey starts and the destination station where the train journey terminates. The delays associated with the primary delay nodes are called primary delays, $d(p)$, and are obtained by finding the time difference in minutes between the disrupted train service and the next passing train through the affected node. When a hazard event delays a train, pending any recovery action, the next train will be delayed by at least $d(p)$.

In rail networks, the operational signalling headway is defined by the minimum safe distance between trains to keep them safely separated without the need to reduce train speed. If $d(p)$ is less than the signalling headway, we assume that the delays are small

enough to be accommodated within the existing network capacity without resulting in the cascade of delays to other trains on the route. Reactionary delays on the other hand are said to occur when the primary delays exceed what is allowed for in the signalling headway. Therefore, to maintain the headway and safe distance between trains, subsequent trains would need to be delayed, resulting in knock-on effect to other trains on the network. To estimate this delay, we first find the delay threshold in minutes, d_{tr} beyond which this delay occurs by calculating the minimum non-disrupted time difference between the times when a primary route train and the next secondary train passes through a Fixed Time Block b (Ilalokhoin et al., 2021). The general sequence of trains through a node is represented by the generalised time sequence

$t_0(p) < t_0(s) < t_1(p) < t_1(s) < \cdots < t_k(p) < t_k(s), where\ t_j(s) - t_j(p) \leq b\ \forall\ j \in \{0, .., k\}$, then

$$d_{tr} = \min_{j \in \{0,..,k\}} \left(t_j(s) - t_j(p)\right) \tag{5.1}$$

Where $t_0(p), t_1(p) \ldots t_k(p)$ and $t_0(s), t_1(s) \ldots t_k(s)$ represents the pre-disruption train times in sequence on the primary and secondary route respectively starting from the first disrupted service to the k disrupted service.

The delay associated with the primary route with trains arriving at times $t_0(p), t_1(p), \ldots, t_k(p)$ before disruptions and delayed times $\tilde{t}_0(p), \tilde{t}_1(p), \ldots, \tilde{t}_k(p)$, where $\tilde{t}_j(p) \geq t_j(p) \forall\ j \in \{0, \ldots, k\}$ after disruption is estimated as:

$$d(p) = \sum_{j=0}^{j=k} \left(\tilde{t}_j(p) - t_j(p)\right) \tag{5.2}$$

Delays on the secondary routes are only triggered if $d(p) \geq d_{tr}$, and can be estimated in terms of the pre- and post-disruption time difference of same trains on such routes:

$$d(s) = \sum_{j=0}^{j=k} \left(\tilde{t}_j(s) - t_j(s)\right) \tag{5.3}$$

Reliability events result in a fixed delay time penalty, $d(c)$ which is based on a set of pre-defined service group delay codes for each route (Ilalokhoin et al., 2021). Cancellation penalties are issued by Service Group based on the location of the route where the

cancellation delay occurs. The cancellation minutes for a particular Service Group reflect the average time in minutes that a passenger has to wait to board the same or alternative train to their destination following a cancellation of a train service. Therefore, at stations where there are more frequent trains going to a specific destination, the minutes attributed to a specific cancellation event will normally be smaller compared with areas with less frequent trains

Reliability events are only triggered when the primary delays exceed the fixed time penalty, i.e., $d(p) \geq d(c)$. This happens when the route capacity is exceeded, as more than the allowable number of trains might need to be accommodated on the route under the planned train timetable, so some trains are cancelled and assigned a fixed time penalty (Ilalokhoin et al., 2021).

The delay minutes on these routes are estimated and collated in sets as $D(P) = \{d(p_1), d(p_2), \ldots, d(p_l)\}$, $D(S) = \{d(s_1), d(s_2), \ldots, d(s_m)\}$, and $D(C) = \{d(c_1), d(c_2), \ldots, d(c_r)\}$.

Total train delays on primary, secondary and cancelled routes are estimated as:

$$v_p = \sum_{i=1}^{i=l} d(p_i) = \sum_{i=1}^{i=l} \sum_{j=0}^{j=k} \left(\tilde{t}_j(p_i) - t_j(p_i)\right) \tag{5.4}$$

$$v_s = \sum_{i=1}^{i=m} d(s_i) = \sum_{i=1}^{i=m} \sum_{j=0}^{j=k} \left(\tilde{t}_j(s_i) - t_j(s_i)\right) \tag{5.5}$$

$$v_c = \sum_{i=1}^{i=r} d(c_i) \tag{5.6}$$

The total train delay is obtained by finding the aggregate of Equations 5.4, 5.5 and 5.6 for all delays at each time block between time intervals $T_1 - T_0, T_2 - T_1, T_3 - T_2, T_4 - T_3$ respectively.

To obtain the passenger delay minutes, we model rail stations as nodes using their geospatial properties. Our network model is set up such that when passenger usage data on a rail network is available, it is possible to assign these to each train service on the rail timetable such that when there is a disruption to any part of the network, the model simulates the rail timetable and extracts the rail stations and number of passengers affected by a hazard event in the disrupted routes *P*, *S* and *C.* For example, in Great Britain, passenger usage data is available from MOIRA (Model of Inter-Regional Activity) which is an elasticity-based travel demand and forecasting passenger usage model that uses a ticketing and revenue database to allocate passengers to trains (Worsley, 2012).

Similar to the train delay methodology, the total number of disrupted passengers following the failure of the nodes in $\bar{A}$ are obtained by first collating the set of all the affected primary routes P, secondary routes S, and cancelled routes C for all trains services scheduled between T_0 to T_4. On each route, the MOIRA model provides the number of passengers loads at each station and on a train between stations. We collate the number of disrupted passengers across the primary, secondary and cancelled route in sets as $\{n(p_1), n(p_2), \dots, n(p_l)\}$, $\{n(s_1), n(s_2), \dots, n(s_m)\}$, and $\{n(c_1), n(c_2), \dots, n(c_r)\}$ respectively, and estimate the number of disrupted passengers using Equations 5.7 – 5.9.

$$w_p = \sum_{i=1}^{i=l} n(p_i) \tag{5.7}$$

$$w_s = \sum_{i=1}^{i=m} n(s_i) \tag{5.8}$$

$$w_c = \sum_{i=1}^{i=r} n(c_i) \tag{5.9}$$

The total passenger delay minutes (PDM) for all disrupted passengers in the time block *b* is obtained by finding the sum for the passengers delayed for all affected routes.

$$Passenger\ delay\ minutes\ (pdm) = v_p w_p + v_s w_s + v_c w_c \quad (5.10)$$

The overall PDM is estimated by aggregating Equation 5.10 between time intervals $T_1 - T_0, T_2 - T_1, T_3 - T_2, T_4 - T_3$ respectively.

5.3 Application of methodology: Case study of the Southern Region passenger network in Great Britain

We demonstrate the application of our model and methodology using a case study of the southern region of the rail network in Great Britain and study its resilience to threats on its traction power systems. In Great Britain, Network Rail owns and manages most of the mainline railway including the southern region of the rail network. The southern region covers a wide range of rail routes connecting Dorset, Hampshire, East and West Sussex, Surrey, Kent and South London including the High Speed route. Stretching over 3,300 miles of railway infrastructure, it is one of country's most strategic rail region, the location of three of the top four busiest train stations nationwide (ORR, 2020a) and a significant contributor to rail public performance measures (PPM) nationally, accounting for a third of all mainline rail journeys (ORR, 2019).

5.3.1 Railway dependence on the traction power network and SCADA systems

Traction power is the electricity supplied from the electricity grid to substations or feeder stations to run electrified trains. The electrified section of the network comprises two main electrification systems which provide Alternating Current (AC) and Direct Current (DC) for traction power supply. Electricity is transmitted at high voltages from a transmission network, usually at 400kv and 275kv over long distances to licensed Distribution Network Operators (DNO) at 132kv and below in England and Wales. The DNOs distribute electricity to a number of strategically located traction grid supply points which serve as entry points for electricity into the rail network and from where traction power is provided to trains via a network of strategically located feeder stations for 25kv AC and substations/track parallel huts (TP huts) for 750v DC. The electrified section of the southern region of the rail network relies on 750v DC third rail traction power. This is typically fed from grid supply points which are connected to conventional 3 phase AC supplies at 33kV and converted to DC at trackside rectifier substations spaced at 6-8km

intervals along the rail network from where traction power is supplied to conductor rails (or third rail) via train conductor shoes. Between several substations, TP huts, which are effectively smaller substations, are used to improve the voltage profile of the third rail and reduce losses (Network Rail, 2017). The traction power grid forms a *'ring'* of power supply such that when a specific grid supply point fails, it is possible to mobilise existing backup power supply from an adjacent functioning grid supply point by closing the circuit breakers on the High Voltage (HV) distribution system.

A core part of the traction power system is SCADA, which is a control system architecture that provides remote control supervisory control and management with plant and equipment through data communication links. The SCADA master station provides a communication interface for Network Rail to remotely control and monitor traction power and distribution for the rail network, including track isolations and implementing automatic execution and service restorations actions. This is made possible by integrating Remote Terminal Units (RTU) in electrical substations to provide telemetry and remote-control links to traction substation equipment including rectifiers, transformers, switchgears and circuit breakers. Using high speed fibre optic connectivity, the RTUs are interfaced with the Master Terminal Units (MTU) which are centrally located at Network Rail's control centres. These RTUs collect details about the traction power equipment on the rail network and are equipped with alarm points inputs. When an input returns information which contains values outside of safe established parameters, the RTU sends alert to the MTU where they are sorted and prioritised to designated responders who assign the necessary response options and actions to the problems.

5.3.2 Interdependent network assembly

We mapped all the system-of-systems assets and interconnections in southern region that included the grid supply points, rectifier substations, TP Huts, signalling supply points and SCADA asset nodes by obtaining their real-world geospatial coordinates from

Network Rail's GeoRINM (Geo-Railway Infrastructure Network Model) asset repository (RailEngineer, 2015). At the time of this study, a complete as-built SCADA dataset for the southern region was unavailable on GeoRINM. However, we relied on available data from the high-level data structure of the Traction Power Centralised Management System (TPCMS) upgrade works to map the SCADA system (Infrarail, 2018). We map the interconnectivities that exist between asset nodes by modelling the physical cables or remote connections between asset nodes as edges in the network graph such that the modelled topology replicates the real-world configuration of the Network Rail's 50Hz HV distribution system for the southern region rail network.

A list of all the asset types and numbers collated for this study is presented in Table 5.1 and a spatial representation is shown in Figure 5.5. All the 34 traction grid supply points in the southern region are shown in Figure 5.5 and are referred to throughout this study according to the labels Grids 1 – 34 as to conceal their actual spatial location.

System	**Asset type**	**No. assets**	**Asset coverage across region**
Electricity	Traction power grid	34	95%
	Substations	390	95%
	TP huts	261	95%
Signalling	Lineside signals	1,774	100%
SCADA	Remote Terminal Units (RTUs)	651	95%
	Master Terminal Units (MTUs)	7	95%
Track	Permanent Way	3,300 miles	100%

Table 5.1 List of rail systems, asset types, number of nodes and regional network coverage in rail network model for the southeast region.

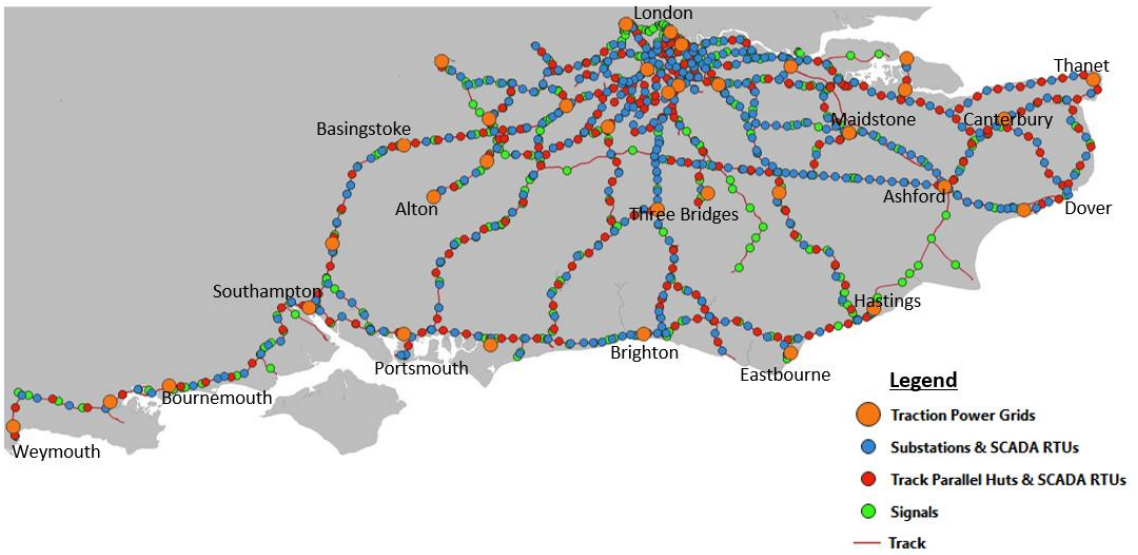

Figure 5.5 Geospatial representation of the high level structure of traction power assets in the southern region of GB's rail network.

5.3.3 Stress testing the model

To initiate failures in our rail model, we performed a stress test analysis which involved simulating the complete failure of a traction power grid supply point. This kind of failure can occur when there is a total loss of functionality or shut down of a specific grid supply point due to extreme weather events or even malevolent attacks. We simulated the exhaustive set of 34 failure scenarios that involved the targeted removal of each disrupted traction grid supply node from the network graph one-by-one. Such exhaustive simulated sampling of 'single point' failure scenarios has shown to be effective in highlighting the criticalities of different types of assets to the systemic performance of networks (Thacker et al., 2017; Thacker et al. 2017a; Pant et al. 2020). For each failure scenario we collated all disrupted sink nodes and functional paths in the set of $\bar{A}$ to create a failure database of directly and indirectly failed assets in accordance with the methodology described in Section 5.2.2. We also stress tested the rail network to 20 failure scenarios involving multi grid supply point failing simultaneously. Though rare, this is a practical failure scenario as evidenced by the national grid power generator failure of August 9, 2019 (ORR, 2020). For this analysis, we set geographical proximities as the criteria for selecting which of the grid supply points to fail in combination. This is similar to the existing approaches that

have looked at spatially correlated failures to Great Britain's rail network bridges in the context of extreme flood events (Lamb et al., 2019) and cyber-physical failures of electricity substations concentrated in a local area that impact several network including railways (Oughton et al., 2019).

To obtain the disruptive effect on train services, we used the rail disruption model to simulate the May 2019 national rail timetable and calculated the disruption to passenger train services and train delay minutes. Our analyses were carried out over two broad timeframes – for disruptions starting during peak and off-peak travel periods.

We replicated the resilience properties of the traction grids by simulating the mobilisation of backup traction power grids, taking into considerations (1) the time taken to deploy backups, (2) the extent of services restored by the backup system. The time taken for these backup systems to be mobilised can be an uncertain variable depending on how long it takes to carry out necessary safety checks before the all-clear is given by the Electric Control Room (ECR) Operator to deploy the backup systems. Even when backup systems are automatically deployed, this does not necessarily guarantee a zero loss time as the power failure of 9th August 2019 in England and Wales confirmed (ORR, 2020; Ofgem, 2019). For this study, we explore this uncertainty by simulating the time taken for backup restoration as a range in time steps starting at $T_1 = T_0 + 5$mins, i.e., 5 minutes from start of disruption event, until $T_1 = T_0 + 30$minutes. This allows us to observe the sensitivity of network performance metrics to the speed of mobilisation of backup systems. We limit our sensitivity analysis to 30 minutes because, first, the *'ring'* of power supply grid on the rail network means that every part of the electrified sections of the rail network has an alternative traction feed which can be mobilised quickly when a particular traction feeder section is out of service which demonstrates there is an inherent plan in the design of the electrified sections of the infrastructure network for power to be restored back to service quickly once there is a disruption. A practical example of this was the

power disruption discussed in ORR (2020) where the power service was restored in 3 mins and 36 seconds.

The nature of service disruption occasioned by power failure to the rail network is such that trains can become permanently locked-out and stranded, requiring a driver reset, and in extreme cases, an external technician to attend site which could lead to substantial knock-on delays (ORR, 2020). The effectiveness of the backup provided can be ascertained by estimating the disruptive impact on the network from varying the level of service. For our analysis, we have simulated service levels of between 50% to 100% of service restored between T_2 and T_3.

Following completion of repair, we simulated the restoration of train services to pre-disrupted levels. The rapidity of service restoration is driven by a number of factors, ranging from the level of disruption to the network, restorative capacity of the network as well as the incentives for quick service regularisation.

5.4 Results

5.4.1 Estimated assets and journey disruptions

In Figure 5.6 we plot the relationship between the failed assets and the number of disrupted services in the southern region of the rail network and this shows the correlation between the number of failed assets and the corresponding number of disrupted journeys. The results from the model simulations are presented in Figure 5.6. Due to unavailability of real-world performance data of these grids, real-world service validation of the output from the simulation has not been carried out, but the Figure 5.4 presents modelled outcomes from our simulation for if the failure of the identified grids occurs. The results show that grids located within the Greater London area accounted for 70% of the most critically affected when the metrics of assets and journeys disrupted were considered. For example, the failure of Grid 33, located in the Greater London area and which affects 2%

of all regional substations and TP Huts results in a disproportionate disruption to 37% and 12% of regional and national passenger train services respectively. Similarly, the failure of Grid 21, also in the Greater London area results in disruption to 75% and 25% of all train services regionally and nationally respectively. It is therefore possible to ascertain from this plot, each grid supply point's criticality to the systemic performance of the regional and national rail network. Also, Grids 4, 9, 12, 33 present interesting findings where very few assets disrupt a disproportionately high number of journeys. Conversely, the relatively high number of assets associated with Grids 11, 29 and 32 do not lead to a significant effect of journey disruptions suggesting that the assets associated with these grids are less critical in terms of number of journeys served.

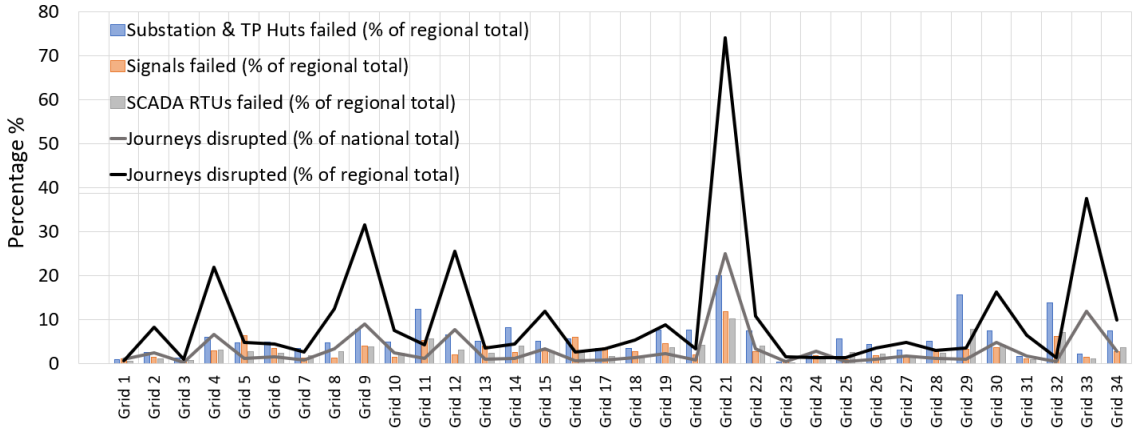

Figure 5.6 Single traction grid failure and interdependency assets affected

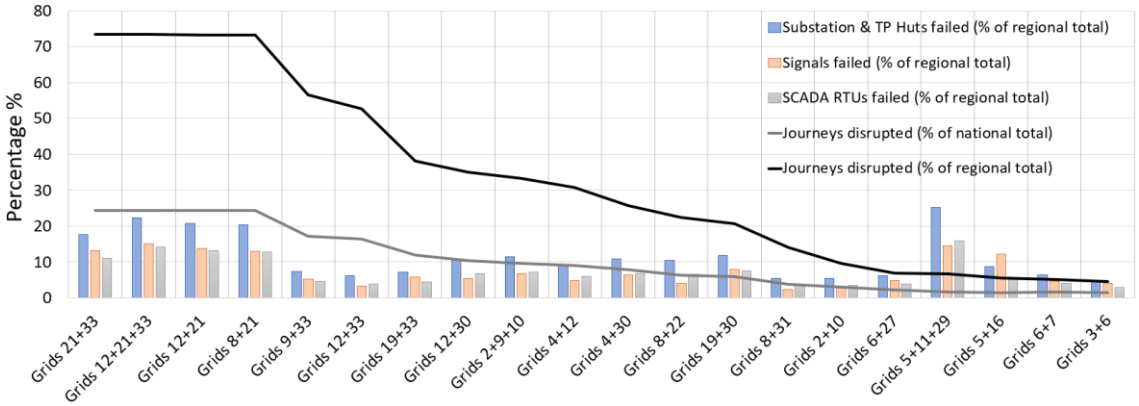

Figure 5.7 Multi traction grid failure and interdependency assets affected

The results shown in Figure 5.7 portray a clear disparity in network performance due to asset failure based on whether these assets were within the Greater London area or not. We find that while the failure of multiple grid supply points located outside London

resulted in increased disruptions to services than for a single grid supply point failure, those for the London area differed from this. For example, the first four failure scenarios shown on the left-hand section of Figure 5.7 which involved the failure of the critical Grid 21 in combination with other grid supply points showed that irrespective of the additional grid supply point failures simulated, as long as they were in combination with Grid 21, this resulted in a 75% and 25% disruption to services regionally and nationally respectively which was the same effect observed from the single failure of Grid 21.

Our multiple failure observation highlights that the southern rail network exhibits what we term a '*funnel phenomenon*' such that it acts like a large funnel, with the Greater London area located at the tip and serves as a conduit through which a disproportionate number of trains in the region navigate through and draw electricity from, on their way to their respective destinations. We find from our analysis of combined grid failures that even though other traction supplies from Grids 4, 9, 12 and 33 individually facilitated a high proportion of train journeys across the network, all these journeys at some point relied on Grid 21 either prior to, or as they arrived at their destination. Therefore, if Grid 21 failed prior to either of these other grids failing, most of the other grids in the region became redundant or significantly reduced in functionality as they wouldn't have trains to feed because these services were either already being delayed or put out of use by the failure of Grid 21 in London. This has a significant implication for the network's robustness as well as the planning and design of resilience alternatives for large, complex infrastructure networks as it presents a single critical point of failure with impact on the overall network performance. This explains why on the rail network in Great Britain, when there is a disruption in the London area, most of the southeast region and a significant portion of the national rail network also experience secondary effects.

5.4.2 Estimated train and passenger delays

In Figure 5.8 and Figure 5.9, we present the resilience performance plots for the respective failure analysis carried out for the traction grids supply points failing individually. Figures 5.8a and 5.8b shows the resilience graphs for failure analysis starting at peak and off-peak times respectively for all 34 traction grid supply points with disruptions occurring at T_0. For these failure scenarios, we simulated the initiation of backup at $T_0 + 15$ minutes. Following this, train delays were observed to accrue until train services were regularised to backup levels at T_2, in this case, assumed at 50% of full service. This continued until the end of asset repair at T_3. In Figure 5.8a, disruption was simulated to start at peak travel time and ended during off-peak travel, while in Figure 5.8b, disruption started at off-peak and service restoration coincided with the start of evening peak travel.

For all scenarios considered, the network resilience to traction grid supply failure is reflected by evolution of passenger delay minutes (PDM) or just train delay minutes following its failure. In Figures 5.8a and 5.8b, we find that the steepest rising gradients occurred in Grid 21 and 33, both of which our study found to be the most critical grid supply points in the region. An important output from this analysis was that for the southern region rail network, when the metric of train delay minutes was used, the calculated values of train delays accrued during peak and off peak travel times were not significantly different. The illustration of this is shown for Grid 21 in Figure 5.8c for peak and off peak train delay minutes. This reason for this can be attributed to the fact that in the southern region of Great Britain's railway, train frequency does not differ much between peak and off peak times. This raises an important consideration for resilience analysis, of whether the use of the metrics of train delay minutes, when used in isolation, is the most appropriate way of measuring the impact of failure on the network. This is because, in Great Britain, like many other western countries, this metric continues to be adopted for measuring network performance (ORR, 2020; NEA, 2003).

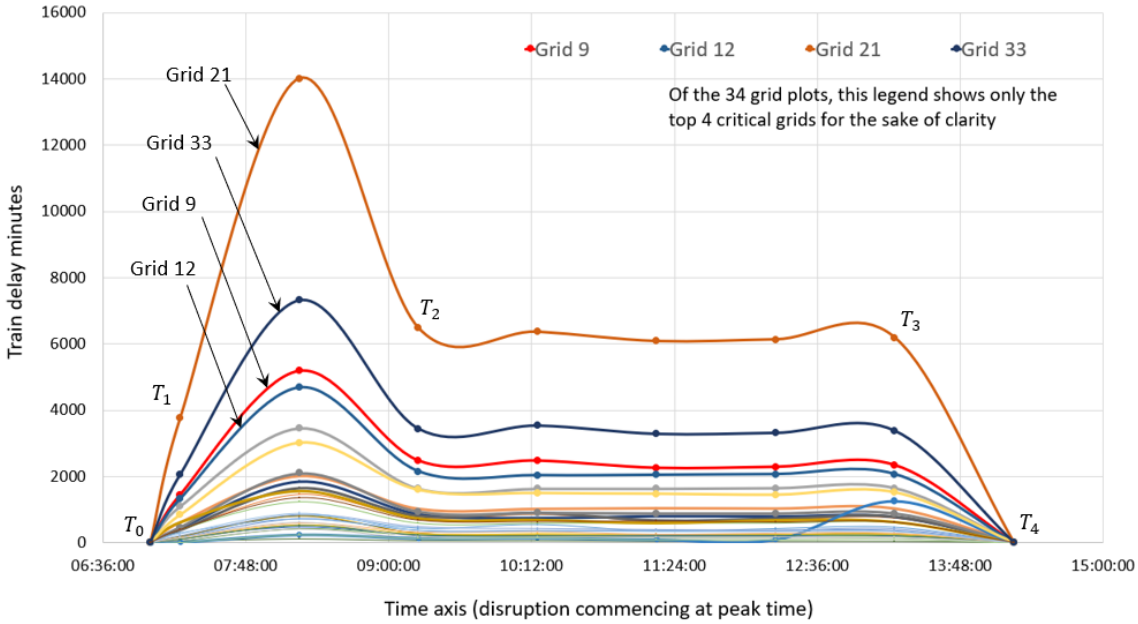

Figure 5.8a – Resilience graphs showing peak time failure analysis for each of the 34 grids using train delay minutes as resilience performance metrics. $T_1 - T_0 = 15mins$; $T_4 - T_3 = 60mins$ *with 50% backup service regularisation. Service recovery occurs during off peak period.*

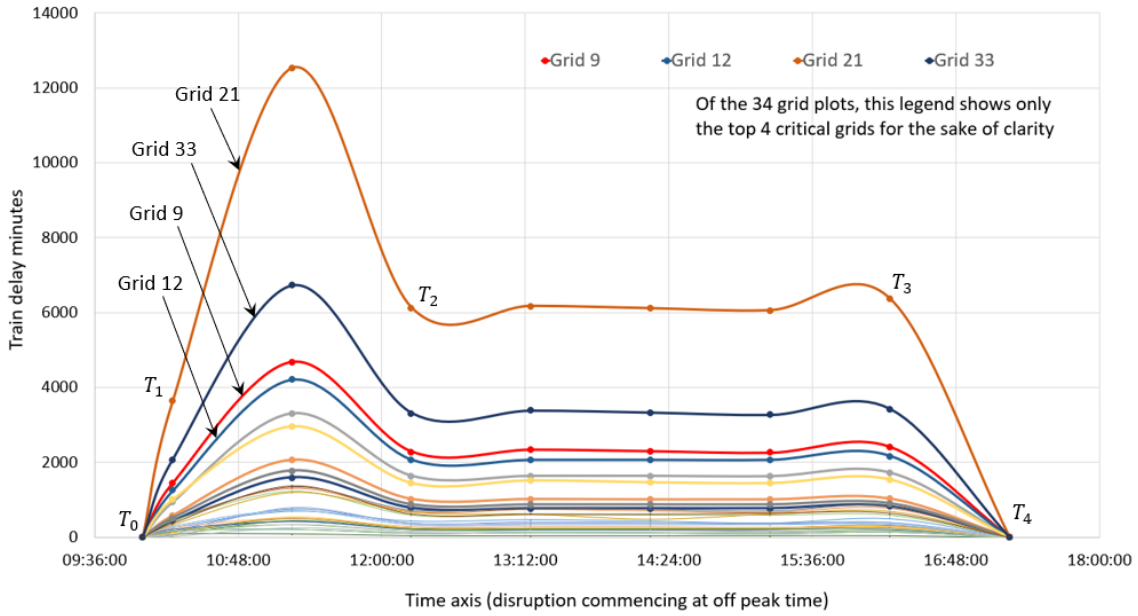

Figure 5.8b – Resilience graphs showing off peak time failure analysis for each of the 34 grids using train delay minutes as resilience performance metrics. $T_0 - T_1 = 15mins$; $T_3 - T_4 = 60mins$ *with 50% backup service restoration. Service recovery occurs at the start of evening peak travel*

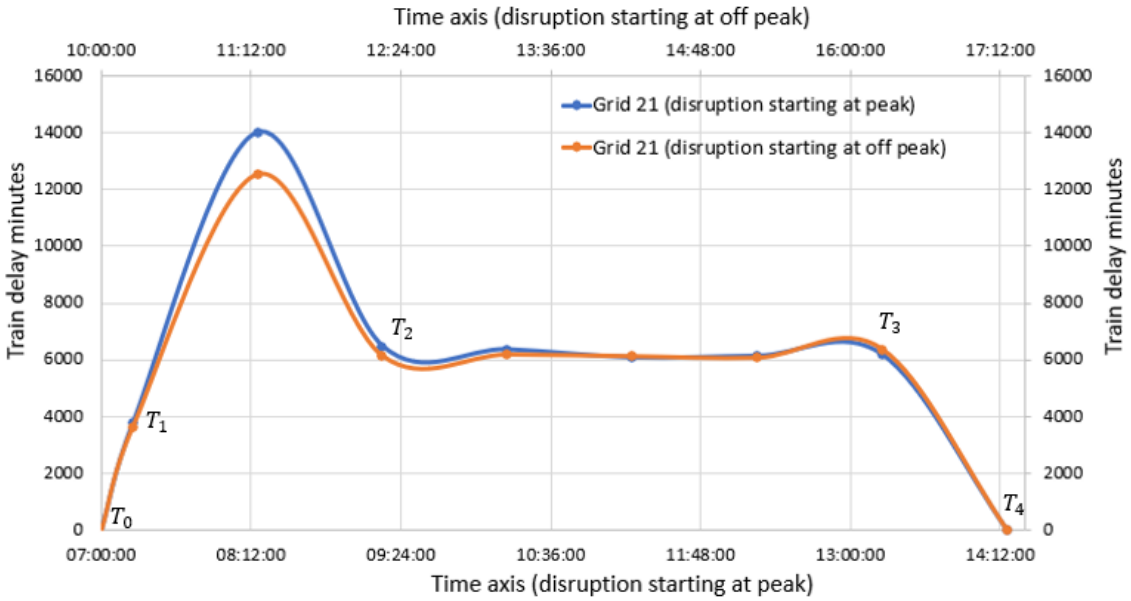

Figure 5.8c – Resilience graphs for Grid 21 showing the difference between disruption commencing at peak and off peak times using train delay minutes as resilience performance metrics. $T_0 - T_1 = 15mins$; $T_3 - T_4 = 60mins$ *with 50% backup service regularisation.*

Figure 5.8 Resilience graphs

Our study finds that the dichotomy between peak and off peak travel times, especially in the major cities, can be better reflected by passenger disruption metrics. To demonstrate this, in Figures 5.9a and 5.9b, we used the metric of passenger delay minutes and the methodology described previously to produce resilience performance graphs using the same resilience assessment analysis parameters considered for Figures 5.8a and 5.8b. The results of this analysis are presented in Figures 5.9a and 5.9b for peak and off-peak travel respectively for all 34 traction grids. Figure 5.9c is also specifically plotted for Grid 21 and shows a four-fold increase in passenger disruptions for disruptions occurring during peak travel when compared with off-peak travel. All three plots show the performance of the network at the respective stages between $T_4 - T_0$ for peak and off-peak travel. From Figure 5.9b, we can see how the restoration of services to pre-disrupted levels, represented by the time interval $T_4 - T_3$, resulted in increased PDM values, reflecting the fact that service restoration occurs at the start of evening peak travel.

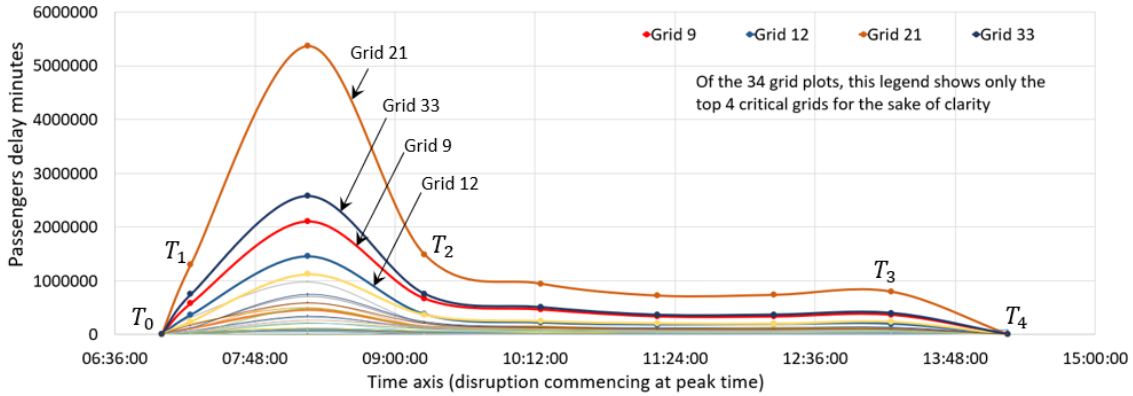

Figure 5.9a – Resilience graphs showing for each of the 34 grids using passenger delay minutes as resilience performance metric for disruption commencing during morning peak and ending during afternoon off team times. $T_1 - T_0 = 15mins$; $T_4 - T_3 = 60mins$ *with 50% backup service regularisation. Service recovery occurs during off peak period.*

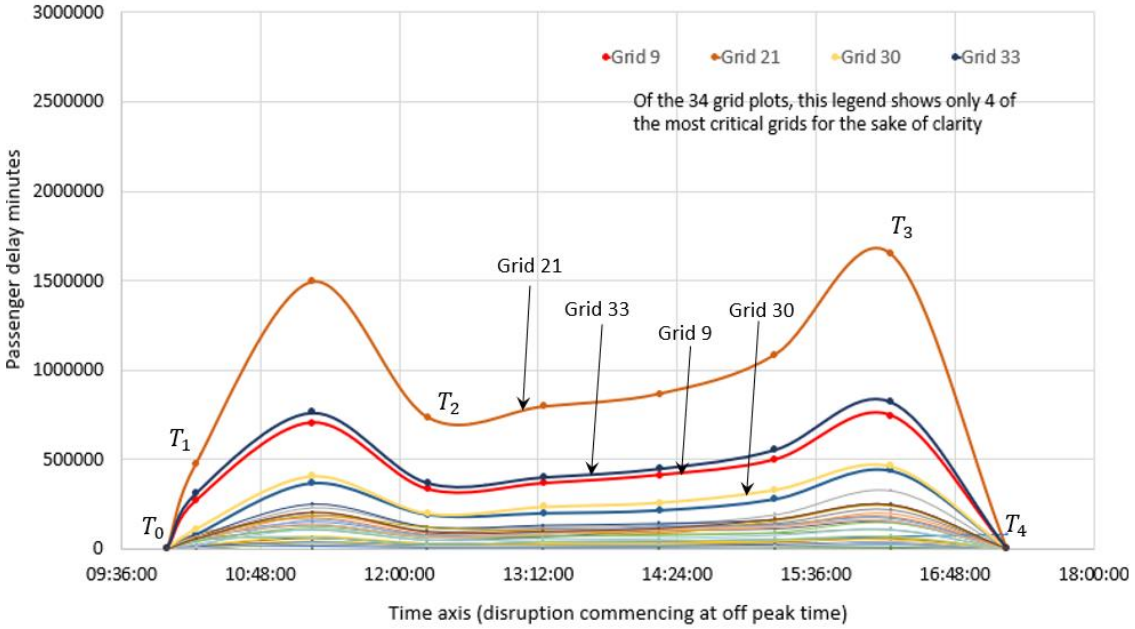

Figure 5.9b – Resilience graphs showing results of failure analysis for each of the 34 grids using passenger delay minutes as performance metric for disruption commencing during morning off peak and ending at evening peak times. $T_1 - T_0 = 15mins$; $T_4 - T_3 = 60mins$ *with 50% backup service regularisation. Service recovery occurs during start of evening peak travel.*

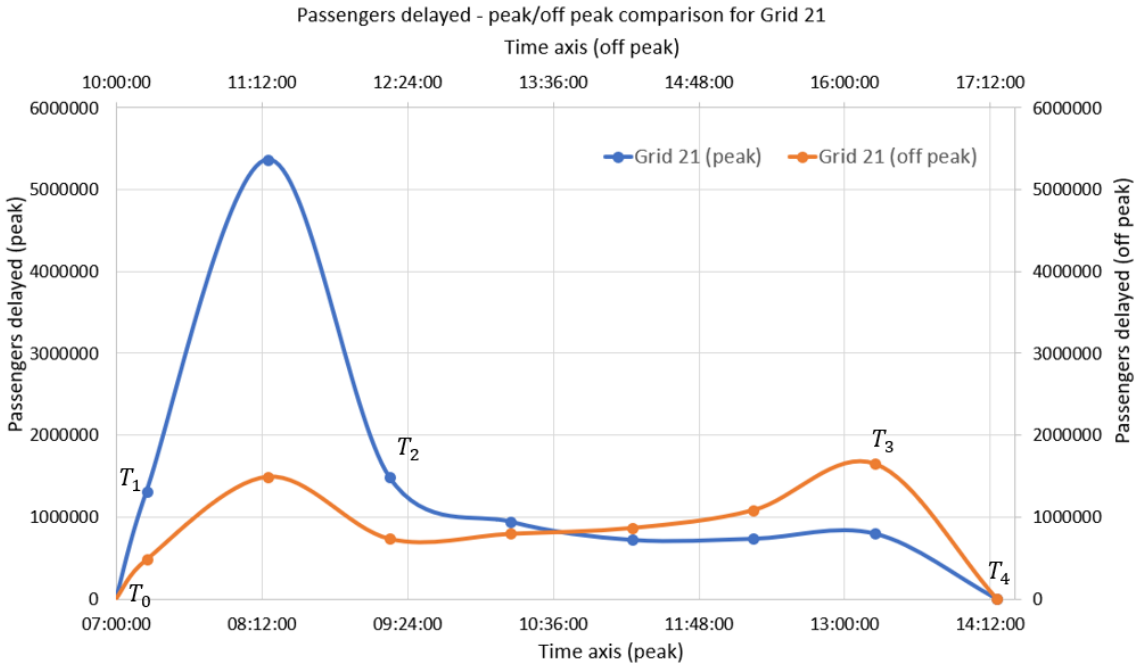

Figure 5.9c – Resilience graphs for Grid 21 showing the difference between peak and off peak time failure analysis using passenger delay minutes as performance metric. $T_0 - T_1 = 15mins$; $T_3 - T_4 = 60mins$ with 50% backup service restoration

Figure 5.9 Resilience graphs

From the resilience plots shown in Figure 5.8 and Figure 5.9, it is possible to ascertain the direct impact on systemic performance at every point during the time series of disruption for each failed traction grid supply points. In Figure 5.10 and 5.11, we focus specifically on the results from our study of the direct impact on systemic performance from varying the restoration of backup systems and plot the resulting delay minutes accrued at $T_1 = T_0 + 5mins$, $T_1 = T_0 + 15mins$, $T_1 = T_0 + 30mins$. This is shown for six of the most critical grids. Our results show that delaying the restoration of backup from 5 to 15 minutes resulted in on average, 2.5 times increase in both train and passenger delay minutes, while delaying backup restoration by 30 minutes resulted in about 4.5 times increase in the train and passenger delay minutes for both peak and off-peak travel. While the rate of increase was similar for both train and passenger delay metrics, when the absolute values were compared, the variations in peak and off-peak train delay minutes were on average 10% whereas this was 63% using the metrics of passenger delay minutes. This reinforces the findings discussed above on the use of

passenger delay minutes as a better metrics for comparing systemic performance and network resilience.

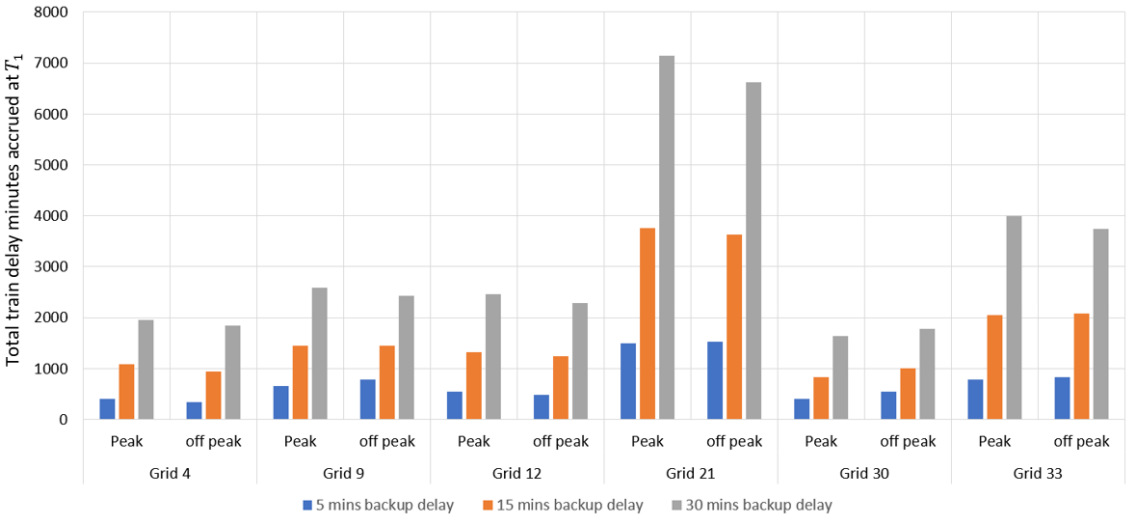

Figure 5.10 Plot showing the total train delay minutes accrued at T_1 when the backup restoration times were varied between $T_1 = T_0 + 5mins$ and $T_0 + 30mins$

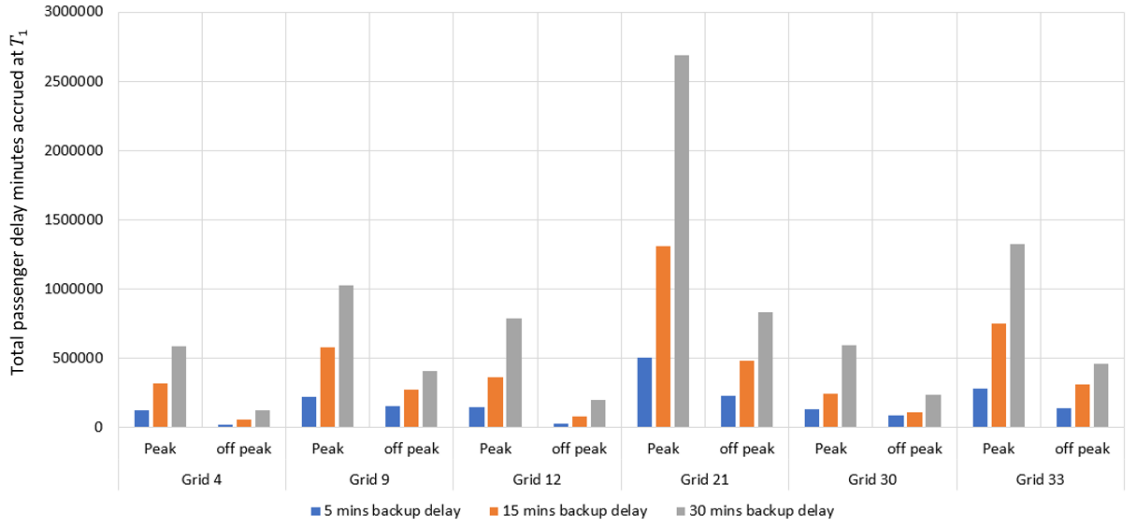

Figure 5.11 Plot showing the total passenger delay minutes accrued at T_1 when the backup restoration times were varied between $T_1 = T_0 + 5mins$ and $T_0 + 30mins$

In Figure 5.12, we present a spatial disaggregation of passengers numbers disrupted for each of the three different backup restoration timescales and plot the results for the failure of Grid 21. We can deduce from these, the spatial spread of passenger disruptions as a function of the time taken to deploy backup systems. We find that at $T_0 + 5minutes$, much of the passenger disruptions happening as a result of failure to Grid 21 was concentrated around the Greater London area which is where this grid is located. As the time taken to mobilise backups increases to $T_0 + 15minutes$, it can be seen from Figure

5.12b that passenger disruptions spread further out from London into the outer parts of the country. For example, passenger disruptions do not occur at Cambridge until $T_0 + 15minutes$. Similarly, at $T_0 + 15minutes$ and onwards, passenger disruptions which were previously limited to the London to Tunbridge Wells to Hastings lines spread across to stations on the line between Tonbridge and Folkestone. Figure 5.12c also shows that delays between Brighton and Littlehampton only start occurring at $T_0 + 30minutes$.

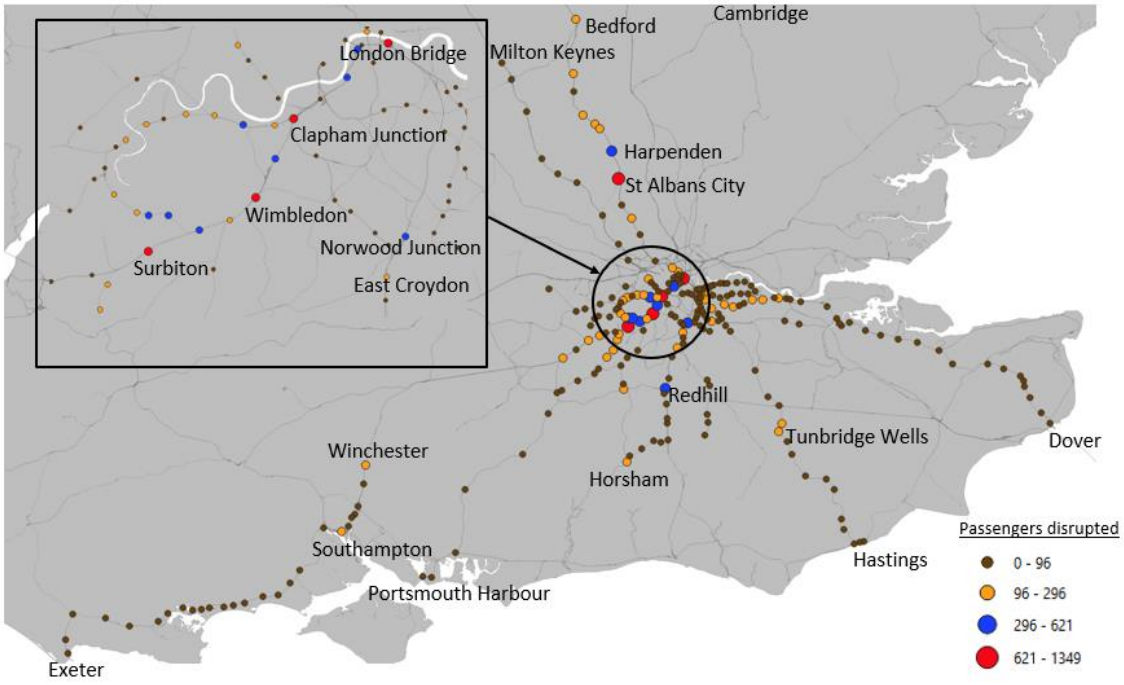

Figure 5.12a – Spatial plot of passenger disruption for Grid 21 based on a backup restoration at $T_0 + 5minutes$ – failure analysis for grid failure commencing during peak time travel times

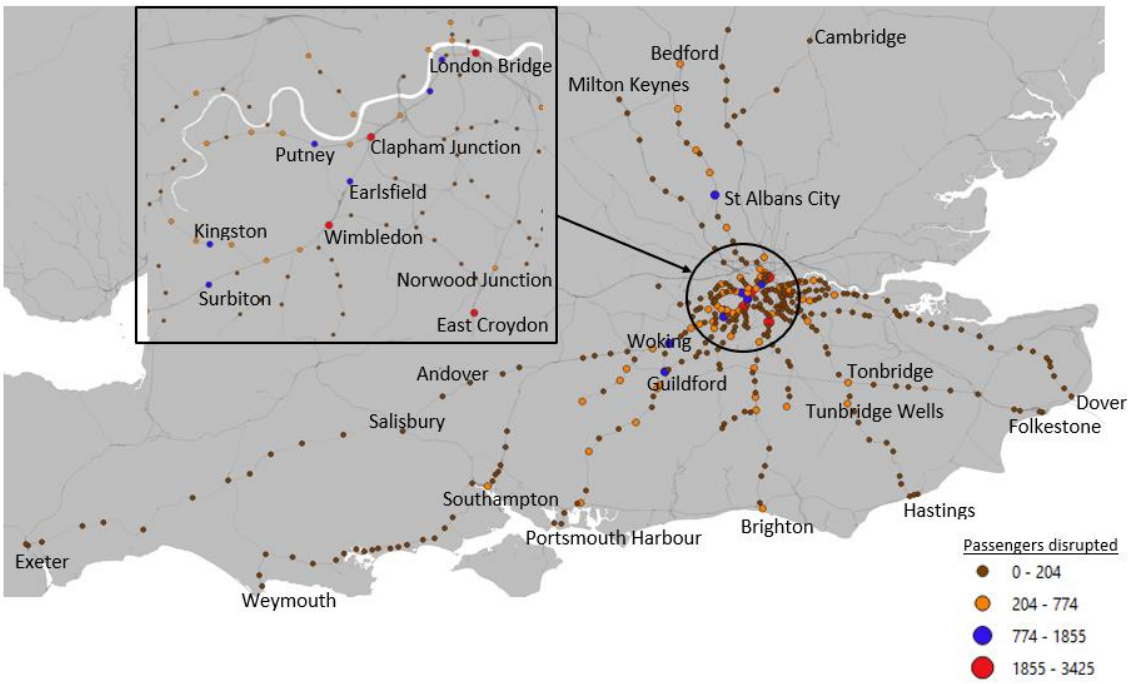

Figure 5.12b – Spatial plot of passenger disruption for Grid 21 based on a backup restoration at $T_0 + 15minutes$ – failure analysis for grid failure commencing during peak time travel times

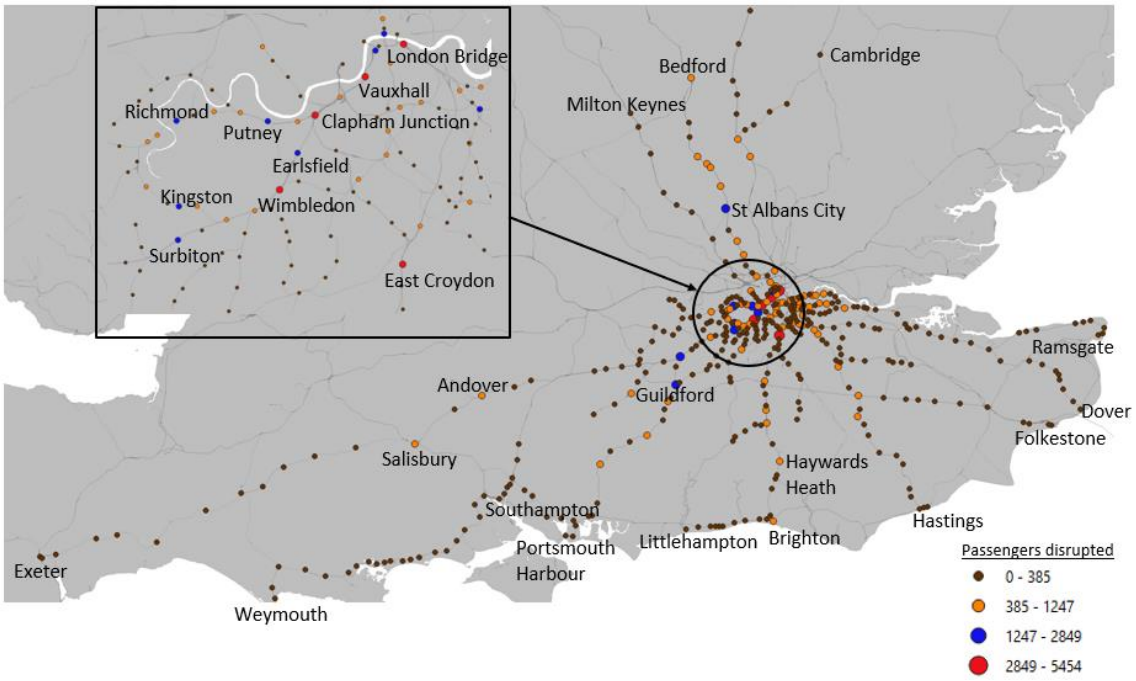

Figure 5.12c – Spatial plot of passenger disruption for Grid 21 based on a backup restoration at $T_0 + 30minutes$ – failure analysis for grid failure commencing during peak time travel times

Figure 5.12 Spatial plots

5.5 Conclusions

In this study we have developed a methodology and model for evaluating systemic performance and resilience of rail networks. System-of-systems models like that developed in this study present an excellent opportunity to correctly represent the complex interdependencies across infrastructure systems. We have demonstrated the development of a replicable model and methodology for rail systems and integrated this with a timetable and journey disruption model to simulate the functionality of real networks. This can be used to stress test the rail network, study systemic response and its resilience to hazard scenarios using the metrics of train and passenger delay minutes. This is a novel contribution to research in this area.

We have also successfully demonstrated the applicability of our model and methodology to stress testing and evaluating the resilience of the southern region rail network in Great Britain to scenarios of failure of the traction power system. The result from our analysis shows the extent of vulnerability of the network to the operational functionality of a small number of assets in the London area. The impact on network vulnerability is measured using the metrics of train and passenger delay minutes and our model produces an output of the spatiotemporal disaggregation of these impacts for each failure scenario, to inform a broad understanding of network performance. From the outputs of our analysis, we find that the southern region exhibits what we term the *"funnel phenomenon"*, with London acting as the tip of the funnel and a conduit which when disrupted, disproportionately affects the network's overall performance across the region and nationally. For example, 70% of all the most critical traction grids in the region are within the Greater London area. Also, the failure of one of the region's most critical electricity traction power grid disrupts 75% of all trains in the southern region and 25% of all trains nationally. Furthermore, we find that disruptions occurring during peak time travel have the most impact on the network when passenger metrics are used, with up to four-fold increase

between peak and off peak disruptions. This is in contrast with when the metric of train delay minute was used. We therefore argue for the use of passenger delay minutes as a more appropriate measure of systemic performance for the resilience assessment of rail networks.

In this study, we have also developed a set of resilience curves for traction grid asset systems of the southern region rail network in Great Britain and have demonstrated the impact on systemic performance metrics from varying the different resilience measures. For example, delaying the mobilisation of backups by 25 minutes resulted in up to 77% increase in passenger delay minutes. It is therefore possible to deduce from these resilience curves important systemic performance metrics that can inform resilience decision making. Our model and methodology and the outputs from this study therefore presents policy makers, engineers, designers, and infrastructure managers with useful evidence based decision support tools for practical and effective resilience decision making approaches on rail networks.

To further enrich the output from this study, we propose that future studies could focus on expanding our model and approach to incorporating the economic modelling of the impact of disruption and different resilience strategies to enhance the resilience assessment scenario planning and the decision making at policy level.

6 A flood risk assessment methodology for complex railway networks: application to the national rail network in Great Britain

Abstract

Rail networks comprise complex interdependent systems with extensive lineside and off-track assets which are exposed to extreme weather-related hazards. In this paper, a methodology is presented for flood risk assessment of large rail networks and is demonstrated on the national rail network in Great Britain which is analysed for the impact of river flood hazards, with the disruptive impacts measured in terms of direct asset damages, disruptions to trains and passengers, and economic losses. Our analysis of the national rail network finds that lineside railway assets are most vulnerable to flood hazards with about 31% of all track assets in Great Britain exposed to river flood hazards. London and the Southeast regions are the most affected by train and passenger disruptions, with both regions incurring about half of all train and passenger disruptions for river flood hazards nationally. Relatively frequent flood events are found to make the greatest contribution to overall risk, with floods with less than a 1 in 20 year return period resulting in 48% of all financial losses on the rail network nationally, most of which occurred in London and the southeast, with the northwest of England having the next highest losses. Our methodology and analysis findings can therefore provide infrastructure managers and decision makers with evidence for prioritising investments for network resilience.

6.1 Introduction

Due to the complex interdependencies that exists across its asset systems, the risk of flooding on rail networks needs to be assessed through an integrated modelling approach which considers the three elements of (i) flood hazard probabilities and magnitudes, (ii) vulnerability of the network to hazards, and (iii) the resulting consequences. While this appears conceptually simple, significant complexities exist in methodological

formulation for large scale interdependent networks which have diverse asset types, multiple failure limit states and potential for widespread disruptions to train services.

With the increasing nature of extreme weather events, the risk of flooding to rail networks has received significant attention (Network Rail, 2020; Rail Journal, 2020; Network Rail, 2016; 2015). In response, infrastructure risk modelling has been advanced in recent years through system modelling approaches that incorporate spatial networks (Thacker et al, 2017; Pant et al, 2018; Koks et al, 2019). Further advancement of network-based approaches to rail modelling has involved building detailed spatial characteristics of these complex infrastructure systems to study their impacts at different scales (Johansson et al, 2011; Pant et al, 2016; Ilalokhoin et al, 2021). While there has been advancement in flood risk analysis studies with application at national scale (Hall et al, 2005; Duman et al, 2013), continental scale (Feyen et al, 2012; Rojas et al, 2013) and even at global scale (Ward et al, 2013; Koks et al, 2019), research studies on flood risk analysis of large scale rail networks which correctly model rail systems interdependencies, integrates these with a timetable model and estimates the disruption using industry-wide performance metrics of train and passenger delays are rare. For large scale networks, this analysis also needs to consider the spatial heterogeneity of flood events across large catchments (Lammersen et al, 2002; Uhlemann et al, 2010; Merz et al, 2014) and the spatial dependence that exist across multiple flood catchments at the same time (Metin et al, 2020). This is the gap in research literature that this study aims to address by presenting a methodology for flood risk assessment of a large spatial railway network which is demonstrated on a case study of the national rail network in Great Britain. A conceptual framework is presented which is used to estimate flood impacts at asset and network levels. These impacts are measured by estimating asset damages using established asset fragility functions. Wider network disruptions are measured using delay minutes metrics (DAB, 2019; NEA, 2003) and economic losses estimates using Value of Time (VoT) metrics (DfT, 2020).

6.2 Overview of flood risk assessment methodology

The methodology, illustrated in Figure 6.1, incorporates the modelling of three key components for the flood risk assessment of rail networks introduced in the previous section. The first step involves flood hazard modelling over a large spatial extent. Secondly, we demonstrate the methodology for assembling a geolocated dataset of the rail assets and their interdependencies that is necessary for operating the railway. Next, we intersect the flood maps with the railway dataset and use asset-specific performance curves to quantify the extent of asset failure for each flood event. Lastly, we estimate the consequence of each railway asset failure in terms of train and passenger delays using a dynamic train disruption model and calculate economic losses.

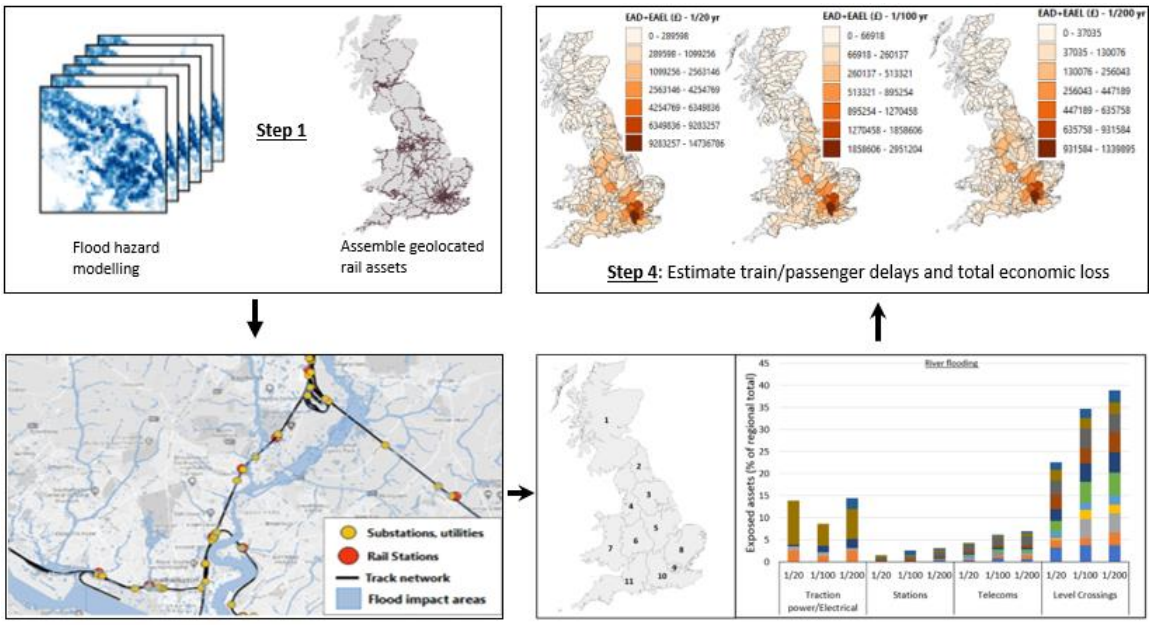

Figure 6.1 Conceptual framework for flood risk assessment of interdependent rail networks

6.2.1 Flood hazard modelling

A traditional approach to flood risk estimation involves using static hazard exceedance probability layers from flood maps which define the return period of a specific hazard event and adopt a specific hazard intensity measure. Each static hazard map is then created for a given return period based on a hazard load with a defined exceedance

threshold to ascertain the risk of flooding. In standard engineering hydrological studies involving flood risk assessment at relatively small spatial scales, the assumption that the flood return period is consistent in space over an area of study with a univariate extreme value theory used to estimate the flood return period severity is understandable (Quinn et al, 2019). However, the challenge of this traditional flood risk assessment approach is the assumption that flood risk probability does not vary within large parts of the network and that large spatial areas of the network will experience the same intensity for a given flood event. In practical real-world scenarios, this is not the case, and for large spatial rail networks, the return period of an event is not uniquely defined. Therefore, when considering flood risk in large scale heterogenous spatial networks like that of rail, it is important to model the risk taking into consideration the spatial dependence which exists across multiple locations during a flood event. This representation of flood hazard in terms of spatially coherent events allows for the possibility that multiple assets in different catchments could fail concurrently within a given flood event.

Our approach involves using available return period flood maps to create flood hazard scenarios which is used to estimate the disruption to assets on the network. The probability of the flood hazard occurring in a given year is therefore defined by its exceedance probability. The risk from a flood event is characterised by a flood hazard footprint, defined as the impact area of a specific flood event and this is estimated over the rail network when a flood hazard introduces failure to rail assets on the network. This allows us to generate a comprehensive and plausible flood hazard footprint which can be used to intersect with asset and depth-damage information to estimate the flood risk to the network. Spatial dependence across flood catchments in large spatial networks is accounted for by sampling an exhaustive set of all possible flood catchments and return periods to arrive at a series of flood scenarios which represent dependence across the network. This methodology is described and applied in detail in Section 6.3.2.

6.2.2 Geolocated dataset of railway asset and mapping of interdependencies

We represent the interdependent infrastructure assets by building a topology-based model to replicate the system-of-systems asset architecture of the rail network using a graph-based network-modelling approach. Details of the network topology models are described in Ilalokhoin et al (2021a) and presented in chapter 5 of this thesis. We represent the network as a collection of nodes and edges with individual assets e.g., rail stations, signal posts, substations designated as nodes while edges are used to represent the connectivity between nodes. This allows us to model a typical railway as a network of 5 core railway systems as shown in Figure 6.2, namely permanent way, signalling, civil engineering, electricity and telecommunications. By representing these as h number of systems, we collate all assets in the entire network in the set $M = \{M^1, \ldots, M^h\}$ where each system, $M^i \in M$ is a graph comprising nodes and edges such that $M^i = (N^i, E^{i,i})$. We denote $N^i = \{n_1^i, \ldots, n_r^i\}$ as the set of *r* nodes and $E^{ii} = \{e_{jk}^{i,i} = (n_j^i, n_k^i) \subseteq N^i \times N^i\}$ as the set of edges which defines the connectivity that exists across nodes in the system M^i. By doing this, we model the edge element $e_{jk}^{i,i}$ to connect the nodes n_j^i and n_k^i in M^i. The interdependencies that exist across the respective infrastructure systems on the rail network are represented in our model by the set $E^{i,v} = \{e_{jk}^{i,v} = (n_j^i, n_k^v) \subseteq N^i \times N^v\}$ and the entire rail network graph is formed by merging all the node and edge sets to form a system-of-systems such that $M = (N, E)$, where $N = \{N^1, \ldots, N^h\}$ and $E = \{E^{i,j} \forall i, j: 1, \ldots, h\}$. Each node in the network model is assigned its location coordinates and elevation to create 3D geospatial properties, mapped to a cartesian coordinate system to represent its true location in space.

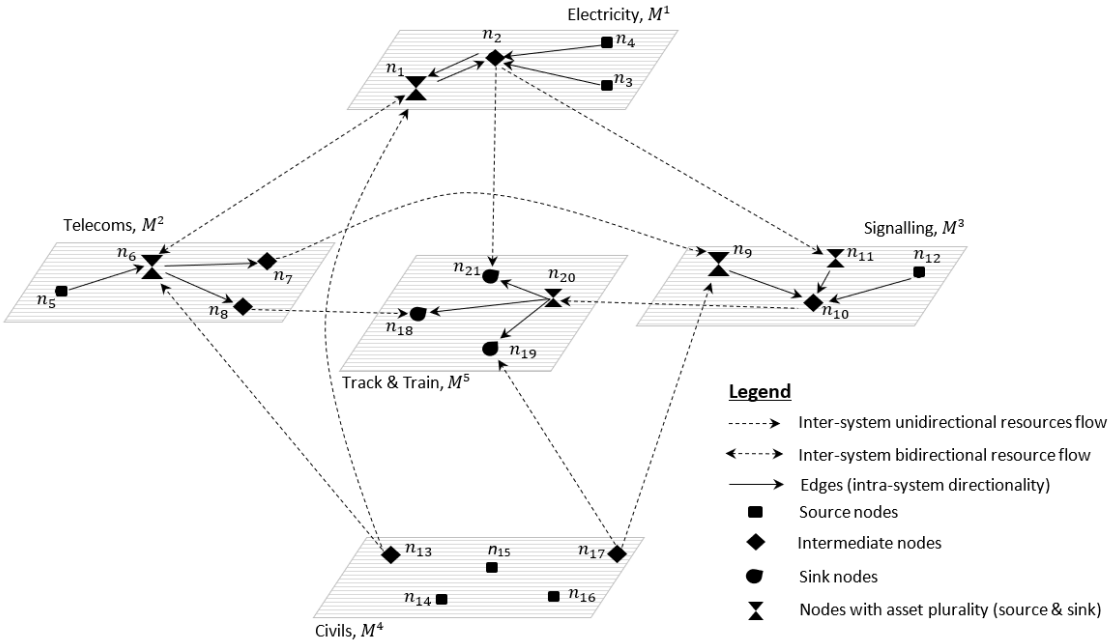

Figure 6.2 Rail interdependent network model showing resource flows across its different systems. Replicated from Ilalokhoin et al (2021a)

6.2.3 Failure analysis

6.2.3.1 Risk formulation

In this section we discuss the formulation of risk and estimation of flood risk probabilities. We represent an asset's failure state by a binary state function $s_i = \{0,1\}$, where $s_i = 0$ means the asset, i, has failed and $s_i = 1$ means the asset is functional. In an interdependent railway network where assets function collectively as a network, there are $2^c - 1$ possible failures states in a network of c assets, with each failure state denoted as $\mathbf{s} = (s_1, \dots, s_c)$. The loss associated with the failure state $\mathbf{s}$ is quantified as $z(\mathbf{s})$ with the conditional probability, $\Pr[\mathbf{s}|\mathbf{y}]$ of the network being in the failure state $\mathbf{s}$ for a given hazard load y described by its fragility.

The risk from the flood hazard event for each network state is estimated from the spatial intersection of the hazard and assets at their spatial locations such that:

$$\mu(\mathbf{s}) = \int_{\mathbf{y}} z(\mathbf{s})\, Pr[\mathbf{s}|y]\, f_{\mathbf{Y}}(\mathbf{y}) d\mathbf{y} \tag{6.1}$$

The total risk across all hazards and network failure states is described in Equation 6.2 and estimated by summing all possible failure states $\{\mathbf{s}_j, j = 1, \ldots, 2^c - 1\}$, the product of the losses incurred $z(\mathbf{s}_j)$ across different failure states, the conditional probability $\Pr[\mathbf{s}_j|\mathbf{y}]$ of the network being in the failure state s_j for a given hazard load y, and the hazard probability function $f_{\mathbf{Y}}(\mathbf{y})$.

$$\mu = \int_{\mathbf{y}} \left\{ \sum_{j=1}^{j=2^c-1} z(\mathbf{s}_j) Pr[\mathbf{s}_j|\mathbf{y}] \right\} f_{\mathbf{Y}}(\mathbf{y}) d\mathbf{y} \tag{6.2}$$

To ascertain which assets have failed, we carry out an intersection of the spatial flood hazard footprints with the different assets in the network model from Figure 6.2 and use asset performance curves to quantitatively assess the physical vulnerability of the assets for a given hydraulic condition. In Table 6.1 we present the asset-specific curves from existing literature which are used to estimate the direct damages to assets. The curves generally comprise two types – (1) fragility curves, which represent the conditional probability of failure given the hazard function e.g., as a function of flood return period and/or flood depth, (2) depth-damage curves, which quantify damage levels for a given flood depth. In each case, the hazard load characterised by the flood intensity is represented by its depth function, y, at the location of an asset, or its return period where a specific asset performance curve does not incorporate a depth function.

For permanent way assets, we adopt the fragility curve by Tsubaki et al (2016) to estimate the probability of ballast scour for varying flood depth. This fragility curve was developed based on a study of ballasted lines and embankments from well-documented track washout events in Japan. Ballasted track types are commonly used for large sections of rail networks across the world. Also, the material properties of ballasted rail networks, irrespective of country, are relatively homogeneous which makes the fragility curves developed by Tsubaki et al (2016) applicable to rail networks of similar configuration. For assets which are supported on structural foundations, we have adopted the fragility

curve by Lamb et al (2019) whose study on foundation scouring of railway bridges involved the assessment of a large dataset of historic bridge failures in Great Britain, culminating in a set of fragility curves based on the maximum likelihood estimation method. In principle, civil engineering foundation design for bridges, structures, signalling, overhead line equipment (OLE) and telecommunication mast assets on the railway follow the same design criteria, which in most of Europe is to the Eurocodes. Also, scouring is considered as the failure mode for all foundation types listed in Table 6.1. Therefore, the fragility curve developed by Lamb et al (2019) can be adopted within acceptable limits for estimating the vulnerability impact due to scouring for all asset foundation types listed in Table 6.1.

The depth-damages curve by Habermann & Hedel (2018) and Kok et al (2004) are used to quantify the damage to stations, operational buildings including signalling control centres and electrical control rooms, and electrical and communication systems which include traction power systems and telecommunication systems. For assets assessed using depth-damage curves, we assume that they become inoperable and when the damage factor, $\alpha \geq 0.25$, i.e., when 25% of the physical asset is damaged. Although we have been unable to validate this assumption using real-world asset performance data, we consider it reasonable to assume that when a quarter of a railway asset becomes non-functional, it becomes too risky to continue to allow it to function as designed. The results discussed in later sections therefore needs to be interpreted taking into context this assumption. In Table 6.1 we present a summary of the asset performance curves for each asset system and a plot of these curves are shown in Figure 6.3. When the total damaged assets for all affected systems are estimated, the expected annual damages (EAD) are calculated from Equation 6.2

It is recognised that the reliability of the flood risk assessment in this study relies on the accuracy of the asset performance curves which contributes to quantifying damages. This

makes the selection of the most appropriate curves of upmost importance to the analysis outputs. While effort has been made in Table 6.1 to source the most relevant asset performance curves for each asset type, it is acknowledged however that the output results of the analysis following the application of the curves need to take into consideration the limitations in rail research literature of directly applicable asset performance curves for each of the respective rail systems. These limitations have been discussed for each rail system in the previous paragraphs when selecting the relevant curves for use.

Rail system	Asset type	Failure mode and limit state	Asset performance functions
Track	PWay, including all track mounted assets located within the vicinity of the running rails between the cess[1] of each adjacent lines	Flooding – ballast scour with $y \geq y_{sleeper}$	Fragility curves adapted from Tsubaki et al (2016)
Civil engineering	Bridges and structures, OLE mast foundations	Foundation scouring	Fragility curves adapted from Lamb et al (2019)
	Buildings including station assets & signalling control centres	Flooding resulting in part of or all of asset becoming inoperable	Depth-damage curves by Habermann and Hedel (2018)
Signalling	Signalling assets	Foundation scouring	Fragility curves adapted from Lamb et al (2019)
Electricity	Traction grids, substations, feeder stations, electrical control rooms	Flooding resulting in part of or all of asset becoming inoperable	Depth-damage curves by Kok et al (2004)
Telecommunication	GSM-R[2] masts, SPTs[3]	Foundation scouring	Fragility curves adapted from Lamb et al (2019)
	FTN/FTNx[4] Location cabinets, Telecoms building and lineside assets	Flooding resulting in part of or all of asset becoming inoperable	Depth-damage curves by Kok et al (2004)

Table 6.1 Failure mode and fragility/depth-damage functions adopted for each asset system

[1] The cess is the area either side of the track, immediately off the ballast shoulder.
[2] GSM-R – Global System for Mobile Telecommunications-Railway
[3] SPTs – Signal Post Telephones
[4] FTN/FTNx – Fixed Telecommunication Network

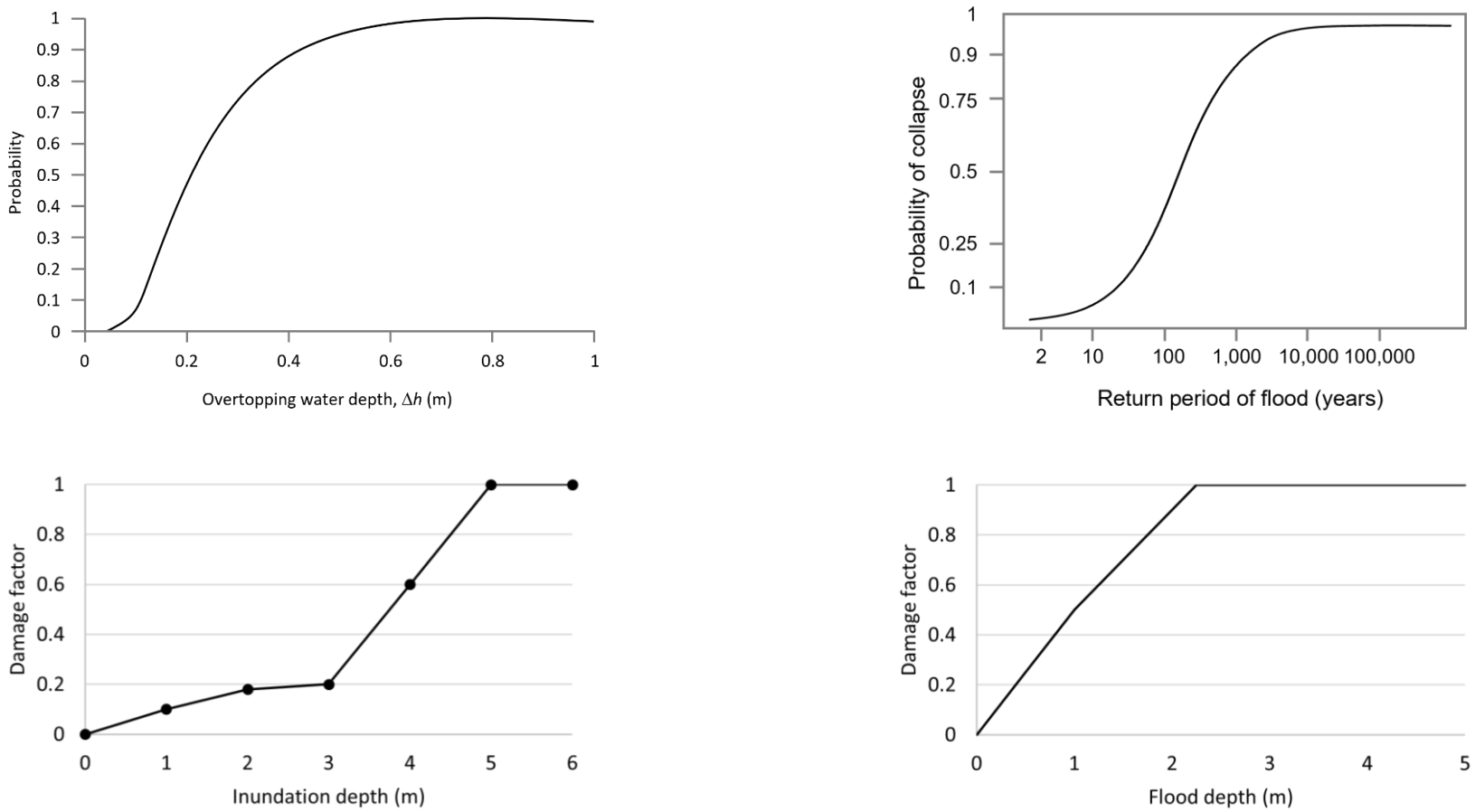

Figure 6.3 Fragility curves and depth-damage functions for rail infrastructure assets

(a) Fragility curve for ballast scour (Tsubaki et al, 2016) (b): Fragility curve for bridge scour damage (Lamb et al, 2019), (c) Depth-damage curve for train stations (Habermann and Hedel, 2018), (d) Depth-damage curve for electricity and communication systems (Kok et al, 2004)

6.2.3.2 Interdependent failure cascade modelling

When failure occurs in one system of the rail network, it can quickly propagate across other interdependent systems with *first-order* single failed asset failures triggering further indirect failures and *higher-order* effects (Rinaldi et al, 2001). To estimate the extent of this failure cascade, we model the operational functionality that exists across assets in terms of resource flows. Resource flow is defined here as the service provided by one asset to another or group of assets to facilitate operational functionality (Thacker et al. 2017). For example, data communication flow through Fixed Telecoms Networks (FTN) to signals and trains. We classify all nodes in the network model as source, intermediary or sink nodes depending on their role in facilitating resource flows. Resource flows are modelled to originate from source nodes and terminate at sink nodes via intermediary nodes, creating functional paths. We represent the set of all source nodes in the graph M as O and the sink nodes as D. For a given source node $n_o \in O$ and sink node $n_d \in D$, the functional path $F(n_o, \ldots, n_d)$ represents the set of all nodes and edges that facilitate an uninterrupted resource flow from the source to the sink. By mapping all functional paths between all sources and sinks in our model, we create a set of all functional paths of resource flows $F = \{F(n_o, \ldots, n_d)\ \forall n_o, n_d \in O, D\}$.

Asset failure is modelled as the removal of failed nodes which results in the disruption of a series of functional paths in the network model. When this happens, the collection of all disrupted functional paths of resource flows between source and sink nodes is denoted the set $\bar{F}$. To represent failure cascades, we assemble the set $\bar{F}$ in an ordered sequence of disrupted assets. Following an external shock event, the *first-order* failed assets are collated in the set of $\bar{A}_0$. Assuming these in turn result in a q ordered sequence of failure cascades, the sets $\bar{F}_1, \ldots, \bar{F}_q$ denote the collection of indirectly failed assets disrupted in the ordered sequence, and the total failure as a result of these is the union of the set, such

that $\bar{F} = \bar{F}_1 \cup \bar{F}_2 \cup \ldots \cup \bar{F}_q$. The complete set of all failed assets, either directly or indirectly are given by the set $\bar{A} = \bar{A}_0 \cup \bar{F}$.

6.2.4 Consequence assessment: train and passenger delay minutes

The consequence of the failure of assets following a flood event is discussed here in terms of the disruption to rail services, modelled and measured in this study in terms of train and passenger delay minutes. *Delay minutes* are a set of regulatory metrics adopted across many large rail networks around the world for measuring the punctuality of trains (NEA, 2003), estimated by finding the time lost, either between two recording points or late departure from a recoding point based on the actual times measured against the planned times from the train timetable (DAB, 2019). The basic concepts of the methodology for estimating delay minutes are discussed in detail in Ilalokhoin et al (2021) and chapter 4 of this thesis and the overall principles from this remain unchanged for this study. Therefore, only a high level summary is explained below, and the reader should refer to this paper for a detailed mathematical formulation of train and passenger delay minutes from first principles.

When a flood hazard results in the failure of an asset and subsequent disruption of train services, these disruptions can either take the form of line speed restrictions or cancellation of part of, or an entire train service. The delays associated with these are classified as *primary delays, reactionary delays* and *reliability or cancellation events* (DAB, 2019). To estimate the delay minutes, we identify the track nodes in the set of $\bar{A}$ which represents the point on the rail network where the resulting train delays are initiated. This is called the primary route and the delay initiated on this route is referred to as the *primary delay*. Train timetables are designed to have a delay threshold in minutes beyond which they result in knock-on effects or *reactionary delays* to other routes. When a hazard event results in a train being cancelled, diverted, or fails to call at some or all its scheduled stops, this is referred to as a *reliability event*. The total train delays associated

with a specific flood hazard event is the total of the primary, secondary and reliability delay minutes. Where passenger usage and disruption data are available for a rail network (Ghaemi et al 2018; Worsley, 2012), it is possible to assign these to rail station nodes on the network model and simulate passenger numbers disrupted for each train journey based on the published timetable (Ilalokhoin et al, 2021). The train and passenger delay minutes can then be calculated using the methodology discussed in Ilalokhoin et al (2021).

6.2.5 Economic loss estimation

The economic losses comprise two main aspects – repair cost and train delay cost. The asset repair costs for damaged assets following exposure to a flood hazard is denoted by the cost repair function, $C(R)$. The economic loss associated with the disrupted train service is estimated using the *value of time* (VoT) approach. This approach has been adopted in a number of model-based transport network vulnerability studies (Pregnolato et al., 2017; Jenelius, 2009; Erath et al., 2009; Taylor et al., 2006) and calculates the economic loss due to passengers arriving at their destination later than expected $C(d) = \Delta T.B\,.\mathrm{VoT}$, where ΔT = increase in journey time, measured in delay minutes, B refers to the number of passengers in each disrupted train service, and VoT = value of time in £/hour. The total economic loss incurred, K is estimated by finding the sum of all individual economic losses for each simulated flood hazard scenario. represented by:

$$K = \sum_{i=1}^{n}(C(R_i) + C(d_i)) \tag{6.3}$$

Where n is the total number of flood hazard scenarios considered.

The expected annual economic loss (EAEL) is obtained from the integral of the product of economic losses and their respective flood exceedance probabilities.

6.3 Case study application to flood risk assessment of Great Britain's rail network

We apply our methodology to a case study of the national rail network in Great Britain. This rail network is owned and operated by Network Rail which is an arm's length public body of the Department of Transport. However, privately owned train operating companies (TOCs) and freight operating companies (FOCs) provide passenger and freight services on the network. Our case study is applied to the entire rail network across Great Britain and covers passenger train services only.

6.3.1 Assembly of national rail assets and interdependency modelling

We collate the geospatial properties of the railway assets which are used to build a national scale rail network model using the asset groups presented in Table 6.2 and the methodology described in Section 6.2.2. These asset datasets are obtained from Network Rail's RINM (Rail Infrastructure Network Model) database which is a repository for asset geospatial data for the entire rail network in Great Britain (RailEngineer, 2015). All assets on the rail network are modelled with the required geometrical properties (x,y,z coordinates) necessary to build a topological model obtained from the Network Rail Standard Design and Detail drawings.

Railway system	Asset type	Numbers
Civil Engineering	Underline bridges (UB)	20,413 nodes
	Stations	2,567 nodes
	Tunnels (portal and shafts)	2,205 nodes
Track	Track/Permanent Way (PWay)	19,511 miles
Electrification and Plant	Traction power – 25kV AC and 75volts DC	1,089 nodes
Telecommunication	Telecommunications	5,474 nodes
Signalling	Signals	10,532 nodes
	Level crossings (LX)	14,762 nodes

Table 6.2 Asset systems used for this building the national rail infrastructure network model

6.3.2 Flood hazard modelling

This case study analysis is based on an assessment of the rail network to scenarios of river flooding hazards created from the JBA comprehensive flood maps for Great Britain. This comprises the mapping of 120,000km of rivers across Great Britain for the following annual exceedance probabilities (AEP): 0.05, (1 in 20 years return period), 0.01 (1 in 100 years RP) and 0.005 (1 in 200 years return periods) and for five banded depth grids.

In producing these maps, estimates of peak flows have been generated by JBA using catchment descriptors, such as rainfall, soil type, urban coverage and reservoir influence. These are extracted from the Flood Estimation Handbook (FEH), software providing guidance and data on rainfall and river flood frequency estimation in the UK with flows calculated from these descriptors using a statistics-based method from the FEH. Flow points are modelled at regular intervals along the 120,000km of river network (spaced at 200m apart in LIDAR areas and 400m apart elsewhere). Only watercourses with a catchment area greater than $3km^2$ in cities and $10km^2$ elsewhere are modelled by JBA. The flow is distributed along the watercourse using flow hydrographs. A hydrograph describes the flow in a watercourse over time. In an event, the hydrograph will provide information about the peak flow. The hydrographs are routed through JBA's JFlow+ modelling software which generates peak flood depth data which are processed into extents of flooding. A spatial plot of the JBA river flood maps is shown in Figure 6.4 (a). In carrying out the flood hazard modelling, the entire GB case study area is discretised into 407 river catchment units defined by the HydroBASINS dataset (Lehner & Grill, 2013). HydroBASINS is a series of hydrologically connected regions which are subdivided into small catchments areas shown in Figure 6.4 (b) through a series of levels from 1 (largest) to 12 (smallest). This is used in this study to create a river flood dataset for the whole of Great Britain. Considering the large spatial area for this study, it is necessary to consider the spatial

pattern of flood hazards that occur across multiple catchments in a given extreme flood event. This means that while flooding is unlikely to be extreme simultaneously across all catchments, it is plausible to consider the scenario where it occurs in more than one catchment at the same time. This dependence between the discreet catchments is accounted for by sampling an exhaustive set of all possible catchment and flood return periods to arrive at a series of flood hazard scenarios. This flood modelling comprises three steps. First, we intersect the flood hazard footprints from the JBA river flood maps with the assembled national scale assets for each of the river flood return periods and use the methodology described in Sections 6.2.3, 6.2.5 and 6.3.3 to calculate the EAD and EAEL for each flood catchment assuming full spatial dependence within a catchment. The next step involves accounting for the spatial dependence of flood events that can occur across multiple catchments. This involves simulating the possibility that for an extreme flood event, more than one catchment could be subject to a flood event at the same time. Estimating this requires the sampling of combinations of catchments experiencing flood events at the same time and estimating the EAD and EAEL for each combination based on their joint exceedance probabilities. To ensure that we are sampling the combination of flood catchments which result in the highest estimate of risk across the network, we rank all the catchments nationally based on the aggregate of their EAD and EAEL values from Figure 6.9 and select the top 20% highest ranked catchments to create five separate clusters of catchments for five key geographical regions of Great Britain. The selection of the top 20% catchments is considered reasonable as they account for over 75% of the total EAD and EAEL estimates nationally. These catchment clusters are shown in Figure 6.4 (b) and it is assumed in our flood modelling analysis that there is homogeneity of flood intensity within the catchments in each cluster due their proximity to one another. Therefore, for the five clusters and three flood return periods, this gives a total of 15 initial separate

combination scenarios. Lastly, from this, we create an exhaustive set of all possible combination of the flood catchment clusters and the three river flood return periods which gives rise to 1023 combinations of flood hazard scenarios which when multiplied by the number of edges removed in each failure scenario for each combination of clusters, gives a total failure simulation of 903,425 removed network edges.

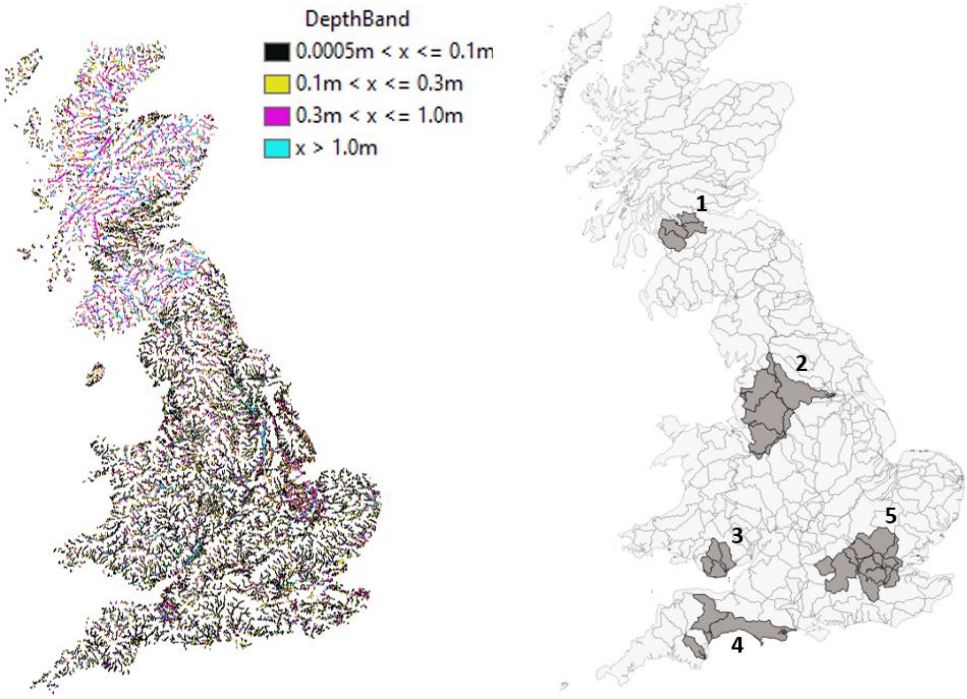

(a) (b)

Figure 6.4 (a) River flood map for GB with the flood depth bands (source JBA). (b) Map of GB showing the geographical boundaries of the HydroBASINs catchment dataset including those that result in the highest risk estimate.

These are grouped in 5 clusters strategically representing five key geographical regions of Great Britain.

1 = Scotland, 2 = North of England, 3 = Wales,
4 = Southwest England, 5 = London and the southeast

6.3.3 Failure analysis

The failure analysis comprises two parts – an exposure analysis and a flood risk analysis.

For this study, we consider an asset to be exposed if the flood event results in its damage.

To ascertain this, all the assets in each catchment area are intersected with the flood hazard footprints and using the asset performance curves in Figure 6.3, we obtain the number of exposed/damaged assets for each flood depth bands. The results of these are presented in Figure 6.5 and Figure 6.6 and discussed in Section 6.4.1.

The flood risk analysis comprises the estimation of the expected annual damages (EAD) and expected annual economic losses (EAEL). The asset performance curves in Table 6.1 and Figure 6.3 are used to estimate the asset damages for each flood hazard scenario. In accounting for the performance of drainage systems and their contribution to the flood risk assessment, the correct approach will be to explicitly model the functional properties of the drainage network. However complete information on this has not been readily available. To therefore account for the drainage system performance which has not been explicitly modelled for this study, the design specification from the flood design protection standards (Network Rail standard, Table 1 of NR/L3/CIV/005/09, 2018) for Great Britain is used to ascertain the threshold beyond which the designed drainage can be considered ineffective for each flood hazard event. This involves estimating the maximum flood levels for the respective flood return periods and assume in our analysis that once flood the flood thresholds exceed the maximum levels for each flood return period mandated in the Network Rail standard, the drainage can be considered ineffective as they would be overwhelmed having been subject to flood levels beyond which they are designed to accommodate. Our analysis is therefore carried out based on this modelling assumption.

The directly failed assets can result in higher order and indirect effects which eventually leads to disruption of track nodes and edges and train delays. This is the interdependent failure propagation whose consequences are obtained by collating the set of failed interdependent assets, $\bar{F}$ together with the set of the directly failed assets, $\bar{A}_0$ and then collating all the track nodes and edges removed as a result of this combined set of

damaged assets to obtain the overall impact disruption to train services and passengers. We do this by overlaying a model of all train paths across the national rail network according to the published rail timetable and using the multi-track journey disruption model discussed in chapter 4 to estimate the number of disrupted train journeys and passengers for each failure scenario. Our analysis is based on a flood hazard resulting in damage and disruption to rail assets and train journeys over a 24 hour period. By doing this, we can estimate results which are based on a daily estimation of risk impacts and which can be easily extrapolated for events which lasts for a longer period.

The economic losses are calculated using the methodology discussed in Section 6.2.5. We estimate repair costs based on cost of a repair gang attending the affected site to remedy damages. Since our analysis is based on each damaged asset being out of use for a 24 hour period, we estimate the asset repair cost in terms of labour cost for a gang of 10 operatives at a day rate of £750 per operative for each disrupted asset. Plant and material repair costs are assumed to be five times the total labour cost for each disrupted asset and the cost is assumed to be the same for all asset groups. The assumption made in this analysis is based on the damaged assets needing minor repairs which the inhouse maintenance teams can carry out successfully. It is however acknowledged that where this involves major repair works, this will result in significantly higher costs than discussed above, but this scenario has not been modelled in this analysis as it will most likely require more than the assumed 24 hours repair timescale. The cost of disrupted train and passenger journeys is calculated using the *VoT* estimates from the UK's Department for Transport TAG Data Book July 2020 (DfT, 2020). From the TAG Data Book, we can extract three different cost rates depending on the type of travel which are classified under (i) business travel, (ii) leisure and (iii) commuting. For business traveling passengers, this value is about 2.5 times the cost for commuting passengers. Leisure travelling is about half the cost for commuting passengers. To accurately adopt this

differential rate across all passenger types requires a correct delineation of all the travelling passengers according to their purpose of travel. As this level of granular data for passenger travel is not readily available for this analysis, we adopt the market rate for commuting passengers as the blanket rate for all travelling passengers. Adopting this rate represents the closest to the average rate for estimating passenger delay costs. Train and passenger delay minutes for each disrupted train journey are calculated using the multi-track journey disruption model by Ilalokhoin et al (2021) discussed in chapter 4 of this thesis. When these values are obtained, we calculate the total economic losses using Equation 6.3.

Finally, the EAD and EAEL are estimated for two separate flood risk scenarios. This includes first, estimating the individual catchment risks and secondly, estimating for all the catchment cluster combinations and failure scenarios discussed in Section 6.3.2 to account for spatial dependence across the catchments. The plots of the result from the former are presented in Figure 6.7 to Figure 6.9.

6.4 Results and discussions

6.4.1 Exposure analysis

The results from the exposure analysis are presented in Figure 6.5 and Figure 6.6. In Figure 6.5 we superimpose the exposed assets on the regional geographical map of Great Britain to present the exposed assets according to their geographical location. The results shows that about 31% of all track assets nationally are installed in areas that are exposed to river flooding. While track assets were the most exposed assets, level crossings were the second most affected asset systems with about 10% of all level crossings spatially intersecting river flood hazards nationally. We find that tunnels, signalling assets and underline bridges were the least exposed to river flood hazards Our results find that non-lineside assets were less likely to be installed in areas where they spatially intersected with a river flood hazard with only 2% of traction power assets found to intersect spatially

with river flood hazards. The high prevalence of lineside assets installed in areas where they intersected with flood hazards can be explained by historical perspectives where it is documented that many sections of the railway in Great Britain were built in flat low-lying land with limited drainage, along river valleys and river flood plains with susceptibility to heavy rain and river flooding, with most of the existing railway network today still following the same routes they were initially built on (Bogart et al, 2017).

West Midlands and the north of England had the highest number of exposed traction power and track assets to river flood hazards. Even though two-thirds of all the traction power assets nationally are located in London and the southeast of England, these regions had one of the lowest exposed traction power assets with only 1% exposed to river flooding.

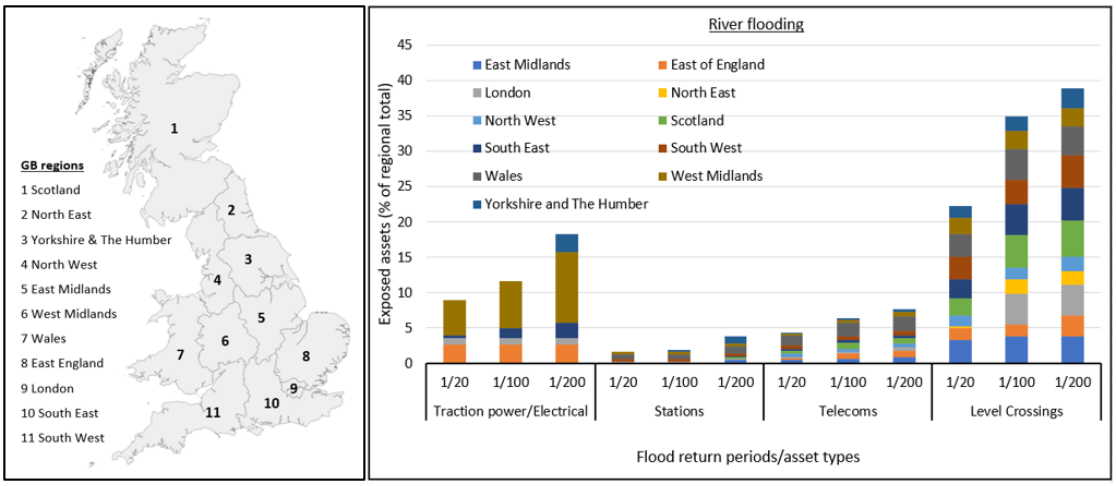

(a) (b)

Figure 6.5 (a) Great Britain's geographical region (b) Output of exposure analysis for all three return periods and assets considered.

The results exclude the plots for underline bridges, tunnels and signalling assets whose exposure numbers were found to be very low.

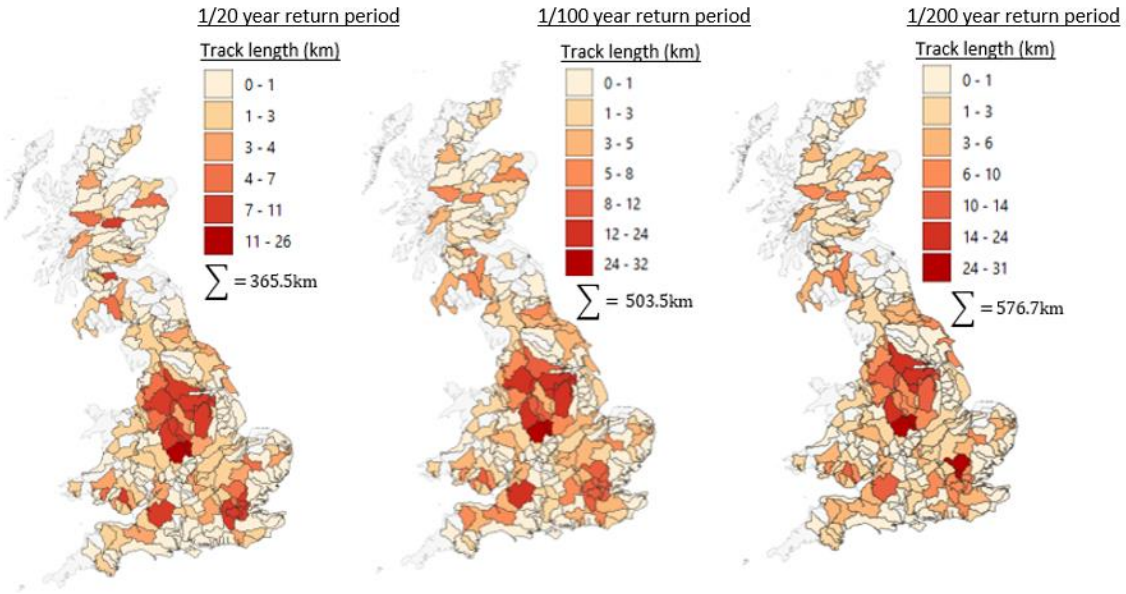
1/20 year return period
Track length (km)
0 - 1
1 - 3
3 - 4
4 - 7
7 - 11
11 - 26
∑ = 365.5km
1/100 year return period
Track length (km)
0 - 1
1 - 3
3 - 5
5 - 8
8 - 12
12 - 24
24 - 32
∑ = 503.5km
1/200 year return period
Track length (km)
0 - 1
1 - 3
3 - 6
6 - 10
10 - 14
14 - 24
24 - 31
∑ = 576.7km

(a) (b) (c)

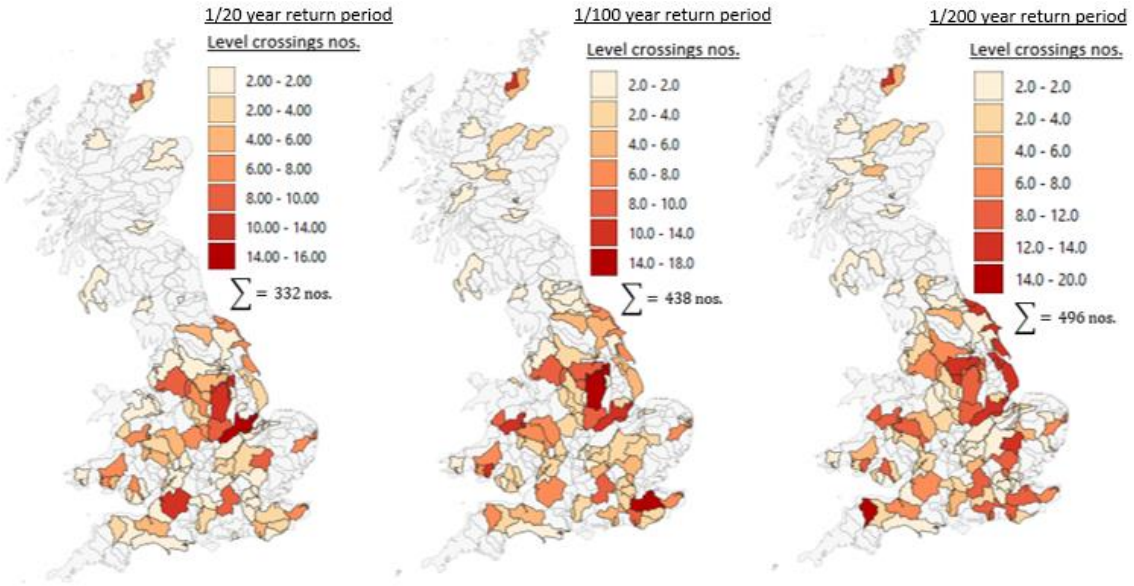
1/20 year return period
Level crossings nos.
2.00 - 2.00
2.00 - 4.00
4.00 - 6.00
6.00 - 8.00
8.00 - 10.00
10.00 - 14.00
14.00 - 16.00
∑ = 332 nos.
1/100 year return period
Level crossings nos.
2.0 - 2.0
2.0 - 4.0
4.0 - 6.0
6.0 - 8.0
8.0 - 10.0
10.0 - 14.0
14.0 - 18.0
∑ = 438 nos.
1/200 year return period
Level crossings nos.
2.0 - 2.0
2.0 - 4.0
4.0 - 6.0
6.0 - 8.0
8.0 - 12.0
12.0 - 14.0
14.0 - 20.0
∑ = 496 nos.

(d) (e) (f)

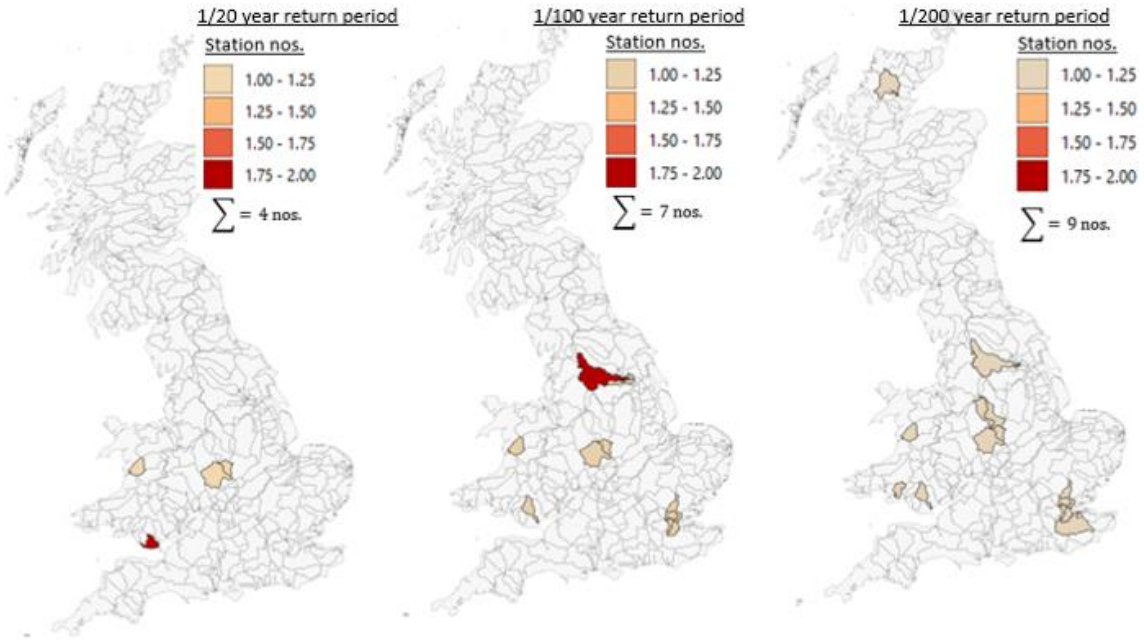

(g) (h) (i)

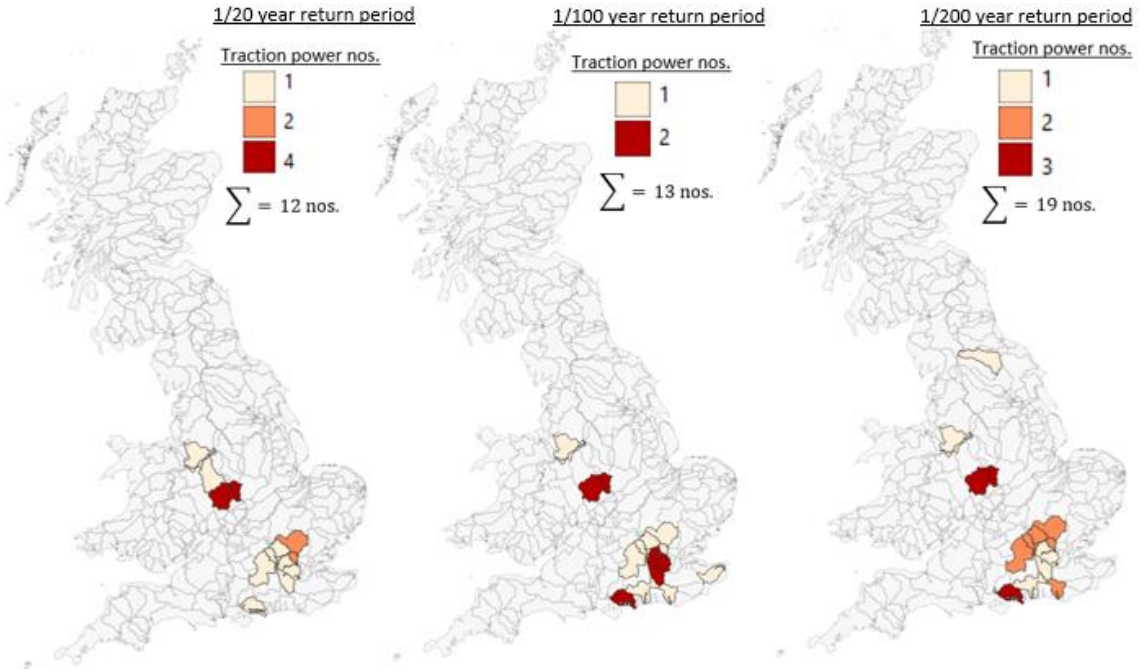

(j) (k) (l)

Figure 6.6 (a-l) Spatial plot of exposure analysis for rail assets for all three river flood return periods.

6.4.2 Results for asset damage and economic losses and risk

In Figure 6.7 to Figure 6.9 we present maps of the results for the expected annual damages (EAD) and expected annual economic losses (EAEL) for individual catchments across the country. In Figure 6.10 and Figure 6.11, graphs of the results from the analysis which considers the spatial dependence of flood events nationally are presented for all the failure scenarios of catchments combinations discussed in Section 6.3.2.

The risk analysis results from Figure 6.7 show that for all the flood return periods considered, the EAD was highest in the East and West Midlands regions of the country followed by sections of the rail network in the Northwest, Southwest and East of England regions. The EAD values for London region were considerably low with the highest EAD value in London about only a quarter of the highest value in the Midlands region. In the London region, our analysis finds that catchments in the east of London had the lowest EAD values in the region.

In contrast with the low EAD risk values obtained in London, our economic loss analysis results, presented in Figure 6.8, shows disproportionately high values for EAEL in London which suggests that small asset damage risks in London give rise to significantly high economic loss risks across the country.

The results presented in Figure 6.9 is the aggregate of the EAD and EAEL values which when compared with Figure 6.7 and Figure 6.8 show that the economic losses account for most risk values, with the EAD accounting for only about 7% the total losses compared with the EAEL's 93% for all the failure scenarios simulated. This output is important for Infrastructure Managers and decision makers when analysing the impact of risk due to flood events as it places emphasis on the need to take a holistic approach when making decisions on the speed of asset repair. This is because a small damage can result in high economic loss when compared with the damage repair cost especially for minor damage type scenarios which was the case tested in this study. However, where this

involves a major damage requiring longer term closure of track and where alternative measures could be implemented to reduce long term passenger delays and therefore decrease economic exposure to these delays, it is possible that the damage costs may be of comparable costs with the overall passenger delay costs.

Of all the catchments analysed and presented in Figure 6.9, London accounted for about 60% of all economic losses with the 1 in 20 year flood event presenting the highest risk estimate. Overall, the highest risk from river flooding was as a result of a 1 in 20 year return period, totalling about 48% of all financial losses on the rail network nationally, most of which occurred in London and the southeast region, with the northwest of England having the next highest losses.

The graphs in Figure 6.10 and Figure 6.11 show the results of our analysis for spatially dependent flood events, with a plot of the flood exceedance probabilities against the disruptions to trains and passengers for scenarios of multiple catchments flooded. The result shows interesting observations about the impact from catchment clusters in combinations with high consequence disruption to trains and passengers, although with very low probability of occurrence. We find that the high consequence catchment combinations almost certainly occurred when they were in combination with catchments located in London and the southeast of England. To demonstrate this, we present in Table 6.3, a snapshot summary of a selection of the catchment combinations including the top ten ranked combinations by train and passenger numbers disrupted. We find that all the top 10 ranked clusters were analysed in combination with C5 which is the cluster of catchments combinations located in London and the southeast. In fact, when we analysed for the consequence of flood hazard to C5 subject to a 1/200 flood return period, the results from Table 6.3 showed that with 9540 trains disrupted, this cluster alone accounted for 64% of the trains disrupted for the highest ranked cluster combination and over 81% of all passengers disrupted. This places emphasis on the significance of this region to

national performance metrics. While the highest ranked combination had a very low probability of occurrence, the cluster C5 combination with a flood return period of 1/20 had a 5% AEP. This shows that in Great Britain, when consideration is made of the impact of spatial dependence of flood events on catchment combinations, while it is possible that the combination with the most onerous consequences has the least probability of occurrence, the chance of a flood event which has 80% of the same level of disruption is much greater, at 5% AEP. This finding throws light on the need to ensure that the strategy for design and planning of critical asset locations on national railway networks takes into consideration their vulnerability impact. In this case, investment on resilience will most certainly need to be focused on key areas of more vulnerability to reduce their impact during disruption.

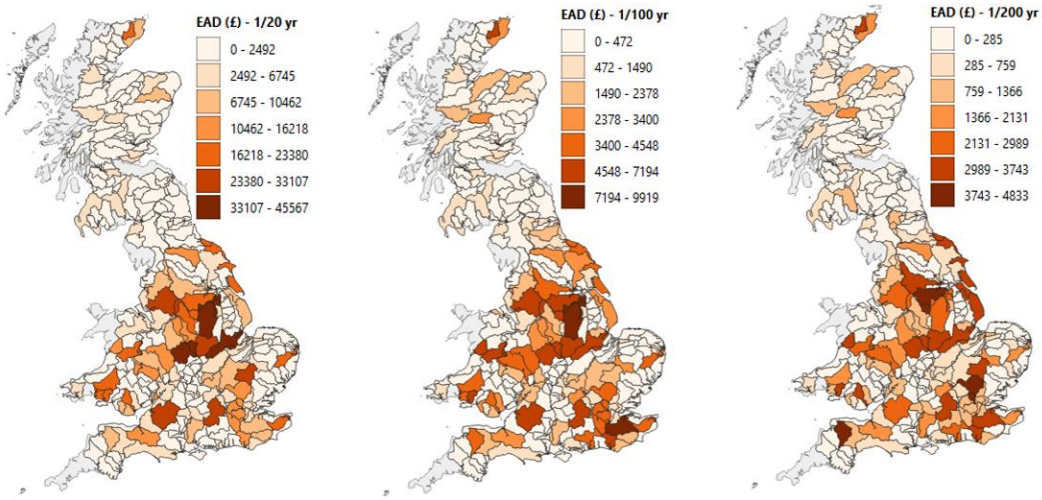

(a) (b) (c)

Figure 6.7 Spatial plot for EAD for all catchments and three river flood return periods

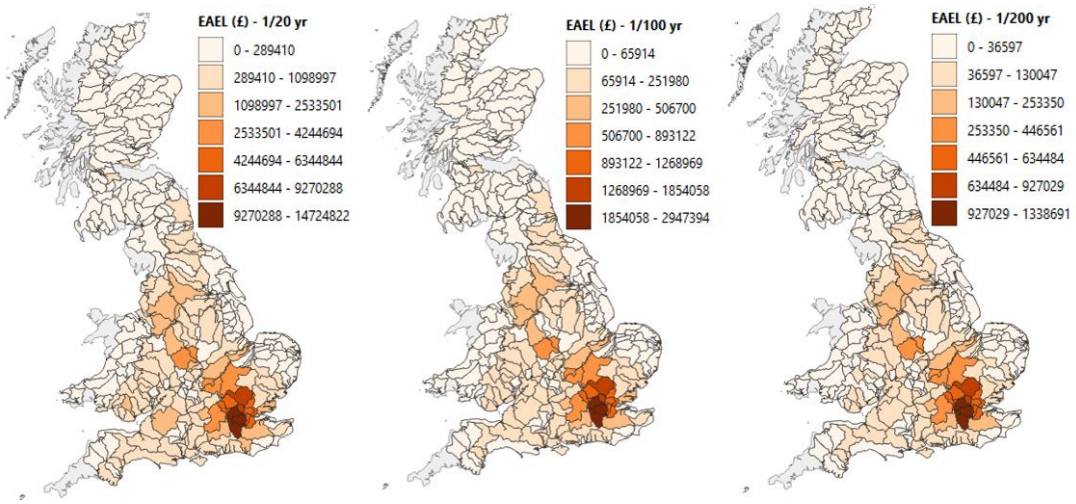

(a) (b) (c)

Figure 6.8 Spatial plot for EAEL for all catchments and three river flood return periods

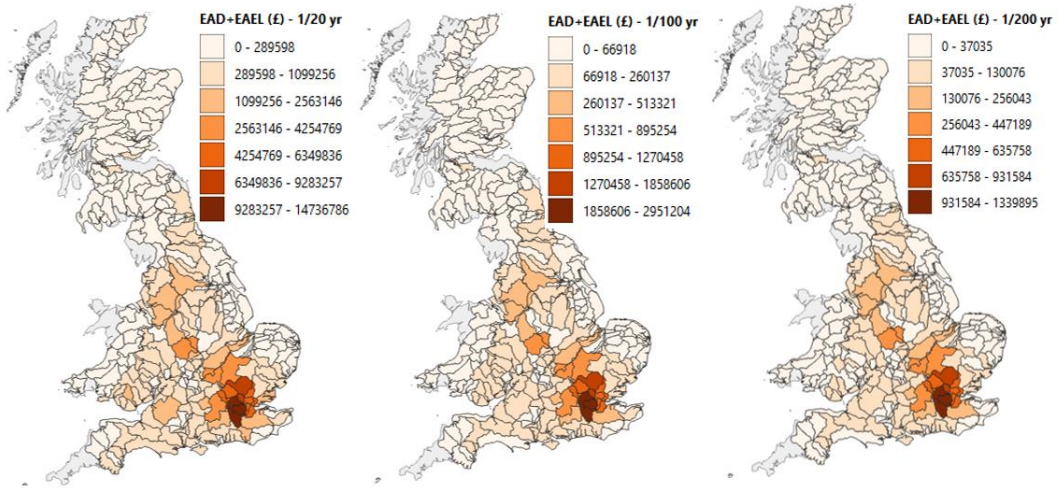

(a) (b) (c)

Figure 6.9 Spatial plot for combined EAD and EAEL for all catchments and river flood return periods

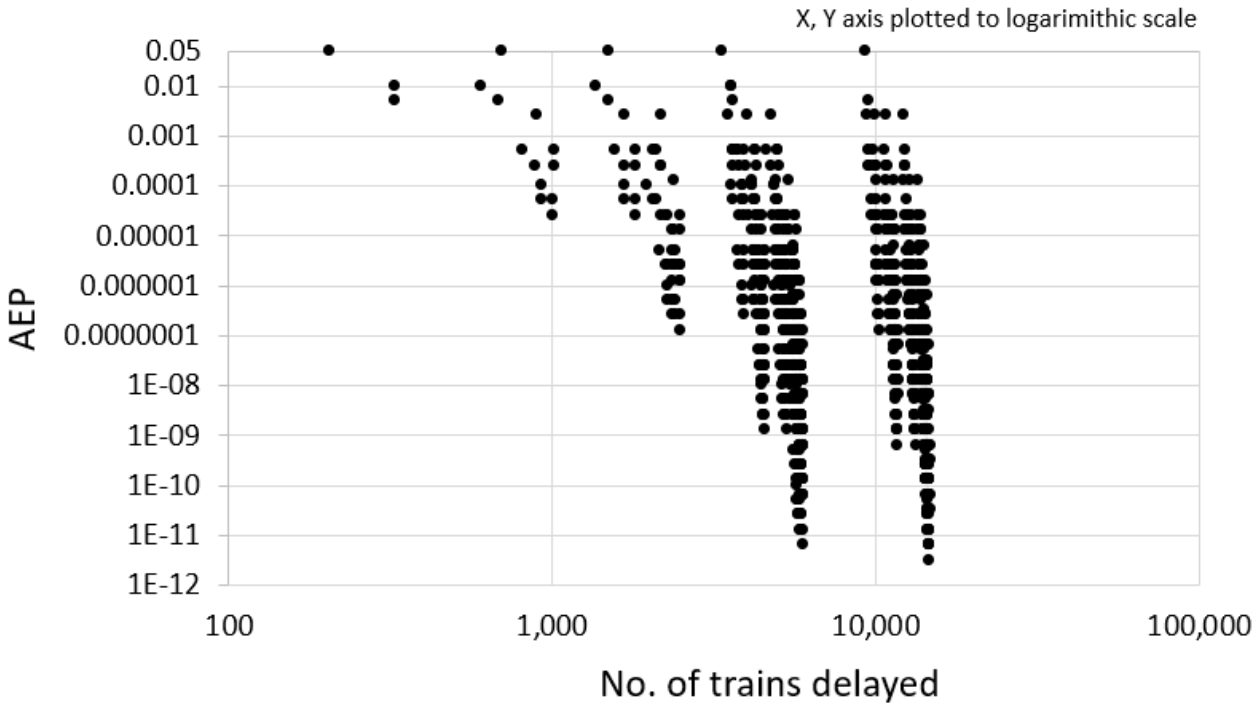

Figure 6.10 Plot showing results for number of trains delayed from analysis for spatial dependence of flood events.

No. of catchment combinations = 1023, no. of failure simulations = 903,425. Analysis is for disruption occurring during weekday for a 24 hour period.

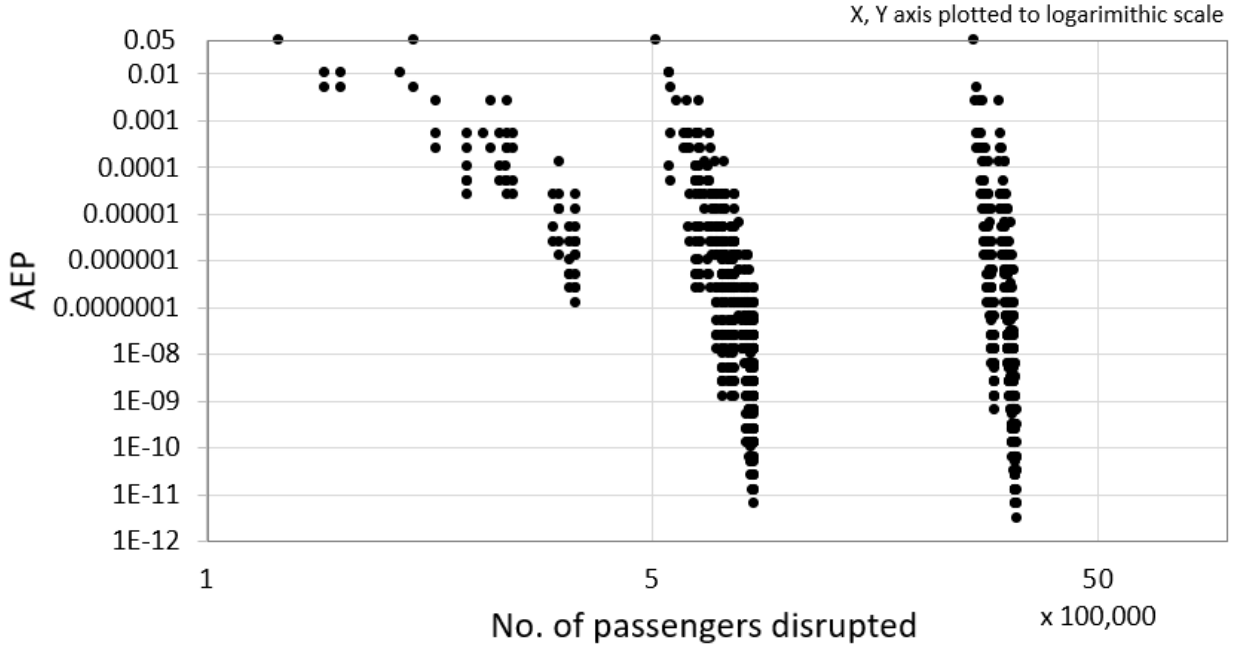

Figure 6.11 Plot showing results for number of passengers disrupted from analysis for spatial dependence of flood events.

No. of catchment combinations = 1023, no. of failure simulations = 903,425. Analysis is for disruption occurring during weekday for a 24 hour period.

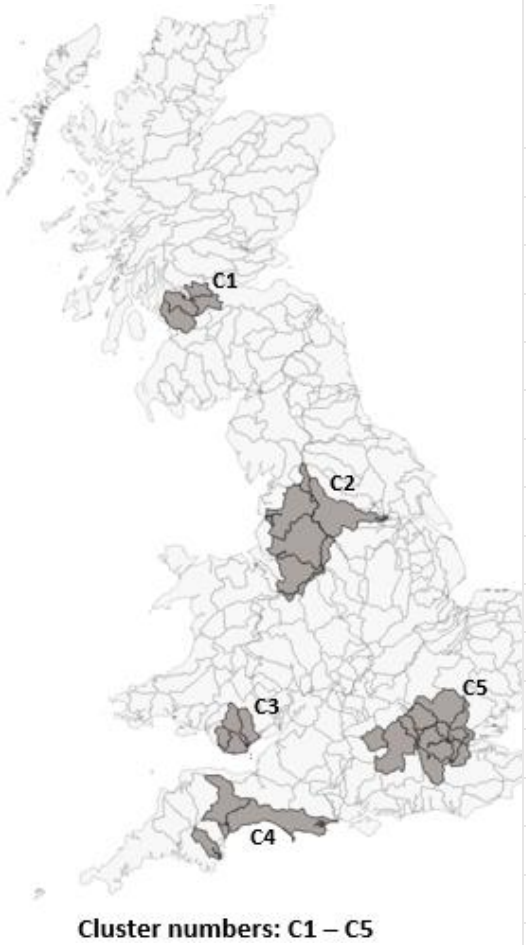

Cluster numbers: C1 – C5

Combinations ranking by trains/passenger nos. disrupted	Catchment combinations/|Return periods					No. of trains disrupted	No. of passengers disrupted
	Cluster no./return period	Cluster no./return period	Cluster no./return period	Cluster no./return period	Cluster no./return period		
1	C1/20	C2/200	C3/20	C4/200	C5/200	14,817	3,294,640
2	C1/200	C2/200	C3/20	C4/100	C5/200	14,816	3,294,638
3	C1/20	C2/200	C3/200	C4/200	C5/100	14,805	3,294,522
4	C1/200	C2/200	C3/200	C4/100	C5/100	14,804	3,294,520
5	C1/200	C2/100	C3/20	C4/200	C5/200	14,776	3,293,166
6	C1/200	C2/100	C3/20	C4/100	C5/200	14,775	3,293,164
7	C1/200	C2/100	C3/200	C4/200	C5/200	14,764	3,293,048
8	C1/200	C2/100	C3/200	C4/100	C5/100	14,763	3,293,046
9	C1/200	C2/200	C3/100	C4/200	C5/100	14,726	3,285,520
10	C1/200	C2/200	C3/100	C4/100	C5/200	14,725	3,285,518
370	C5/200	C2/100				12,618	3,074,562
510	C5/200					9,540	2,692,819
513	C5/20					9,361	2,647,327
942	C2/200	C4/20				3,828	608,776
954	C2/200					3,651	550,871
958	C2/100					3,610	549,397
1023	C4/20					205	72,767

Table 6.3 An abbreviated summary of the analysis output of catchments analysed in combination to simulate the impact of spatial dependence of flood events.

The result in this table shows the top 10 highest ranked combinations including 7 other selected combinations

6.5 Conclusion

In this paper, a methodology has been presented for flood risk assessment of large, complex rail networks. While several flood risk assessment methodologies exist in research literature for infrastructure networks, the complexity of the systemic interactions that make up a typical large rail network often requires tailored methodologies for its analysis. In this study, a methodology has been presented that considers the modelling of rail interdependencies at national scale and the integration with a timetable model for the estimation of disruptive impacts on the network in terms of train and passengers.

Methodologies such as that developed and demonstrated in this paper provide useful tools that can assist infrastructure managers and policy makers with informed, effective and sustainable asset policies that inform robust decision making through the testing of a range of scenarios. The economic loss modelling discussed in this study can be easily extrapolated for application to longer event disruption scenarios. The network model methodology developed in this study and the demonstration of its use with real-world dataset in Great Britain means that it can easily be transferrable for use in similar rail networks, especially across rail networks which are interoperable with that of Great Britain.

7 Conclusion

7.1 Thesis summary

This thesis presents methodologies and models for analysing the risk and resilience of critical infrastructure networks with a specific focus on rail networks. The railway in Great Britain is one of its most complex critical infrastructure network and the interdependencies that exists across its asset systems mean that small perturbations can quickly result in widespread disruption beyond the immediate disrupted system with greater impacts to the wider society. These layers of interdependencies, coupled with the large spatial scale that the networks cover, introduces complexities in the understanding of their risk estimation. In this thesis, this challenge has been addressed by the development of system-of-systems methodologies and modelling approaches for analysing them. A network-based approach has been applied to modelling the topological characteristics of a typical rail network by representing assets as nodes, with edges used to represent the connections between nodes. The functional characteristics have been modelled in the form of resource flows between interdependent asset systems. The building of a rail network model requires a high-resolution (asset level) modelling of a large dataset of multiple sector assets, from electricity to civil engineering, telecommunications, permanent way and signalling assets. This thesis has focussed on analysis at national scale to allow for a complete, holistic overview of the network's performance. Train network performance in real-world networks is measured by its ability to facilitate train journeys on the track network. To reflect this, the thesis has also incorporated a national scale timetable dataset as a modelled layer on the infrastructure network model and by combining the asset network model with the train journey model, an integrated infrastructure network disruption model of the rail network is created that allows for the simulation of asset disruption and performance measure in a single model. The modelling and methodological approach adopted in this thesis therefore makes a

significant contribution to rail research literature, because for the first time in research literature, a complete national scale multi-track model is developed that analyses train journeys on the rail network through their actual multi-track pathways. The benefit of this is that, with a correctly calibrated model, it is possible to analyse the potential impacts from disruption more accurately than previous models based on single-track models. This methodology and model have been tested using real-world asset dataset and the national rail timetable in Great Britain. An empirical dataset of previous disruptions on the network has been used to calibrate the model to facilitate the correct estimation of the impact from extreme weather events, culminating in a predictive model which can be used to analyse multiple scenarios at national scale. In the integrated infrastructure network model, the performance of the rail network is measured in terms of the metrics of delay minutes to replicate how this is carried out in real-world networks. This thesis represents the first time in academic research literature that disruptions to rail networks have been modelled and analysed using the metrics of train and passenger delay minutes.

Equally relevant to the study of risk in complex systems is their resilience to vulnerability. The resilience of an infrastructure network allows it to retain some, or most of its functionality during perturbation. The railway, like many other critical national infrastructure networks, has in-built resilience properties to maintain some level of network robustness under threat scenarios. This has informed the development of a resilience methodology and model in Chapter 5 of this thesis. This involved the representation of the network's redundancy, robustness and recovery with the development of resilience performance curves for different failure scenarios of traction power failure to the rail network using a case study of the southern region rail network of Great Britain.

One of the major causes of disruption to the rail network today is flood events as evidenced by the recent flooding events across rail networks in Great Britain (Network

Rail, 2021; New Civil Engineer, 2021), other parts of Europe (Trains, 2021), North America (Nytimes, 2021), China (BBC, 2021) within a short space of time in the month of July 2021. This points to the potent threat from extreme flood events on rail networks that were designed hundreds of years ago to engineering standards which may not have accounted for the climatic conditions experienced today. In Chapter 6, a methodology is therefore presented for analysing fluvial flood risk assessment, taking into account the spatial dependence of flood events on large spatial networks. This methodology is demonstrated on a comprehensive national scale flood risk assessment for Great Britain with interesting insights into the risk formulation and pattern for the respective regions and nations that make up the country.

An integration of the methodologies, models and analysis outputs from Chapters 4, 5 and 6 of this thesis results in a holistic approach to understanding and studying the risk and resilience of complex rail networks. Research models and tools are developed that can be applied to actual failure scenarios to inform decision making by Infrastructure managers and policy makers. This can inform the testing of multiple scenarios and appraisal of often very complex options to arrive at optimal and evidence based decision making.

7.2 Main research contributions

The main research contributions of this research thesis are in the areas of:

- The development of a multi-track disruption network model for analysing the disruptive impacts of perturbations on large scale rail networks.
- Methodological development and modelling of performance metrics in rail networks using real-world train performance metrics.
- The development of a calibrated integrated infrastructure network model using real-world asset data and empirical case studies.
- Methodology for assessing the resilience of rail networks.

- The presentation of methodology that is applied to a comprehensive flood risk assessment of rail networks taking into account the spatial dependencies on large spatial networks.

7.3 Implication of this research thesis for engineering, regulatory and policy making

The methodological advancements made in this thesis present useful outputs which have implications for engineering and regulatory policy making for critical infrastructure networks especially that of rail.

First, this thesis has demonstrated that the complex nature of large infrastructure networks and their interdependencies can be better understood using modelling methodologies. As these networks become more complex and sophisticated, it is important to expand the effectiveness of policy and decision using modelling methodologies and a broader expansion of modelling skills across academia and industry circles is key to achieving this.

Secondly, the analysis carried out in this thesis for the vulnerability and resilience of the rail network in Great Britain, point to the contribution of rail assets within the London region to network vulnerability and resilience nationally. For example, three of the four busiest stations in the country are fed by a traction power grid located in London. The region also contributes to over a third of the network's overall performance. Also, train journeys to most part of the southeast and southern parts of Great Britain need to connect via stations in London. The implication of having such a critical region is the potential for it to be an area of key vulnerability on the network. It is therefore important in the future resilience policy formulation on the railway network to consider the cost benefit implications of investing in more geographical resilience on the network. However, such geographical resilience consideration cannot be accomplished in isolation from the wider

government policy on addressing the concentration of large sections of economic activities in Great Britain around London.

Thirdly, careful consideration is needed in the area of policy formulation for addressing the risk from climate change and extreme weather-related hazards on the network. With the historic construction flaws of building large sections of the current network in Great Britain in areas which were already susceptible to flooding (Bogart et al, 2017), the output from the flood risk analysis in chapter 6 points to the potential for this problem to persist with increased asset exposure levels as weather becomes more extreme. While it may be unreasonable to completely change the geographical location of the existing railway network, there needs to be an acknowledgement of the potential for increase in investment for asset maintenance as the risk profile increases with climate change. Technology for asset monitoring and routine maintenance can be deployed more widely to tackle this challenge but needs careful consideration and policy formulation to ensure the network remains resilient to the challenges of an uncertain climatic future.

Lastly, there is a need to address the suitability of engineering design standards and asset performance specification to meet the growing challenges of an uncertain future. Many of the assets which are used across the rail network in Great Britain today were designed over 50 – 100 years ago. Some signalling assets and underline bridges are even older, and they remain in service as originally designed despite the changing risk from environmental and physical threats over the years. Also discussed in chapter 3, despite the increase in hot weather across the national network over the years, the stress-free temperature for track assets remains unchanged for Great Britain. The same is the case for flood protection assets, many of which have been in place for a considerable period of time, and subject to increasing extreme flood events. It is therefore important for organisations which are responsible for managing critical infrastructures which by their

nature are subject to increased climate related hazards, to ensure that they sufficiently address the changing nature of these threats.

7.4 Research limitations

While significant methodological advancement has been made in this thesis, there are several opportunities to improve the research presented here. This section discusses these limitations and in the following section, highlights areas of consideration for further future research.

(i) In Chapter 4, a methodology for journey disruption on a multi-track model is presented. The accuracy of calculating the cascading effect from knock-on delay across the network rely on how the model can simulate trains across junction points. With the digitalisation and technological advancement in Command and Control Systems, many real-world networks are now being controlled by Automatic Route Settings (ARS) which is a major subsystem of railway traffic management system that automatically sets train routes according to published timetables and can help to solve conflicts and establish train priority across route to minimise train delays and deadlock. The complexities in modelling journey prioritisation and regulatory preferences across junction points with complex interlocking arrangements to match often complicated regulated delay policies at national scale exceeds the capability of the network model developed in this thesis. However, for weather related hazard events, which this thesis is mainly focussed on, the principles discussed in the model provide a very good estimation of the delays accrued as discussed in Chapter 4.

(ii) While this thesis has involved the collation, modelling and analysis of arguably the most extensive dataset of national scale railway assets in Great Britain, there are still gaps in the dataset collated for certain asset systems. This is because at the time of collation of the data in 2019, certain technical discipline datasets were missing from the Network Rail's GeoRNIM database. The implication of this is the limitation in

the presentation of the results for the missing systems in the analysis outputs. However, because the network models developed in this thesis are expandable to include new datasets, it is possible to improve the model when such data becomes available in the future.

(iii) In modelling passenger disruption data output from the MOIRA database in Chapter 4, there is an acknowledged gap in the passenger data across a number of routes, for example, in Scotland where the number of passengers disrupted can be underestimated due to gaps in data available for this part of Great Britain.

(iv) The study of interdependencies in this thesis is limited to technical systems. In reality, other systems exist beyond just technical, for example, rolling stock maintenance, supply chain, political subsystems, and these often need to be considered in interdependency modelling. It will therefore be important for the consideration of whole-systems modelling to consider the incorporation of these systems to ascertain their impact when carrying out vulnerability and resilience analysis.

(v) The analysis in this thesis is limited to passenger disruptions only and does not consider freight transport.

(vi) While this thesis has extensively covered the area of vulnerability and resilience of rail networks, it is silent on the cost benefit analysis of different resilience options. Such information can be useful in informing a robust vulnerability framework and resilience strategy of critical infrastructure systems.

(vii) An area which has been highlighted during the development of this thesis is the need for appropriate validation of research models which can be applied to real-world scenarios. While the journey disruption multi-track model was validated against empirical failure data, this wasn't the case for the economic modelling due to the challenge of getting access to commercially sensitive economic data. This limitation

could therefore lead to assumptions in the modelling process which may not necessarily represent operational reality. While the basis for these assumptions is clearly spelt out in the thesis, nevertheless, this remains a limitation of this study for applicability to real-world scenarios and the results of the economic modelling need to be interpreted, taking this into consideration.

7.5 Future research direction

While acknowledging the substantial methodological advancements and contributions made in this thesis, the study of risk and resilience of large interdependent networks, particularly in the transportation sector, and indeed rail, is still growing and a lot still remains to be done. The paragraphs below discuss future research areas that can be developed to improve the understanding and research knowledge of the subject area covered in this thesis.

(i) There is a need to further expand existing knowledge of asset vulnerability studies in rail to reflect the different limit state of failures for the respective asset types. Depending on the hazard type, failure to an asset system can take different forms and the incorporation of these failure modes into a complete study is a research gap that needs to be explored further.

(ii) The sparce nature of studies focussed on developing fragility functions for rail systems has been highlighted in this study. This is an interesting area for future research study that can contribute to vulnerability analysis of rail networks.

(iii) Extending system-of-systems methodologies to other aspects of infrastructure interdependencies beyond geographical and physical. With the increasing digitalisation of infrastructure systems, there is a need to extend methodologies and models towards studying the impact of cyber interdependencies. Digital technologies can connect very large group of assets at the same time which means disruptions can

have wider impacts when compared with physically and geographically interdependent assets. The speed at which networks which are subject to cyber interdependencies can become degraded and/or recover is also an interesting area for future study.

(iv) The advancement of current methodologies and research models to analysing real-time simulation of transportation systems. Many existing train systems in real-world scenarios can show network performance in real time. For example, the tracking of real-time train movements on the network on digital platforms. This can be integrated with the network models developed in this thesis to analyse real-time disruption consequences and network resilience under failure scenarios.

(v) With future projections of more extreme weather events occasioned by climate change, it is expedient for existing models to be extended to allow for a robust analysis of current and future projection of flood risks to the railway network. With the potential for hotter summers, more studies on this area of risk remain under-developed in rail networks. There is therefore a need to extend existing methodologies and models to study the impact of increased heat to asset systems at national scale.

(vi) An advancement in the contributions of this research can be made in the area of incorporating freight transport to the passenger models already extensively covered in this thesis. This will allow for a complete and extensive coverage of all forms of rail transport types.

(vii) The incorporation of cost benefit analysis of resilience options into the modelling framework for this study will help to improve the applicability of the model and methodology and its practical usage for decision and policy making.

Ohis Ilalokhoin,
Oxford, England,
2021 AD

Bibliography

Adjetey-Bahun, K., Birregah, B., Châtelet, E., Planchet J.L., (2016), 'A model to quantify the resilience of mass railway transportation systems', Reliability Engineering & System Safety 153, 1-14

Albert, R., Albert, I., and Nakarado, G. L., (2004), 'Structural vulnerability of the North American power grid', Phys. Rev. E, 69(2), 025103

Anelli, A., Mori, F., Vona, M., (2020), 'Fragility Curves of the Urban Road Network Based on the Debris Distributions of Interfering Buildings', Appl. Sci., 10, 1289, doi:10.3390/app10041289

Armstrong, J., Preston, J., Ortega Hortelano, A., (2017), 'Enabling Resilient Railway Operations in the Context of Climate Change', At *7th International Conference on Railway Operations Modelling and Analysis*, Lille, France. 04 - 07 Apr 2017

Baker, J.G., (2015), 'Efficient analytical fragility function fitting using dynamic structural analysis', Earthq. Spectra, 31, 579–599, doi:10.1193/021113EQS025M

Bendfeldt J.P., Mohr, U., Muller L., (2000), 'RailSys, a system to plan future railway needs', Computers in Railways, VII: 249-255

Bešinović, N., (2020), 'Resilience in railway transport systems: a literature review and research agenda', Transport Reviews, 40(4), pp.457-478

Bogart, D., Xuesheng You and Leigh Shaw Taylor (2017), 'The development of the railway network in Britain 1825-1911', in The Online Historical Atlas of Transport, Urbanization and Economic Development in England and Wales c.1680-1911. Eds. L. Shaw-Taylor, D. Bogart and A.E.M. Satchell, 2017

Bradley BA, Dhakal RP, (2008), 'Error estimation of closed-form solution for annual rate of structural collapse', Earthquake Engineering and Structural Dynamics; 37(15): 1721–1737. DOI: 10.1002/eqe.833

Bruneau, M., Chang S.E., Eguchi, R.T., Lee, G.C., O'Rourke, T.D., Reinhorn, A.M. (2003), Shinozuka, M., Tierney, K.,) M.EERI, Wallace, W.A., vonWinterfeldt, D. (2003), 'A framework to quantitatively assess and enhance the seismic resilience of communities', Earthq Spectra; 19:733–52

Cabinet Office (2011), 'Keeping the Country Running: Natural Hazards and Infrastructure', downloaded on 13/04/2020 from https://www.gov.uk/government/uploads/system/uploads/attachment_data/file/61342/natural-hazards-infrastructure.pdf

Cadwallader, L.C. (2012), Review of maintenance and repair times for components in technological facilities', Idaho National Laboratories

Chang, S. E., & Shinozuka, M. (2004), 'Measuring Improvements in the Disaster Resilience of Communities', Earthquake Spectra, 20(3), 739–755

Chopra, S.S., Dillon, T., Bilec, M.M., Khanna, V., (2016), 'A network-based framework for assessing infrastructure resilience: a case study of the London metro system', J R Soc Interface 13 (118)

Cimellaro, G.P., Reinhorn, A.M., Bruneau, M., (2006), 'Quantification of seismic resilience', Proceedings of the 8th U.S. National Conference on Earthquake Engineering April 18-22, 2006, San Francisco, California, USA Paper No. 1094

Cimellaro, G.P., Reinhorn, A.M., Bruneau, M., (2010), 'Framework for analytical quantification of disaster resilience', Engineering Structures, 32 (2010), 3639–3649

Collins, M., R. Knutti, J. Arblaster, J.-L. Dufresne, T. Fichefet, P. Friedlingstein, X. Gao, W.J. Gutowski, T. Johns, G. Krinner, M. Shongwe, C. Tebaldi, A.J. Weaver and M. Wehner, 2013, 'Long-term Climate Change: Projections, Commitments and Irreversibility. In: Climate Change 2013: The Physical Science Basis. Contribution of Working Group I to the Fifth Assessment Report of the Intergovernmental Panel on Climate Change [Stocker, T.F., D. Qin, G.-K. Plattner, M. Tignor, S.K. Allen, J. Boschung, A. Nauels, Y. Xia, V. Bex and P.M. Midgley (eds.)]. Cambridge University Press, Cambridge, United Kingdom and New York, NY, USA.

Cui Y., Martin, U., (2011), 'Multi-scale simulation in railway planning and operation', Traffic & Transportation; 23(6): 511 – 517

D'Ariano, A., Corman, F., Pacciarelly, D., Pranzo, M., (2008), 'Reordering and local rerouting strategies to manage train traffic in real time', Transportation Science, vol 42, No. 4, pp 405 – 419

DAB (2019), 'Delay Attribution Principles and Rules', Delay Attribution Board, published September 2019, retrieved on 29/10/2019 from http://www.delayattributionboard.co.uk/DAPR.htm

Department of Defense, (1997), 'High Level Architecture Run-Time Interface Programmers Guide', pg 7-13

DfT (2020), 'Department for Transport Tag Data Book v1.13.1', accessed on 19/05/2021 from https://www.gov.uk/government/publications/tag-data-book

DMF (2015), 'Holding the line? Reviewing the impacts, responses and resilience of people and places in Devon to the winter storms of 2013/2014', A Summary Report from the Devon Maritime Forum

Duenas-Osorio, L., Craig, J.I., Goodno, B.J., Bostrom, A., (2007), 'Interdependent response of networked systems', J Infrastruct Syst 185–194

Dumas, P., Hallegatte, S., Quintana-Segui, P. and Martin, E., (2013), 'The influence of climate change on flood risks in France – first estimates and uncertainty analysis', Nat. Hazards Earth Syst. Sci., 13(3), 809–821, doi:10.5194/nhess-13-809-2013, 2013.

Eidsvig, U., Ekeheien, C., Tanasic, N., Hajdin, R., (2020), 'Vulnerability and resilience factors', Safeway Gis-Based Infrastructure Management System For Optimized Response To Extreme Events Of Terrestrial Transport Networks, WP 2: risk factors and risk analysis

Emanuelsson, M.A.E, McIntyre, N., Hunt, C.F., et al (2014), 'Flood risk assessment for infrastructure networks', J Flood Risk Management, 7, 31-41

EPCIP (2008) European Council, On the identification and designation of European critical infrastructures and the assessment of the need to improve their protection. Official Journal of the European Union. Council Directive 2008/114/EC; 8 December2008

Erath, A., Birdsall, J., Axhausen, K.W., Hajdin, R., (2009), 'Vulnerability assessment methodology for Swiss road network', Transportation Research Record 2137, 118–126

Eusgeld I, Nan C, Dietz S., (2011), 'System-of-systems approach for interdependent critical infrastructures', Reliability Engineering and System Safety, 96(6):679–686

Feyen, L., Dankers, R., Bódis, K., Salamon, P. and Barredo, J. I., (2012), 'Fluvial flood risk in Europe in present and future climates, Clim. Change, 112(1), 47–62, https://doi:10.1007/s10584-011-0339-7

Francis, R., and Bekera, B., (2014), 'A metric and frameworks for resilience analysis of engineered and infrastructure systems', Reliability Engineering and System Safety, 121, p90 – 103

FT (2019), 'National Grid chief questions hospital power cuts', accessed on 16/08/2020 from https://www.ft.com/content/1308e19c-bdf4-11e9-89e2-41e555e96722

Ganguli, P., and Reddy, M.J., (2013), 'Probabilistic assessment of flood risks using trivariate copulas', Theor Appl Climatol, 111:341–360, DOI 10.1007/s00704-012-0664-4

Ghaemi N, Zilko AA, Yan F, et al., (2018), 'Impact of railway disruption predictions and rescheduling on passenger delays', Journal of Rail Transport Planning & Management, 8(2):103-122

Ghaemi, N., Zilko, A.A., Yan, F., Cats, O., Kurowicka, D., Goverde, R.M.P., (2018), Impact of railway disruption predictions and rescheduling on passenger delays, Journal of Rail Transport Planning & Management, Vol: 8, Issue: 2, Page: 103-122

Ghafory-Ashtiany, M., Mousavi, M., Azarbakht, A., (2011), 'Strong ground motion record selection for the reliable prediction of the mean seismic collapse capacity of a structure group'. Earthquake Engineering and Structural Dynamics 2011; 40(6): 691–708. DOI: 10.1002/eqe.1055

Gouldby B. & Samuels P., (2005), 'Language of risk – project definitions', Floodsite Project Report T32-04-0, pp. 1–56

Gouldby B., Sayers P., Mulet-Marti J., Hassan M.A.A.M. & Benwell D., (2008), 'A methodology for regional-scale flood risk assessment', Proc Inst Civ Eng Water Manag, WM3, 169–182

Grubesic, T.H., and Matisziw, T.C., (2013), 'A typological framework for categorizing infrastructure vulnerability', GeoJournal, Vol. 78, No. 2, pp. 287-301

Habermann, N. and Hedel, R., (2018), 'Damage functions for transport infrastructure', International Journal of Disaster Resilience in the Built Environment Vol. 9 No. 4/5, pp. 420-434

Hall J.W., Dawson R.J., Sayers P.B., Rosu C., Chatterton J.B. & Deakin R., (2003), 'A methodology for national-scale flood risk assessment', Proc Inst Civ Eng Water Marit Eng, 156, (3), 235–247

Hall, J.W., Henriques, J.J., Hickford, A.J. and Nicholls, R.J. (2013), 'Systems-of-systems analysis of national infrastructure', Engineering Sustainability, ICE, 166(5): 249-257

Hall, J.W., Sayers, P.B., Dawson, R.J., (2005), 'National-scale Assessment of Current and Future Flood Risk in England and Wales', Natural Hazards, 36: 147–164

Hall, J.W., Tran, M., Hickford, A.J. and Nicholls, R. (2016), 'The Future of National Infrastructure: A System-of-Systems Approach', Cambridge University Press, UK. ISBN: 9781107066021

Hashimoto, T., J. R. Stedinger, and D. P. Loucks (1982), 'Reliability, resiliency, and vulnerability criteria for water resource system performance evaluation', Water Resources Research, 18(1), 14–20

Hickford, A.J., Blainey, S.P., Hortelano, A.O. and Pant, R., (2018), 'Resilience engineering: theory and practice in interdependent infrastructure systems', Environment Systems and Decisions, 38(3), pp.278-291

Holing, C.S. (1973), 'Resilience and stability of ecological systems', Annual Review on Ecology and Systematics, Vol 4, pp. 1-23

Hong, L., Ouyang, M., Peeta, S., He., X., Yan, Y., (2015), 'Vulnerability assessment and mitigation for the Chinese railway system under floods', Reliability Engineering and System Safety, 137, p58-68

Hosseini, S., Barker, K. and Ramirez-Marquez, J.E., (2016), 'A review of definitions and measures of system resilience', Reliability Engineering & System Safety, 145, pp.47-61

House of Lords, (2015); 'The resilience of the electricity system', House of Lords Science and Technology Select Committee, 1st Report of Session 2014 – 15

Ibarra, L. F., and Krawinkler, H., (2005), 'Global collapse of frame structures under seismic excitations', John A. Blume Earthquake Engineering Center, Stanford, CA, 324

Ilalokhoin, O., Pant, R. and Hall, J., (2021), 'A multi-track rail model for estimating journey impacts from extreme weather events Case study of Great Britain's rail network, International Journal of Rail Transportation, DOI: 10.1080/23248378.2021.1891582

Ilalokhoin, O., Pant, R. and Hall, J., (2021a), 'A model and methodology for risk and resilience assessment of interdependent rail networks – case study of Great Britain's rail network, JRESS-D-21-00945, submitted to the Journal of Reliability Engineering and System Safety, in Review

Infrarail (2018), 'The future of railway electrification control' by Dr Paul Hodgson, accessed on 08/05/2020 from http://www.infrarail.com/2018/assets/Future_of_Electrification_Control_RIA_May_2018.pdf

IRGC (2006), 'White Paper no. 3 on Managing and reducing social vulnerabilities from coupled critical infrastructures', International Risk Governance Council, Geneva

Janić, M., (2018), 'Modelling the resilience of rail passenger transport networks affected by large-scale disruptive events: the case of HSR (high speed rail)', Transportation (2018) 45:1101–1137

JBA (2013), 'JBA comprehensive flood map: Environmental and Perils Data', https://www.esriuk.com/~/media/esriuk/productsheets2015/ProductSheet_JBA_2015.pdf?la=en

Jenelius, E., (2009), 'Network structure and travel patterns: explaining the geographical disparities of road network vulnerability', Journal of Transport Geography 17 (3), 234–244

Johansson, J., Hassel, H. and Cedergren, A. (2011), 'Vulnerability analysis of interdependent critical infrastructures: case study of the Swedish railway Johansson, J., Hassel, H. and Cedergren, A. (2011),system', Int. J. Critical Infrastructures, Vol. 7, No. 4, pp.289-316

Kariyazaki, K., Hibino, N. and Morichi, S., (2013), 'Simulation mode for estimating trian operation to recover knock-on delay earlier', Asian Transport Studies, Volume 2, Issue 2, p284-294

Keef, C., Tawn, J. A., & Lamb, R., (2012), 'Estimating the probability of widespread flood events' Environmetrics, 24(1), 13–21. https://doi. org/10.1002/env.2190

Kelly-Gorham, M.R., Hines, P.D.H., Dobson, I. (2019), 'Using historical utility outage data to compute overall transmission grid resilience', Computer Science, Physics, Mathematics, ARXIV

Kok, M., Huizinga, H.J., Vrouwenvelder, A. and Barendregt, A. (2004), 'Standard method 2004 damage and casualties caused by flooding', Road and Hydraulic Institute

Koks, E.E, Rozenberg, J., Zorn, C., Tariverdi, M., Vousdoukas, M., Fraser, S.A, Hall, J.W and Hallegatte, S., (2019), 'A Global Multi-Hazard Risk Analysis of Road and Railway Infrastructure Assets', Nature Communications 10 (1): Article: 2677

Kong, J., Simonovic, S.P., and Zhang, C. (2018), 'Sequential Hazards Resilience of Interdependent Infrastructure System: A Case Study of Greater Toronto Area Energy Infrastructure System', Risk Analysis

Lam, J.C., Heitzler, M., Hackl, J., Adey, B.T., & Hurni, L., (2020), 'Modelling the functional capacity losses of networks exposed to hazards', Sustainable and Resilient Infrastructure, 5:1-2, 30-48

Lamb, R., Garside, P. Pant, R. and Hall, J.W., (2019), 'A network-scale analysis of the risk of railway bridge failure from scour during flood events in Britain', Risk Analysis, 39(11): 2457-2478. DOI: 10.1111/risa.13370

Lammersen, R., Engel, H., Van de Langemheen, W. and Buiteveld, H., (2002), 'Impact of river training and retention measures on flood peaks along the Rhine', J. Hydrol., 267(1–2), 115–124, doi:10.1016/S0022- 1694(02)00144-0

Latora, V., Marchiori, M., (2005), Vulnerability and protection of infrastructure networks, Physical review. E, Statistical, nonlinear, and soft matter physics, Vol.71(1 Pt 2)

Lee, E. E., Mitchell, J.E., Wallace, W.A., (2007), 'Restoration of services in interdependent infrastructure systems: a network flow approach', IEEE Trans Syst Man Cybern Part C 37(6):1303–1317

Lehner, B., and Grill, G., (2013), 'Global river hydrography and network routing: Baseline data and new approaches to study the world's large river systems', Hydrological Processes, 27(15), 2171–2186. https://doi.org/10.1002/hyp.9740

Li, A. and Hensher, D.A., (2013), 'Crowding in Public Transport: A Review of Objective and Subjective Measures', Journal of Public Transportation, Vol. 16, No. 2

Li, Tao & Rong, Lili, (2021), 'Impacts of service feature on vulnerability analysis of high-speed rail network', Transport Policy, Elsevier, vol. 110(C), pp 238-253

Lu, M., Nicholson, G.L., Schmid, F., Dai, L., Chen, L., Roberts, C., (2013), 'A Framework for the Evaluation of the Performance of Railway Networks', International Journal of Railway Technology, Volume 2, Issue 2, 2013

McDaniels, T., Chang, S., Cole, D., Mikawoz, J., Longstaff, H. (2008), 'Fostering resilience to extreme events within infrastructure systems: Characterizing decision contexts for mitigation and adaptation, Global Environmental Change, Vol. 18, No. 2, p. 310-318

Merz, B., Elmer, F., Kunz, M., Mühr, B., Schröter, K. and Uhlemann-Elmer, S., (2014), 'The extreme flood in June 2013 535 in Germany', La Houille Blanche, 5–10, doi:10.1051/lhb/2014001

Merz, B., Elmer, F., Kunz, M., Mühr, B., Schröter, K. and Uhlemann-Elmer, S., (2014), 'The extreme flood in June 2013 535 in Germany', La Houille Blanche, 5–10, doi:10.1051/lhb/2014001

Metin, A. D., Dung, N. V., Schröter, K., Vorogushyn, S., Guse, B., Kreibich, H., and Merz, B., (2020), 'The role of spatial dependence for large-scale flood risk estimation', Nat. Hazards Earth Syst. Sci., 20, 967–979, https://doi.org/10.5194/nhess-20-967-2020

MTI (2015), 'Passenger Flows In Underground Railway Stations And Platforms', Mineta Transportation Institute, REPORT 12-43, assessed on 14/10/2020 from https://www.its.ucla.edu/wp-content/uploads/sites/6/2015/11/passenger-flows-in-underground-railways-stations-platform.pdf

Nan, C., and Sansavini, G., (2017), 'A quantitative method for assessing resilience of interdependent infrastructures', Reliability Engineering and System Safety, 157:35-53

NEA Transport research and training (2003), 'BOB railway case – Benchmarking passenger transport in railways – Final report', Rijswijk, The Netherlands

Network Rail (2017), 'Delays explained: What we 're doing to minimize disruption and how delays can affect your journey', Retrieved from https://www.networkrail.co.uk/running-the-railway/looking-after-the-railway/delays-explained/ on 01/12/2019

Network Rail (2017), 'Electric Current for Traction (EC4T) Knowledge, by Authored by Alan Bullock

Network Rail (2018), 'Signals explained, accessed on 03/05/2020 from https://www.networkrail.co.uk/stories/signals-explained

Network Rail (2019), 'How a delay to services in one area can affect trains elsewhere in the country', Retrieved on 01/12/2019 from https://www.networkrail.co.uk/running-the-railway/looking-after-the-railway/delays-explained/knock-on-delays

Network Rail (2020), 'Network Rail Sectional Appendix', Accessed on 20/05/2020 from https://www.networkrail.co.uk/industry-and-commercial/information-for-operators/national-electronic-sectional-appendix

Network Rail (2020), 'Resilience of rail infrastructure: Interim report to the Secretary of State for Transport following the derailment at Carmont, near Stonehaven', by Andrew Haines, Chief executive officer 1 September 2020

Network Rail, (2015), 'Dawlish', Network Rail: London. https://www.Networkrail.Co.Uk/Timetables-and-travel/storm-damage/dawlish/(accessed 16/01/2021)

Network Rail, (2016), 'Dover to Folkestone railway will reopen this autumn, retrieved on 09/05/2020 from https://www.networkrailmediacentre.co.uk/news/dover-to-folkestone-railway-will-reopen-this-autumn

Network Rail, (2017a), 'Delays explained: What we 're doing to minimize disruption and how delays can affect your journey, retrieved from https://www.networkrail.co.uk/running-the-railway/looking-after-the-railway/delays-explained/ on 01/12/2019

Network Rail, (2017b), 'Knock-on delays: How a delay to services in one area can affect trains elsewhere in the country', retrieved on https://www.networkrail.co.uk/running-the-railway/looking-after-the-railway/delays-explained/knock-on-delays/ from on 05/07/2020

New Civil Engineer (2015), 'Flood damaged railway reopens', accessed on 12/05/2020 from https://www.newcivilengineer.com/archive/flood-damaged-railway-reopens-21-12-2015/

Neves, D., Geurs, K., La Paix, L., Lindhout, E., & Zanen, M., (2021), 'A vulnerability analysis of rail network disruptions during winter weather in the Netherlands', European Journal of Transport and Infrastructure Research, 21(2), 19–40, https://doi.org/10.18757/ejtir.2021.21.2.3956

Newman M.E.J., (2010), 'Networks: An Introduction', Oxford, UK: Oxford University Press. 2010; 720 pp

Ng, K., (2020), 'Crowd control measures introduced at stations and on trains amid fears of surge in passenger numbers', retrieved on 14/10/2020 from https://www.independent.co.uk/news/uk/home-news/coronavirus-lockdown-crowd-control-measures-public-transport-overcrowding-a9519506.html

NR/L2/TRK/2102 (2021), 'Level 2 Specification: Design and Construction of Track', Network Rail, Issue date 06/03/2021, compliance date 05/06/2021

NR/L3/CIV/05/09 (2018), 'Drainage Design Module 9', Network Rail, Issue 1, 02 June 2018, compliance date 03 December 2018

O'Rourke, T.D., (2007), 'Critical Infrastructure, Interdependencies, and Resilience', *The Bridge*, vol 37, No. 1, p22 – 29

Ofgem (2019), 'Technical report on the events of 9 August 2019', retrieved on 25/09/2020 from https://www.ofgem.gov.uk/system/files/docs/2019/09/eso_technical_report_-_final.pdf

ORR (2018), '2018 Periodic review final determination', retrieved on 22/09/2020 from https://www.orr.gov.uk/sites/default/files/om/pr18-final-determination-review-of-network-rails-proposed-costs.pdf

ORR (2019), 'Passenger Rail Performance: Quality and Methodology Report', Office of Road and Rail, Accessed on 25/10/2019 from https://dataportal.orr.gov.uk/media/1235/performance-quality-report.pdf

ORR (2020), 'Rail Infrastructure and Assets 2019-20', retrieved on 13/05/2021 from Rail Infrastructure and Assets 2019-20 (orr.gov.uk)

ORR (2020), 'Report following rail power disruption on 9th August 2019', Office of Rail and Road, Accessed on 16th August 2020 from https://orr.gov.uk/__data/assets/pdf_file/0017/42164/railway-power-disruption-on-2019-08-09-report.pdf

ORR (2020a), 'Estimates of station usage 2018 – 19', Office of Rail and Road', Accessed on 09/08/2020 from https://dataportal.orr.gov.uk/media/1668/estimates-of-station-usage-2018-19-key-facts.pdf

Ortega-Arranz, H., Llanos, D.R., Gonzalez-Escribano, A., (2014), 'The Shortest-Path Problem: Analysis and Comparison of Methods', Morgan & Claypool

Ossimitz, G., and Mrotzek, M., (2008), 'The Basics of System Dynamics: Discrete vs. Continuous Modelling of Time', International System Dynamics Conference 2008, Athens/Greece

Oughton, E.J., Ralph, D., Pant, R., Leverett, E., Copic, J., Thacker, S., Dada, R., Ruffle, S., Tuveson, M. and Hall, J.W., (2019), 'Stochastic Counterfactual Risk Analysis for the Vulnerability Assessment of Cyber-Physical Attacks on Electricity Distribution Infrastructure Networks', Risk Analysis, 39(9), pp.2012-2031

Ouyang, M. (2014), 'Review on modeling and simulation of interdependent critical infrastructure systems', Reliability Engineering & System Safety, 121(1), 43–60

Özgün, O., and Barlas, Y., (2009) 'Discrete vs. Continuous Simulation: When Does It Matter?', Proceedings of the 27th International Conference of The System Dynamics Society, July 26 – 30, 2009, Albuquerque, NM, USA

Pagani A., Mosquera G., Alturki A., et al., (2019), 'Resilience or Robustness: Identifying Topological Vulnerabilities in Rail Networks, R.Soc. open sci. 2019; 6

Pagani, A., Mosquera, G., Alturki, A., Johnson, S., Jarvis, S., Wilson, A., Guo, W., Varga, L., (2019), 'Resilience or Robustness: Identifying Topological Vulnerabilities in Rail Networks', 6., R.Soc. open sci

Pant R., Hall, J.W., Blainey, S.P., (2016), 'Vulnerability assessment framework for interdependent critical infrastructures: a case study for Great Britain's rail network', European Journal of Transport and Infrastructure Research, 16(1):174-194

Pant, R., Russell, T., Zorn, C., Oughton, E. and Hall, J.W, (2020), 'Resilience study research for NIC - Systems analysis of interdependent network vulnerabilities', Environmental Change Institute, Oxford University, UK

Pant, R., Thacker, S., Hall, J.W., Alderson, D., and Barr, S., (2018), 'Critical infrastructure impact assessment due to flood exposure', Journal of Flood Risk Management, 11, p22-33

PCCIP (1997) President's Commission on Critical Infrastructure Protection, Critical Foundations: Protecting America's Infrastructures (1997). Assessed online on 18/04/2020 from https://fas.org/sgp/library/pccip.pdf

Pederson, P., Dudenhoeffer, D., Hartley, S., & Permann, M. (2006), 'Critical infrastructure interdependency modeling: a survey of US and international research'. *Idaho National Laboratory*, 1-20

Pitts, F.R., (1965), 'A graph theoretic approach to historical geography', The Professional Geographer, 17(5): 15 – 20

Porter, K., Kennedy, R., and Bachman, R. (2007), 'Creating Fragility Functions for Performance-Based Earthquake Engineering' Earthquake Spectra, 23(2), 471–489

Pregnolato M., Ford, A., Glenis, V., Wilkinson, S., Dawson, R., (2017), 'Impact of Climate Change on Disruption to Urban Transport Networks from Pluvial Flooding', J. Infrastruct. Syst., 23(4)

Preston J, Wall G, Batley R et al., (2009), 'Impact of Delays on Passenger Train Services: Evidence from Great Britain', Transportation Research Record, 2117(1): 14–23

Quinn, N., Bates, P. D., Neal, J., Smith, A., Wing, O., Sampson, C., et al. (2019), 'The spatial dependence of flood hazard and risk in the United States', Water Resources Research, 55, 1890–1911, doi.org/10.1029/2018WR024205

Rail Journal (2020), 'RAIB confirms landslip caused Stonehaven derailment', assessed on 19/09/2020 from https://www.railjournal.com/regions/europe/raib-confirms-landslip-caused-stonehaven-derailment/

Rail Technology (2013), retrieved on 21/03/2020 from https://www.railway-technology.com/uncategorised/newsedf-energy-signs-ten-year-deal-power-uk-rail-network/

RailEngineer (2015), 'RINM Asset Viewer', . Accessed on 02/08/2021 from https://www.railengineer.co.uk/rinm-asset-viewer/

Rinaldi, S.M., Peerenboom, J.P., Kelly, T.K., (2001), 'Identifying, understanding, and analysing critical infrastructure interdependencies', Control Systems, IEEE, 2001; 21(6):11–25

Rojas, R., Feyen, L. and Watkiss, P., (2013), 'Climate change and river floods in the European Union: Socio-economic consequences and the costs and benefits of adaptation', Glob. Environ. Chang., 23(6), 1737–1751, https://doi:10.1016/j.gloenvcha.2013.08.006, 2013

RSSB (2016), 'Tomorrow's Railway and Climate Change Adaptation: Executive Report, written by Olivier Marteaux, Rail Safety and Standards Board

Rudnicki, A. (1997), 'Measures of regularity and punctuality in public transport operation', Transportation system, Proceedings volume from the IFAC symposium, Chania, Greece, 16-18 June 1997, Vol. 2, pp 661-666

Rungskunroch P., Jack A., Kaewunruen S., (2022), 'Risk and Resilience of Railway Infrastructure: An Assessment on Uncertainties of Rail Accidents to Improve Risk and Resilience Through Long-Term Data Analysis' In: Pal I., Kolathayar S. (eds) Sustainable Cities and Resilience, Lecture Notes in Civil Engineering, vol 183. Springer, Singapore. https://doi.org/10.1007/978-981-16-5543-2_2

Salkonen, R., & Paavilainen, J., (2010), 'Measuring railway traffic punctuality from the passenger's perspective', 12th WCTR, July 11-15, 2010 – Lisbon, Portugal

Salvadori, G., De Michele, C., (2004), 'Frequency analysis via copulas: theoretical aspects and applications to hydrological events', Water Resources Research, vol 40, W12511, doi:10.1029/2004WR003133

Schmöcker, J.-D., Cooper, S. and Adeney, W., (2013), 'Metro service delay recovery: compassion of strategies and constraints across systems', Transportation Research Record: Journal of the Transportation Research Board, No. 1930, Transportation Research Board of the National Academies, Washington D.C., 2005, pp. 30–37

Sen P, Dasgupta S, Chatterjee A, et al., (2003), 'Small-world properties of the Indian Railway Network', Phys. Rev.; E67. 036106

Setola, R., and Theocharidou, M., (2016), 'Modelling Dependencies Between Critical Infrastructures', Chapter 2 (eds.), in Managing the Complexity of Critical Infrastructures, Studies in Systems, Decision and Control 90

Simonovic, S.P., & Peck, A., (2013), 'Dynamic resilience to climate change caused natural disasters in coastal megacities quantification framework', British Journal of Environment & Climate Change, 3(3): 378-401

Tang, Junqing & Xu, Lei & Luo, Chunling & Ng, Tsan Sheng Adam, (2021), **'**Multi-disruption resilience assessment of rail transit systems with optimized commuter flows**',** Reliability Engineering and System Safety, Elsevier, vol. 214(C).

Taylor, M.A.P., Sekhar, S.V.C., D'Este, G.M., (2006), 'Application of accessibility based methods for vulnerability analysis of strategic road networks', Networks and Spatial Economics 6 (3–4), 267–291

Thacker, S., Kelly, S., Pant, R. and Hall, J.W., (2017), 'Evaluating the benefits of adaptation of critical infrastructures to hydrometeorological risks', *Risk Analysis,* DOI: 10.1111/risa.12839

Thacker, S., Pant, R. and Hall, J.W., (2017), 'System-of-systems formulation and disruption analysis for multi-scale critical national infrastructures', Reliability Engineering and Safety, 167, p30 – 41

The Guardian (2018), 'Beast from the East meets storm Emma, causing UK's worst weather in years', Accessed on 06/06/2020 from https://www.theguardian.com/uk-news/2018/mar/01/beast-from-east-storm-emma-uk-worst-weather-years

TRCCA (2016), 'Tomorrow's Resilience and Climate Change Adaption: Final Report', Task 4: Systems modelling appendices, Railway Safety and Standards Board, Published May 2016

Tsubaki, R., Bricker, J.D., Ichii, K., Kawahara, Y., (2016), 'Development of fragility curves for railway embankment and ballast scour due to overtopping flood flow', Nat. Hazards Earth Syst. Sci., 16, 2455–2472, doi:10.5194/nhess-16-2455-2016

Uhlemann, S., Thieken, A. H. and Merz, B., (2010), 'A consistent set of trans-basin floods in Germany between 1952- 2002', Hydrol. Earth Syst. Sci., 14(7), 1277–1295, doi:10.5194/hess-14-1277-2010

UN (2015), 'Transforming our world: the 2030 Agenda for Sustainable Development, Seventieth Session', The UN General Assembly, September 2015

Veiseth, M., & Bititci, U.S., (2005), 'Performance measurement in railway operations - improvement of punctuality and reliability', Proc. of the 5th Int. Conf. on Performance measurement and management, eds. A. Neely M. Kennerly & A. Walters, Cranfield University: Stirling, UK, pp. 801- 808, 2005

Wang, Q., Liu, K., Wang, M. et al., (2021), 'A River Flood and Earthquake Risk Assessment of Railway Assets along the Belt and Road', Int J Disaster Risk Sci, 12, 553–567, https://doi.org/10.1007/s13753-021-00358-2

Ward, P. J., Jongman, B., Weiland, F. S., Bouwman, A., Van Beek, R., Bierkens, M. F. P., Ligtvoet, W. and Winsemius, H. C., (2013), 'Assessing flood risk at the global scale: Model setup, results, and sensitivity', Environ. Res. Lett., 8(4), doi:10.1088/1748-9326/8/4/044019, 2013

Wheater H.S., (2006), 'Flood hazard and management: a UK perspective', Philos Trans R Soc, 364, 2135–2145

Williams Rail Review, (2019), 'Rail in the future transport system', Evidence Paper, UK Department for Transport

Worsley, T. (2012), 'Rail Demand Forecasting Using the Passenger Demand Forecasting Handbook: On the move' – Supporting paper 2, London, UK

Zobel, C. W. (2011), 'Representing perceived trade-offs in defining disaster resilience', Decision Support Systems, 50(2), 394– 403

Appendix A: Co-Author paper contribution statements

Co-author paper contribution statements

To the Director of Graduate Studies,
School of Geography and the Environment
Environmental Change Institute
South Parks Road, Oxford OX1 3QY

I, Jim W. Hall, certify that Ohiowaobo Ilalokhoin completed the majority of the work in each of the chapters that form part of his DPhil thesis, as well as any associated articles that have already been published or may be published in the near future.

Signature:

Professor Jim W. Hall

Date: 17/08/21

School of Geography and the Environment
Environmental Change Institute
South Parks Road, Oxford OX1 3QY

Co-author paper contribution statements

To the Director of Graduate Studies,
School of Geography and the Environment
Environmental Change Institute
South Parks Road, Oxford OX1 3QY

I, Raghav Pant, certify that Ohiowaobo Ilalokhoin completed the majority of the work in each of the chapters that form part of his DPhil thesis, as well as any associated articles that have already been published or may be published in the near future.

Signature:

Dr Raghav Pant

Date: 18/08/2021

School of Geography and the Environment
Environmental Change Institute
South Parks Road, Oxford OX1 3QY

Appendix B: Overview of data and software processing tools used in this thesis

Tool name	Tool type	Tool used within this thesis	Link to tool
QGIS	GIS platform	For plotting and visualising database outputs	http://www.qgis.org/en/site/
ESRI-ArcGIS	GIS platform	For visualising database outputs and geo-spatial functionality	http://www.esri.com/software/arcgis/
Python	Programming language	For building the infrastructure network model, general algorithm implementation, failure analysis, rail timetable simulation	https://www.python.org/
Python-igraph	Python library	Package containing network functions for building the infrastructure network model	https://igraph.org/python/
Microsoft Excel and VBA applications	Spreadsheet	Spreadsheet, graphic tool, programming	https://www.microsoft.com/en-gb/microsoft-365/excel/